EXAMINING THE ROLES OF DIR1 AND DIR1-LIKE DURING SAR

EXAMINING THE ROLES OF DIR1 AND DIR1-LIKE DURING SYSTEMIC ACQUIRED RESISTANCE IN *ARABIDOPSIS* AND CUCUMBER

By MARISA ISAACS, B.Sc

A Thesis Submitted to the School of Graduate Studies in Partial Fulfilment of the Requirements for the Degree of PhD in Biology

McMaster University

DR OF PHILOSOPHY SCIENCE (2013) McMaster University Hamilton, Ontario (Biology)

TITLE: EXAMINING THE ROLES OF DIR1 AND DIR1-LIKE DURING SYSTEMIC ACQUIRED RESISTANCE IN *ARABIDOPSIS* AND CUCUMBER

AUTHOR: Marisa Isaacs, B.Sc (McMaster University)

SUPERVISOR: Dr. Robin K. Cameron

NUMBER OF PAGES: 152

Abstract

Systemic Acquired Resistance (SAR) is a plant defense response induced by an initial infection in one part of the plant that leads to broad-spectrum resistance to normally virulent pathogens in distant naïve leaves. As part of the Cameron research team, I contributed to demonstrating that the lipid transfer protein, DIR1 is required for SAR long distance signaling in *Arabidopsis* and travels from induced to distant tissues during SAR. A highly similar *Arabidopsis* protein DIR1-like was identified and is thought to be responsible for the occasional SAR-competent phenotype observed in the *dir1-1* mutant. This work provides evidence for the idea that DIR1 and DIR1-like are paralogs created by a recent duplication event and that similar to DIR1, DIR1-like may travel to distant tissues during SAR. To better understand DIR1 and DIR1-like contribution during SAR, *dir1-1dir1-like* double mutant transgenic plants were created as well as transgenic plants expressing epitope- (HA and FLAG) and fluorescent- (iLOV and phiLOV) tagged DIR1 and DIR1-like to facilitate visualization of movement during SAR. Several putative DIR1 orthologs were identified in crop plants and cucumber CucDIR1 was shown to be functionally equivalent to AtDIR1 in *dir1-1* complementation studies providing further evidence that DIR1 plays an important role in SAR across plant species. By analyzing conservation between DIR1, DIR1-like and the putative DIR1 orthologs, several protein residues were identified that may be important for DIR1 function during SAR. DIR1 proteins were modified at these sites and the importance of these residues was supported by the reduced binding of the TNS hydrophobic probe in these DIR1 variants. Taken together, this thesis suggests that DIR1 and DIR1-like both participate in SAR in *Arabidopsis*, that DIR1 crop orthologs are also important for the SAR

response and that DIR1 possesses several sites that are critical for its function in long distance SAR signaling.

Acknowledgements

First and foremost I would like to thank my supervisor Dr. Robin K. Cameron for her unending encouragement over the years. She has taught me to grow as a researcher in a productive and supportive environment. We have also shared many laughs and fun times at the Phoenix, in her office or at her wonderful lab get togethers. You have made the lab seem like a family.

I would also like to thank my committee members Dr. Weretilnyk and Dr. Elliot who have always provided thoughtful comments and suggestions. Your honest and constructive feedback has always been appreciated. I would also like to thank Dr. Dan Yang for advice on homology modeling, Yifei Huang and Wilson Sung for their bioinformatics guidance, and Dr. Jocelyn Rose for helping us with the TNS experiments. Thank you also to Zohaib Ghazi for providing essential restriction enzymes.

My family has been an enormous source of strength for me and I would like to thank them as well. Thank you to The Isaacs, The Melases, and The Propers. A super thanks to husband Chris for always being interested in my research, for picking me up during late nights at the lab and for taking up the slack around the house while I was preparing for committee meetings, conferences, and writing my thesis. Thank you also to my unborn baby boy! Two brains are better than one when you are writing a thesis.

I would also like to thank past and present Cameronites: Philip C., May Y., Dan W., Jen F., Marc C., Jen C. Jean F. Jessie C., Zainab R., Nick N., Salima C., Dan D., and Matt, T. You have all been such wonderful lab mates and friends and I truly appreciate your help over the years. The lab is a very positive and fun filled environment because you are all such amazing people. Special thanks to Philip C. who has been my partner in crime for many projects. Dan W. and May Y. you are two of the kindest people I know and I have really enjoyed your company. Thanks also to Marc C. for being a great teacher and always having time for my questions.

Table of Contents

List of Figures

List of Tables

List of Abbreviations

µg	microgram
µl	microliter
5FLC	5-Formyltetrahydrofolate cycloligase
AA	Azelaic Acid
AId1	*Agd2-like defense response protein1*
Avr	Avirulence gene
AZI1	*Azelaic acid induced 1*
BLAST	Basic Local Alignment Search Tool
BSA	Bovine serum albumin
cDNA	Complementary DNA
Cfu	Colony forming units
Col-0	Columbia
DA	Dehydroabietinal
DHAP	Dihydroxyacetone Phosphate
DIR1	*Defective in Induced Resistance 1*
DMSO	Dimethyl sulfoxide
dpi	Days post inoculation
DTT	Dithiothreitol
EMBOSS	European Molecular Biology Open Software Suite
ER	Endoplasmic Reticulum
ETI	Effector-Triggered Immunity
ETS	Effector-Triggered Susceptibility
EYFP	Enhanced Yellow Fluorescent Protein
FAD7	*Fatty Acid Desturase7*
FMO1	Flavin-Dependent Monooxygenase1
G3P	Glycerol-3-Phosphate
GFP	Green Fluorescent Protein
Gus	β-glucuronidase
Hpi	Hours post inoculation
HR	Hypersensitive Response
HSF1	*heat shock factor TL1-binding factor1*
iLOV	Light, oxygen or voltage sensing domain
IP	Isoelectric Point
IPTG	Isopropyl β-D-1-thiogalactopyranoside
kDa	Kilo Dalton
LB	Luria Bertani media
ld	Leaf disc
LPC	Lysophosphatidylcholine
LTP	Lipid Transfer Protein
LTP2sw	*Lipid Transfer Protein 2 similar to wheat*

MAMPS	Microbe-Associated Molecular Patterns
MAPK	*Mitogen-Activated Protein Kinase*
MDG1	*Monogalactosyldiacylglycerol Synthase1*
MES	2-(N-morpholino)ethanesulfonic acid
MeSA	Methyl Salicylate
$MgCl_2$	Magnesium Chloride
MIQE	Minimum information for publication of quantitative real-time PCR experiments
ml	Milliliter
mM	Millimolar
MMLV-RT	Moloney Murine Leukemia Virus Reverse Transcriptase
MS	Murashige and Skoog
NCBI	National Center for Biotechnology Information
NEB	New England Biolabs
NO	Nitric Oxide
NPR1	*Nonexpresser of PR genes 1*
OD	Optical density
PA	Pipecolic Acid
PAMPS	Pathogen-Associated Molecular Patterns
PCR	Polymerase Chain Reaction
phiLOV	Photostable light, oxygen or voltage sensing domain
PMSF	Phenylmethanesulfonylfluoride
PR	Pathogenesis-Related Proteins
Psm	*Pseudomonas syringae pv. maculicola*
Pss	*Pseudomonas syringae pv. syringae*
Pst	*Pseudomonas syringae* pv. *tomato*
PTGS	Post translational Gene Silencing
PTI	PAMP-Triggered Immunity
qRT-PCR	Quantitative Real Time PCR
RIN4	*RPM1-interacting protein 4*
RNAi	RNA interference
ROS	Reactive oxygen species
rpm	Rotations per minute
SA	Salicylic Acid
SABP2	SA Binding Protein 2
SAR	Systemic Acquired Resistance
SDS	Sodium dodecyl sulfate
SFD1	*Suppressor of Fatty Acid Desaturase Deficiency 1*
SS	Signal Sequence

T3SS	Type III Secretion System
TAIR	The *Arabidopsis* Information Resource
TGA	TGACG Motif-Binding Factor
TGS	Transcriptional Gene Silencing
TMV	Tobacco Mosaic Virus
TNS	6,P-toluidinylnaphthalene-2-sulfonate
Tris	Tris(hydroxymethyl) aminomethane
wpg	Weeks post germination
Ws	Wassilewskija
XVE	Estrogen inducible promoter
YEP	Yeast Extract Peptone

Introduction

The continuing loss of arable land due to urban sprawl and changing climate conditions combined with an increasing world population is putting pressure on the world's food supply. To maintain food security the need to increase crop yields is critical. Approximately 30% of crops are lost to biotic stress each year in North and Central America (Oerke and Dehne, 2004). Manipulation of plant defense signaling pathways may provide a way to enhance the plant defense response, increasing crop yield and reducing our reliance on environmentally destructive pesticides. Unlike animals, plants lack an adaptive immune system composed of dedicated, circulating immune cells. Instead each plant cell relies on intricate networks of innate defense response pathways that allow effective and coordinated protection against pathogen ingress (Nürnberger et al., 2004; Dong and Spoel, 2013). Understanding plant defense responses may reveal targets to enhance plant resistance to pathogens.

1.1 Plant-Pathogen Interactions

Plants have several mechanisms of pathogen detection, including recognition of conserved molecules on the pathogen surface and identification of pathogen effector molecules that have been injected directly into the plant cell. However, upon discovery of infection these separate alarm systems converge on key hubs of plant resistance. One of these key hubs is the transcriptional regulator protein Nonexpresser of PR genes 1 (NPR1) which induces the expression of pathogenesis related (PR) genes. PR proteins are mediators of plant resistance and include proteins like β1-3 glucanase, chitinases and defensins which act as antimicrobial

compounds. Thus several plant disease-monitoring systems rely on a similar downstream network of defense proteins and molecules (Dong and Spoel, 2013). Below is a review of the plant disease recognition systems.

1.2 Basal and R Gene-Mediated Resistance

The interaction between the plant innate immune system and pathogens is a constant battle can be depicted by a "zigzag model" which describes the biological arms race between plant and pathogen (Figure 1.1) (Jones and Dangl, 2006).

Basal resistance is the first class of pathogen perception, providing non-specific resistance to a broad range of pathogens. Basal resistance includes constitutive defenses, such as barriers to pathogen ingress, for example the cuticle and cell wall. Basal inducible defenses are initiated when pathogen- or microbe-associated molecular patterns (PAMPs or MAMPs), for example flagellin, are recognized as non-self by pattern recognition receptors on the plant membrane initiating PAMP-triggered immunity (PTI) (Reviewed in Schwessinger and Zipfel, 2008 & Booler and He, 2009). Plant basal inducible defenses include the fortification of the cell wall by callose deposition (Boller and Gomez-Gomez, 1999), salicylic acid-dependent PR (Pathogenesis-Related) gene expression (Zeidler et al., 2004), as well as production of antimicrobial compounds. The phenolic plant hormone salicylic acid (SA) is an essential signaling compound in many defense responses including basal resistance (Vlot et al., 2009). SA signaling leads to activation of the transcription factor Nonexpresser of PR genes 1 (NPR1) leading to PR gene expression. Basal defense is effective against the majority of pathogens.

To counter this plant response, some bacterial pathogens have evolved a type III secretion system (T3SS) to inject effector proteins into the plant cell. These effector molecules promote pathogen virulence by interfering with plant basal resistance, resulting in effector-triggered susceptibility (ETS) (Reviewed in Jones and Dangl, 2006 & Cunnac et al., 2009). For example, *Pseudomonas syringae* pv *tomato* (*Pst*) avirulence effector protein, AvrRpt2, along with approximately 40 other effectors, is secreted into the *Arabidopsis* cell via the T3SS (Mudgett and Staskawicz, 1999). Once inside the *Arabidopsis* cell, the cysteine protease AvrRpt2 proteolitically cleaves RPM1-interacting protein 4 (RIN4), a plant defense protein whose cleavage products suppresses PTI (Afzal et al., 2011). RIN4 is targeted by several effectors (AvrRPM1, AvrB), illustrating its importance in plant immunity (Reviewed in Dodds and Rathjen, 2010). In addition, AvrRpt2 undermines plant disease resistance by proteolytically cleaving proteins involved in repression of the plant hormone auxin (Chen et al., 2007; Cui et al., 2013). Auxin accumulation antagonizes salicylic acid defense pathways (Wang et al., 2007) thereby compromising SA-dependent plant disease resistance and promoting pathogen growth.

It is believed that plants countered pathogen effectors by evolving the ability to detect pathogen virulence effectors using plant Resistance (R) receptors. If the plant receptor interacts directly or indirectly with the pathogen effector then R gene-mediated resistance also known as effector triggered immunity (ETI) is established (Jones and Dangl, 2001; Jones and Dangl, 2006). R gene-mediated resistance is characterized by elevated SA levels, PR gene expression and the hypersensitive response (HR) (Dodds and Rathjen, 2010). The HR is a form of plant-controlled programmed cell death that is thought to limit pathogen spread. The HR is

characterized by a calcium influx followed by an oxidative burst leading to production and release of two cell death signals: reactive oxygen species (ROS) and nitric oxide (NO) (Mur et al., 2008). If a plant R receptor interacts with a pathogen effector, fast and successful defense is inititated and the pathogen is considered avirulent. However, if the pathogen effector remains undetected then effector-mediated suppression of plant immunity allows pathogen proliferation and the pathogen is considered virulent. Several R receptors have been shown to monitor proteins important for plant defense and therefore targets of pathogen effectors. This R receptor protection of an effector target is known as the "guard hypothesis" (Jones and Dangl, 2001). For example, the plant R gene product, RPS2 indirectly recognizes the *Pst* AvrRpt2 pathogen effector protein (Kunkel et al., 1993). In *Arabidopsis,* the RPS2 R receptor protects the pathogen effector target RIN4 (Mackey et al., 2003). When AvrRpt2 mediates cleavage of the RIN4 protein, RPS2 senses this modification and quickly activates R gene-mediated resistance (Kim et al., 2005).

Finally, new pathogen effectors may evolve allowing the pathogen to circumvent basal or R gene-mediated resistance (Figure 1.1, panel 4). The nature of the plant-pathogen interaction leads to this back and forth evolution, selecting for new strategies to outcompete one another. The zig-zag model will likely continue as long as this interaction persists (Jones and Dangl, 2006).

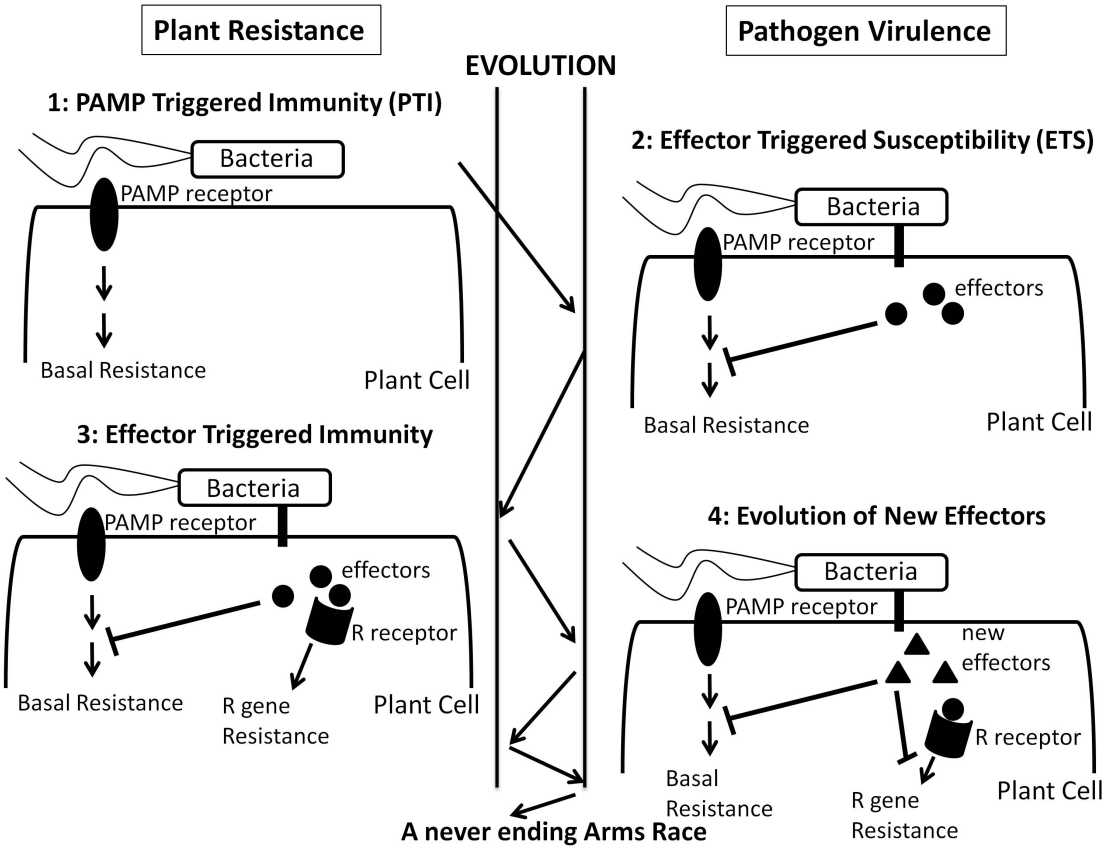

Figure 1.1: Illustration of the zig-zag model which summarizes the evolutionary arms race between plant and pathogen. This figure was loosely based on that found in (Jones and Dangl, 2006). First bacterial pathogen associated molecular patterns (PAMPS) such as flagellin are detected by plant PAMP receptor and trigger basal resistance or PAMP triggered immunity (PTI). Next, the pathogen employs a type III secretion system (T3SS) to inject susceptibility promoting effector molecules into the plant cell. These pathogen effectors reduce basal resistance leading to effector triggered susceptibility (ETS). Subsequently, the plant develops receptor molecules to identify effectors either directly or indirectly. If the plant receptor senses a pathogen effector then R-gene mediated resistance is triggered leading to effector triggered immunity (ETI). Next new pathogen effector molecules evolve allowing the pathogen to circumvent plant immune system. New effectors may target and suppress basal or R-gene mediated resistance. As long as there is selective pressure either from the plant or the pathogen, this arms race will continue on.

1.3 Systemic Acquired Resistance (SAR)

Systemic Acquired Resistance (SAR) is a plant defense response induced by an initial priming infection in one part of the plant that leads to broad-spectrum resistance to normally virulent pathogens in distant naïve tissues (Ross, 1961b). This resistance is long lasting (20 days in tobacco (Ross, 1961a), can prime subsequent generations in *Arabidopsis* (Luna and Ton, 2012; Luna et al., 2012; Slaughter et al., 2012)) providing rapid induced defense upon secondary infection. Studies using tobacco, cucumber and the *Arabidopsis* SAR models show that SAR occurs in four distinct stages: induction, long distance signaling, establishment and manifestation (Champigny and Cameron, 2009) (Figure 1.2).

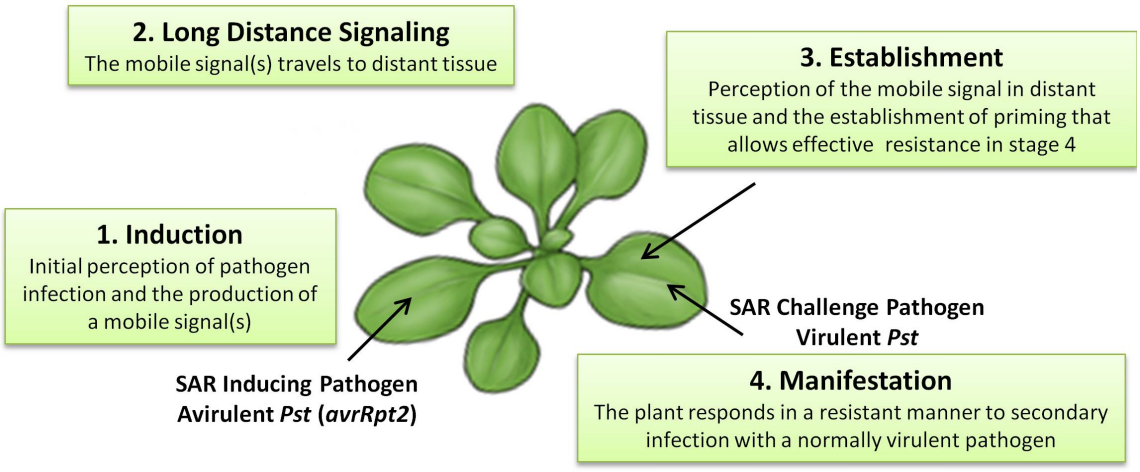

Figure 1.2: The four stages of SAR.

1.3.1 SAR Induction

The SAR induction phase is initiated by pathogen-induced cell death which could be caused by the HR as part of the plant ETI response or by virulent infections that cause necrosis (Reviewed in Kuc, 1982; Dong and Durrant, 2004). Originally it was believed that SAR was initiated only in response to pathogen-induced cell death. A recent study demonstrated that non-host pathogens and even exposure to MAMPs can trigger the SAR response in the absence of macroscopic cell death (Mishina and Zeier, 2007). However, microscopic cell death was not monitored during this study and therefore cell death may still be essential for SAR induction. Perception of a SAR-inducing pathogen is quickly followed by the accumulation of salicylic acid (SA) and expression of pathogenesis related (PR) proteins. The degree of SA accumulation and PR gene expression depends on the pathogen used. Some virulent pathogens that suppress plant defense induce less SA accumulation and PR gene expression compared to avirulent pathogens but SAR is induced to both (Reviewed in Dong and Durrant, 2004). A SAR long distance signal is produced and/or activated and begins its journey to distant leaf tissue.

1.3.2 Movement of the SAR Long Distance Signal

In the second stage of SAR, the mobile signal travels to distant tissue. The *Arabidopsis-Pst* (Cameron et al., 1994), tobacco-*Tobacco mosaic virus* (*TMV*) (van Loon and Dijkstra, 1976) and cucumber-*Pseudomonas syringae pv. syringae* (*Pss*) (Smith et al., 1991b) models have served as systems for the investigation of the SAR mobile signal. Seminal

studies by Kus and Jenns (1979) showed that cucumber contained a long distance graft transmissible signal that traveled from SAR-induced rootstocks (bottom of the plant) into a grafted scion (upper grafted plant) to initiate SAR (Jenns and Kuc, 1979). The SAR signal likely moves either through the phloem and/or cell-to-cell. This is supported by girdling experiments in tobacco and cucumber where phloem and cell-to-cell movement are reduced and this resulted in the elimination of SAR (Guedes et al., 1980; Tuzun and Kuc, 1985). Cucumber, tobacco and *Arabidopsis* may have differing routes for SAR signal movement based on the amount of time it takes for the SAR signal to travel to distant tissues. The cucumber SAR signal is transported very rapidly to distant tissues. Cucumber leaf detachment studies showed that the SAR signal left SAR-induced local tissue 4 hours after inoculation and SAR was established by 24 hours in distant tissues (Smith et al., 1991a). This suggests that cucumber may rely on rapid movement via the phloem rather than slower cell-to-cell movement. Full establishment of SAR in tobacco takes 7 days (Ross, 1961a), however, putative Tobacco SAR signal methyl salicylate accumulates in the phloem by 48hpi (Park et al., 2007) and SAR-induced tobacco leaves can be detached 60 hours after inoculation. This suggests tobacco may rely on phloem movement but SAR establishment in distant tissues is slow. In *Arabidopsis,* the SAR signal moves out of the induced leaf within 4-6 hours (Truman et al., 2007; Chaturvedi et al., 2012) but it takes 36-48 hours for the SAR signal to prime distant tissues (Cameron et al., 1994). This may suggest some combination of phloem and cell to cell movement. This is supported by Kiefer et al. (2003) who examined SAR signal movement in relation to source and sink phloem connections (orthostichies) in *Arabidopsis* rosette leaves. They found that SAR was

established in leaves inside and outside of the phloem connection patterns (orthostichies) suggesting that in *Arabidopsis* the SAR signal may move cell-to-cell as well as through the phloem (Kiefer and Slusarenko, 2003).

1.3.2.1 Salicylic Acid is not likely the SAR mobile signal

The phytohormone salicylic acid (SA) is required for SAR establishment as SA deficient mutants such as *sid2* and *NahG* are SAR-defective (Gaffney et al., 1993; Delaney et al., 1994; Vernooij et al., 1994; Lawton et al., 1995). Initially, SA was considered to be a candidate for the Cucumber and Tobacco SAR mobile signal (Malamy et al., 1990; Metraux et al., 1990). However, a series of elegant tobacco grafting experiments demonstrated that SA-deficient *NahG* rootstocks that were induced for SAR produced the mobile signal and induced SAR in grafted wild type scions, suggesting that SA is not required for the production and propagation of a mobile signal (Vernooij et al., 1994). Moreover, in a series of clever experiments in cucumber Rasmussen et al. (2001) severed the primary inoculated leaf at various time-points to collect highly enriched phloem sap from the petiole ends. They showed that SA did not enter the phloem until 8 hours post inoculation but SAR-induced leaves severed after only 6 hours induced SAR in upper leaves. This suggests that the SAR signal moves out of the induced leaf before SA (Rasmussen et al., 1991). These experiments helped to show that although essential for SAR establishment in distant tissues, SA is probably not a SAR mobile signal candidate.

Several SAR mobile signal candidates have been proposed including the lipid transfer protein DIR1 (Maldonado et al., 2002), methyl

salicylate (MeSA) (Park et al., 2007; Vlot et al., 2008; Liu et al., 2011b), a lipid derived glycerol-3-phosphate (G3P) derivative (Chaturvedi et al., 2008; Chanda et al., 2011), azelaic acid (AA) (Jung et al., 2009), pipecolic acid (PA) (Navarova et al., 2012), and dehydroabietinal (DA) (Chaturvedi et al., 2012) (Signals reviewed in Dempsey and Klessig, 2012; Fu and Dong, 2013; Shah and Zeier, 2013). Figure 1.3 illustrates the structure of the putative SAR long distance signals and shows that all of these molecules have hydrophobic and hydrophilic regions.

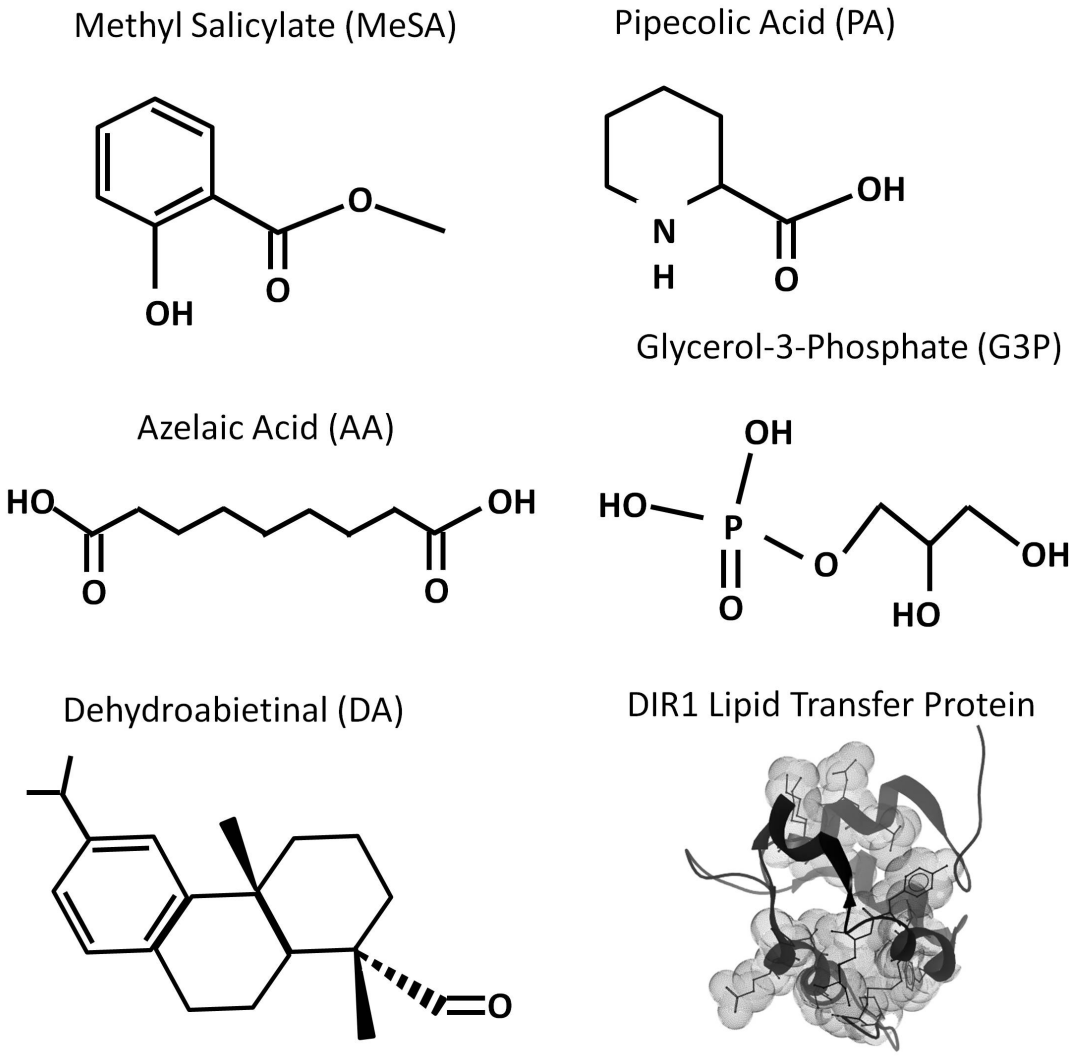

Figure 1.3: Candidate mobile SAR signals.

1.3.2.2 Defective in Induced Resistance 1 (DIR1)

In a genetic screen of a T-DNA-tagged population of Wassilewskija (Ws) *Arabidopsis* plants (11,000 lines), *dir1-1* (*defective in induced resistance 1-1*) was identified (Maldonado et al., 2002). The *dir1-1* mutant was competent in both basal resistance and R gene-mediated resistance, making *dir1-1* the first mutant specifically compromised in SAR (Maldonado et al., 2002). The *dir1-1* mutant is competent for the first stage of SAR, induction, however, the absence of PR1 expression and SAR establishment in distant leaves suggests that DIR1 may be involved in long distance signaling or signal perception (Maldonado et al., 2002). Protein gel blot analysis demonstrated that DIR1 accumulates in phloem sap-enriched petiole exudates collected from SAR-induced wild type, but not mock-induced, wild type, or *dir1-1* leaves. Furthermore, petiole exudates collected from SAR-induced wild type plants were able to induce PR1 gene expression in the distant leaves of the *dir1-1* mutant suggesting that *dir1-1* is competent to establish SAR in distant tissue if the missing phloem mobile molecule is provided (Maldonado et al., 2002). Taken together, this data suggests that DIR1 is involved in SAR long distance signaling. However, the presence of DIR1 is not sufficient to activate SAR as transgenic plants expressing high levels of DIR1 do not display enhanced resistance without pathogen exposure (Maldonado et al., 2002) This suggests that pathogen exposure is essential for DIR1 activation during SAR (Maldonado et al., 2002).

DIR1 movement was previously monitored by probing local or distant petiole exudates with a DIR1 antibody. Petiole exudates collected from locally treated and distant leaves of SAR-induced versus mock-inoculated plants are lyophilized and subjected to protein gel blot analysis. DIR1 was found in SAR-induced but not mock exudates

(Champigny et al., 2013). The constitutive plant wide expression of DIR1 (Champigny et al., 2011) hampered efforts to monitor movement since protein detected in petiole exudates may not have originated from the SAR-induced leaf but from the petiole tissues themselves.

DIR1 encodes a putative lipid transfer protein (LTP) (Maldonado et al 2002), part of the LTP2 family (Lascombe et al., 2008). Plant LTP proteins have been grouped into two families, LTP1 and LTP2 (Reviewed in Carvalho and Gomes, 2007). Both share 8 conserved cysteine residues that participate in four disulfide bonds that stabilize the central hydrophobic cavity, however the cysteine bond pairing is different between the two groups (Douliez et al., 2001). In addition, LTP1 proteins are larger (9 kDa) compared with LTP2 proteins (7 kDa). Both LTP1 and LTP2s contain N-terminal signal sequences that are predicted to target these proteins for secretion to the cell wall. Several LTPs have been shown to be targeted to the apoplast *in vivo* including DIR1 (Thomas et al., 1993; Pyee et al., 1994; Champigny et al., 2011). Using fluorescence and X-ray diffraction studies, Lascombe et al. found that DIR1 has unique features which set it apart from other LTP2s (Lascombe et al., 2008). For example, DIR1 has an acidic IP (isoelectric point) while most LTP2 proteins have a basic IP. Additionally, DIR1 is able to bind two parallel mono-acylated lipids in its active site (Lascombe et al., 2008). In comparison, a wheat LTP2 was crystallized with two L-α-palmitoyl-phosphatidyl glycerol molecules, however these lipids entered the hydrophobic cavity from opposite ends in a tail-to-tail arrangement (Hoh et al. 2005). The only other LTP2 whose structure has been solved is a rice LTP2 (Samuel et al., 2002) which was crystallized without a ligand. Thus it remains to be determined if the side by

side binding of two mono-acylated lipids is unique to DIR1 or a common feature of LTP2 proteins.

1.3.2.3 Methyl Salicylate (MeSA)

Although SA is probably not a mobile SAR signal, the conjugated form, methyl salicylate (MeSA) may participate in long distance signaling. Park et al. (2007) hypothesize that SA is converted to MeSA by SA methyl transferase (NtSAMT1 or AtBSMT1) in local SAR-induced tissue and travels through the phloem to distant tissue where it is converted back to SA by SALICYLIC ACID BINDING PROTEIN 2 (SABP2), leading to SAR establishment (Figure 1.3). This is based on tobacco grafting experiments that show that SABP2 is required in distant tissue to respond to the SAR signal (Park et al., 2007) and that the tobacco SABP2 mutant and a triple mutant of *Arabidopsis* SABP2 orthologs (AtMES 1, 7 and 9) are both SAR-defective (Kumar and Klessig, 2003; Park et al., 2007; Vlot et al., 2008). Tobacco contains a single SABP2 protein while *Arabidopsis* has three. Furthermore, addition of a SABP2 inhibitor to distant tissue in tobacco and *Arabidopsis* inhibited the SAR response (Park et al., 2009). Contradictory evidence by Attaran et al. (2009) showed that in *Arabidopsis* most locally produced MeSA is released to the atmosphere as a volatile molecule and that an MeSA production mutant *bsmt1* is SAR competent suggesting that MeSA is not required for the SAR response (Attaran et al., 2009). However, Liu et al. discovered that the hours of light received after infection affects MeSA participation during SAR and suggest that this may account for different results obtained by various labs (Liu et al., 2011a). Exogenous application of MeSA induced SAR in wild type but not *dir1-1* mutant plants suggesting that MeSA-activated SAR requires DIR1 (Liu et al., 2011b). Liu et al. (2011)

show that *dir1-1* mutants have elevated AtBSMT1 expression in both induced and distant tissues suggesting that DIR1 may be required to balance SA to MeSA ratios during SAR. DIR1 may reduce AtBSMT1 levels in distant tissues to reduce reconversion of SA to MeSA, thereby preventing reduction in SA levels and allowing a low accumulation (less than 2-fold) of SA required for SAR establishment (Delaney et al., 1995; Lawton et al., 1995; Cameron et al., 1999).

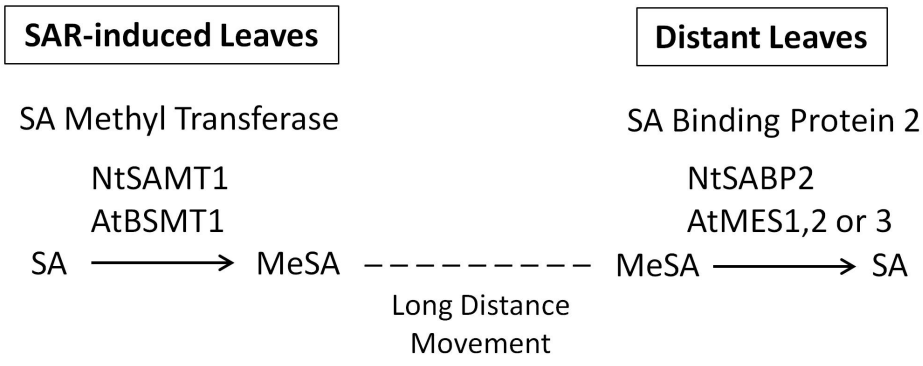

Figure 1.4: Illustration of enzymes involved in maintaining the balance of SA and MeSA in SAR-induced and distant leaves. In SAR-induced leaves SA methyl transferase (NtSAMT1 in tobacco and AtBSMT1 in *Arabidopsis*) convert SA into the putative SAR long distance signaling molecule MeSA. MeSA is thought to travel to distant tissues where SA Binding Protein 2 (NtSABP2 in tobacco and AtMES1,2 or3 in *Arabidopsis*) converts MeSA back into SA where it participates in SAR.

1.3.2.4 A lipid derived glycerol-3-phosphate (G3P) derivative

Evidence that a lipid-derived molecule is required for SAR emerged from the discovery of the SAR-deficient *suppressor of fatty acid desaturase deficiency 1* (*sfd1*) mutant. *SFD1* encodes an *Arabidopsis* dihydroxyacetone phosphate (DHAP) reductase involved in lipid metabolism (Nandi et al., 2004). Nandi et al. (2004) showed that the *sfd1* mutant appears to be wild type for SAR induction, but defective in establishment of SAR in distant tissues. Mutations in two other enzymes also required for plastid localized glycerolipid synthesis, *fatty acid desaturase7* (*fad7*) and *monogalactosyldiacylglycerol synthase1* (*mgd1*), resulted in SAR-deficient phenotypes providing additional evidence of lipid involvement during SAR (Chaturvedi et al., 2008). Unlike SAR-induced petiole exudates collected from wild type plants, SAR-induced petiole

exudates from *sfd1*, *fad7*, and *mgd1* single mutants were unable to induce SAR when applied to wild type plants suggesting that *sfd1*, *fad7*, and *mgd1* exudates lacked SAR-inducing activity. However SAR-inducing activity was restored when mixed with petiole exudates from *dir1-1* plants. This suggests that the SAR-defective phenotype of these mutants is derived from their inability to produce a SAR signal, and that a lipid derived signal and DIR1 are both required for long distance signaling and are mobilized into the phloem independently (Chaturvedi et al., 2008). A mutagenesis study of *SFD1* revealed that its dihydroxyacetone phosphate (DHAP) reductase activity and its targeting to the chloroplast are both required for its participation in SAR (Lorenc-Kukula et al., 2012).

SFD1 reductase converts dihydroxyacetonephosphate to glycerol-3-phosphate (G3P), the precursor molecule in plastid glycerolipid synthesis. Studies with G3P indicate that when mixed with SAR-induced or mock-inoculated wild-type petiole exudates it is an inducer of SAR in *Arabidopsis* and soybean (Chanda et al., 2011). This suggests that G3P requires a component present in untreated petiole exudates for SAR-inducing activity. When G3P is mixed with petiole exudates from the *dir1-1* mutant, SAR is not established suggesting that SAR activation by G3P requires DIR1 (Chanda et al., 2011). Furthermore, when G3P is mixed with wild-type exudates (SAR-induced or uninduced) and inoculated into *dir1-1* (Chanda et al., 2011) or *azi1* plants, SAR is not established suggesting that G3P requires both DIR1 and AZELAIC ACID INDUCED1 (AZI1) for SAR establishment (Yu et al., 2013). AZI1 is upregulated by another potential SAR mobile signal and will be discussed in the next section.

Chanda et al. predicted that G3P movement required DIR1 and conducted several experiments to test this hypothesis. Exogenously

applied radiolabeled G3P did not move on its own but required coinfiltration with recombinant DIR1 protein and was detected as a derivative in distant tissues (Chanda et al., 2011). However, Chanda et al. (2011) failed to test if the recombinant DIR1 protein made in *E.coli* was folded properly. Additionally, the level of DIR1 protein applied may have induced cell death and cell death has been shown to induce SAR possibly accounting for G3P movement. In addition G3P was tested for its ability to cause DIR1 movement in tobacco by co-infiltration of *Agrobacterium* transiently expressing DIR1-RFP and TMV movement protein tagged with GFP. Although not clearly stated, it is assumed that TMV movement protein-GFP is used as a plasmodesmata marker to show that DIR1 is traveling through the phloem plasmodesmata. However, TMV movement protein is known to affect plasmodesmata size exclusion limits (Wolf et al., 1989) by modifying the cytoskeleton (Liu and Nelson, 2013) and therefore is a poor choice of marker for DIR1 movement through the plasmodesmata as it could enhance movement. In addition, this group failed to include a random similarly sized protein as a control to ensure that the addition of TMV movement protein did not cause all proteins to move through the plasmodesmata. Therefore additional evidence is required to determine if G3P moves to distant tissue and if this movement is dependent on DIR1. G3P synthesis may be regulated by DIR1 and AZI1 as mutants in these genes are compromised in G3P production during SAR (Yu et al., 2013). Therefore Chanda et al. hypothesize that a derivative of G3P is a mobile SAR signal.

1.3.2.5 Azelaic Acid (AA)

Screening petiole exudates for accumulation of small molecules that may participate in long distance signaling led to the discovery that azelaic acid (AA) is enriched 6-fold in petiole exudates from leaves SAR-induced with avirulent *Pseudomonas syringae pv. maculicola* (*Psm*DG6-*avrRpt2*) compared to mock-inoculated leaves (Jung et al., 2009). Elevated levels of AA in SAR-induced exudates led to the idea that AA maybe involved in SAR long distance signaling. Therefore Jung et al. tested AA's SAR-inducing potential by spraying plants. At concentrations higher than 10 μM AA treatment enhanced resistance to virulent *Psm*DG6 in both local and distant leaves (Jung et al., 2009). Isotopically labeled AA traveled from leaves where it was applied to distant tissues suggesting that it is mobile (Jung et al., 2009). AA treatment induced resistance in *sfd1* and *fad7* mutant plants suggesting that AA and the lipid-derived molecule are likely independent SAR signals. However, AA did not induce SAR in the *dir1-1* mutant, suggesting that DIR1 is required for AA-induced resistance. It is important to note that AA application does not cause elevated levels of SA or PR gene expression compared to mock-inoculated plants until after secondary infection. Therefore Jung et al. hypothesize that AA is involved in the priming/establishment phase of SAR.

AA treatment induced modest upregulation of *AZI1* (1.8-fold), an LTP1-type LTP (Jung et al., 2009). The *azi1* mutant is defective in establishing resistance in response to AA application. Jung et al. demonstrated that petiole exudates collected from SAR-induced *azi1* leaves do not contain the SAR mobile signal(s), but application of SAR-induced wild-type petiole exudates to *azi1* can establish SAR. Thus, *azi1* mutant is competent for SAR induction, but defective in establishing SAR in distant tissues in response to pathogen infection. This suggests that like

DIR1, AZI1 is involved in production or translocation of a SAR long distance signal. Using bimolecular fluorescence complementation and co-immunoprecipitation, DIR1 and AZI1 were shown to form homo and heterodimers in tobacco (Yu et al., 2013). Furthermore, overexpression of *DIR1* in *azi1* and overexpression of *AZI1* in *dir1-1* complemented the SAR-defective phenotypes of these mutants (Yu et al., 2013).

Recently several studies have questioned the importance of AA. Zoeller et al. (2012) found that AA increased in local leaves inoculated with avirulent *Pst* (*avrRpm1*) but, unlike Jung et al. (2009) this group did not find any elevation in AA levels in distant tissues. In addition, Zoeller et al. (2012) could not replicate the finding that exogenous AA application induced resistance in response to virulent *Pst*. Furthermore, they point out that there is a lack of genetic evidence for the involvement of AA in SAR in that no AA deficient mutant has been shown to be SAR-defective (Zoeller et al., 2012). This group provides evidence that AA is a byproduct and marker of lipid oxidation and fragmentation initiated by pathogen-associated oxidative stress. Navarova et al. found that AA did not increase in petiole exudates when SAR was induced by virulent *Psm* ES4326 (Navarova et al., 2012). Variability in the SAR response due to differing environmental conditions or differences in pathogens used have been reported. Jung et al. induced plants for SAR with avirulent *Psm*DG6 (*avrRpt2*) and distant leaves were inoculated with virulent *Psm*DG6. Zoeller et al. induced plants for SAR using avirulent *Pst* (*avrRpm1*) and distant leave were inoculated with virulent *Pst*. Navarova et al. induced for SAR using virulent *Psm*ES4326. Thus, there is no consistency in the use of pathogens between these experiments which could account for some of the differences observed. Together this data suggests that AA is involved

in distant leaves in the priming stage, but it may not be essential in the SAR response induced by all *Pseudomonas* pathovars.

1.3.2.6 Pipecolic Acid

Comparisons of free amino acid content in mock- versus SAR-induced (virulent *Psm* ES4326) *Arabidopsis* leaves revealed an accumulation of lysine, as well as a 70-fold increase in the lysine catabolite, pipecolic acid (PA) (Navarova et al., 2012). PA levels were also elevated in leaves inoculated with avirulent *Psm* ES4326 (*avrRpm1*) or the PAMP, flagellin (flg22). The increase in PA in local leaves led Navarova et al. to wonder if this amino acid might act as a SAR long distance signal and travel to distant tissues. This group observed elevated PA in exudates collected from SAR-induced compared to mock-inoculates leaves. PA levels were 10-fold higher in distant leaves of SAR-induced compared to mock-inoculated plants. Watering with PA resulted in resistance to virulent *Psm* in distant leaves. Enhanced resistance after PA application was not observed in *fmo1*, *sid-2* or *npr1* mutants suggesting that PA functions upstream of FM01 and SA during SAR establishment. The *flavin-dependent monooxygenase1* (*fmo1*) mutant is impaired in SA accumulation and SAR establishment in distant leaves and *FM01* is upregulated in local and distant leaves in response to virulent or avirulent pathogen infection (Mishna and Zeier, 2006). FMO proteins have been shown to detoxify xenobiotics in animal systems (moth and human) (Schlaich, 2007) and therefore Mishna et al. (2006) suggest that FMO1 may detoxify pathogen compounds. An alternative hypothesis is that FMO1 participates in modifying the redox state of the plant during the infection

process (reviewed in Schlaich, 2007). Both ideas require further investigation. PA also accumulated after virulent pathogen infection in tobacco leaves and similar to *Arabidopsis*, root application of PA enhanced resistance to virulent and non-host pathogens (Vogel-Adghough et al., 2013). Navarova et al. demonstrated that the SAR-defective mutant *agd2-like defense response protein1* (*ald1*) (Song et al., 2004) produced little PA in untreated or SAR-induced leaves. The ALD1 aminotransferase is known to convert lysine to PA *in vitro* and Navarova et al. hypothesize that ALD1 is responsible for converting lysine to PA during SAR. When the *ald1* mutant was watered with PA, SAR to virulent *Psm* was restored and PA was detected in distant tissues (Navarova et al., 2012). This suggests that PA is mobile, a key characteristic of a SAR long distance signal. Many putative SAR signals require functional DIR1 to induce SAR in distant tissues. It would be informative to examine the requirement of DIR1 for PA activity, however this has yet to be tested.

1.3.2.7 Dehydroabietinal (DA)

Dehydroabietinal (DA) was identified by screening SAR active fractions of petiole exudates collected from SAR-induced *Arabidopsis* leaves (Chaturvedi et al., 2012). When applied to *Arabidopsis*, tobacco and tomato, DA (1 pM) acts as a powerful inducer of SAR. In *Arabidopsis,* DA induced resistance in distant tissues to virulent *Psm*, virulent *Pst* and the fungal pathogen *Fusarium graminearum* (Chaturvedi et al., 2012). Leaf detachment experiments revealed that resistance in distant tissues was observed as little as 30 minutes after DA application. Radiolabeled DA applied to plants quickly migrated thoughout the plant reaching distant leaves within 15 minutes suggesting that DA may act as a mobile SAR

signal. Interestingly, DA is present in mock- and SAR-induced *Arabidopsis* petiole exudates, however, after SAR induction there is a shift from low molecular weight DA-containing complexes (30kDA) to high molecular weight DA-containing complexes (100kDa). This observation suggests a SAR-activating DA modification is necessary for SAR activity. Exogenously applied radiolabeled DA was recovered in distant leaves as a high molecular weight complex, suggesting that DA was incorporated into a complex after application. DA present in high molecular weight complexes is trypsin-sensitive indicating proteins are present in the complex. DA treatment induces increased SA and PR gene expression in distant leaves. DA-induced resistance is dependent on SA as DA application to *nahG* and *npr1* induced little resistance in distant tissues. DIR1 and AZI1 are required for the DA-induced resistance and DA appears to be upstream of FM01. DA is capable of inducing resistance in MeSA and AA production mutants albeit to a lesser extent than wild type, suggesting a synergistic multi-signal interaction between DA, MeSA and AA is required to fully activate SAR (Chaturvedi et al., 2012).

1.3.2.8 DIR1-like

The occasional appearance of a DIR1-sized band in protein gel blots of *dir1-1* exudates and the rare partial SAR$^+$ phenotype in *dir1-1* led us to believe that a DIR1-like protein may be recognized by our antibody and occasionally participate in SAR. A Basic Local Alignment Search using the NCBI database of the DIR1 coding sequence revealed the *DIR1-like* locus adjacent to *DIR1* on chromosome 5 (Champigny et al., 2011). DIR1 (At5g48485) and DIR1-like (At5g48490) are 88% similar at the amino acid level and yet only the *dir1-1* mutant was identified in a forward genetic mutant screen (Maldonado et al., 2002). To investigate the ability

of DIR1-like to participate in SAR, the Cameron lab developed the Agro-SAR assay (Figure 1.5). *Agrobacterium tumefaciens* transfers its T-DNA into *Arabidopsis* cells where the T-DNA-encoded genes are expressed transiently before integration of the T-DNA into the *Arabidopsis* genome (Wroblewski et al., 2005). In the Agro-SAR assay, *Agrobacterium* T-DNA is used to transiently express a protein of interest in one leaf of *Arabidopsis dir1-1* followed by inoculation of the same leaf with a SAR-inducing pathogen. Distant leaves are inoculated two days later with virulent *Pst* and the ability of the expressed protein to complement the SAR defect in *dir1-1* can be assessed (Figure 1.1). Using *Agrobacterium*-mediated transformation Champigny et al. expressed 35S:DIR1-like in the *dir1-1* mutant to investigate DIR1-like involvement in SAR (Champigny et al., 2011). Unlike the EYFP alone control, *Agrobacterium*-mediated expression of DIR1-like complemented the *dir1-1* SAR defect. Thus DIR1-like can complement the *dir1-1* mutation when transiently expressed by *Agrobacterium*, suggesting that DIR1-like is capable of participating in SAR (Champigny et al., 2011).

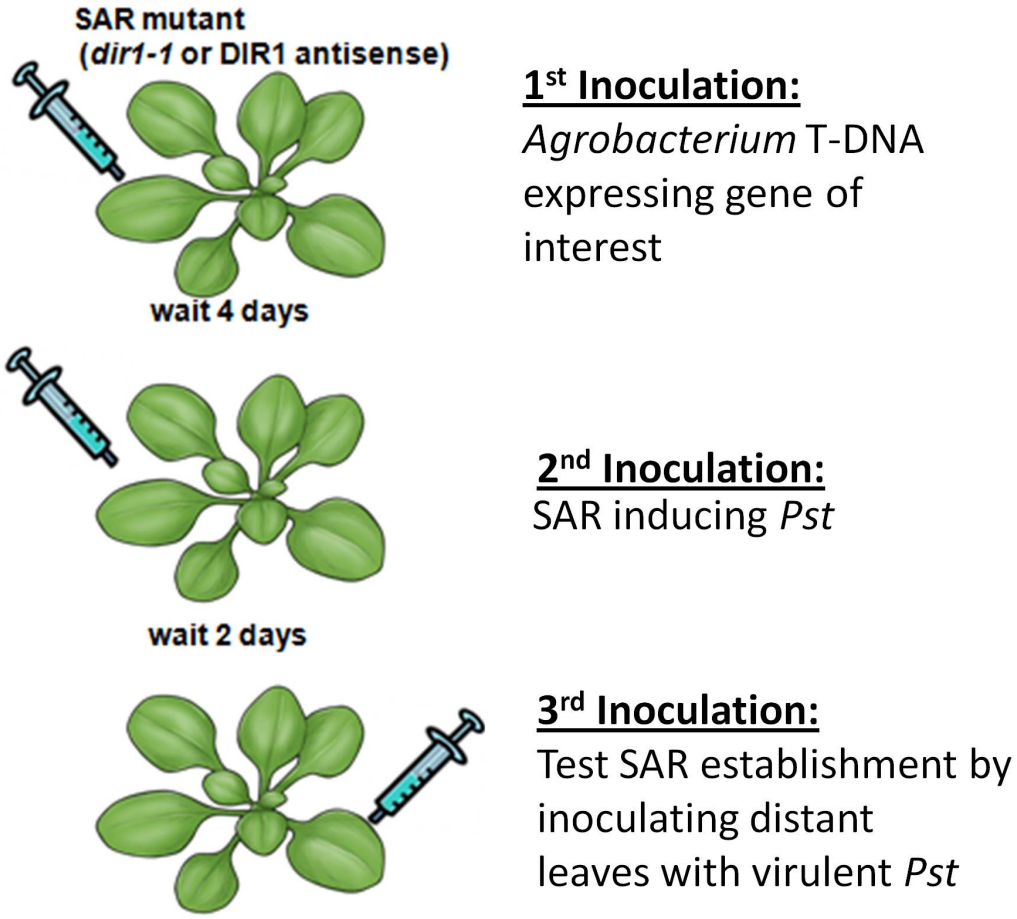

Figure 1.5: Illustration of the Agro-SAR assay. First, *Agrobacterium* is inoculated into two lower leaves. The second inoculation occurs four days post *Agrobacterium*-inoculation in the same leaves with either 10 mM $MgCl_2$ (Mock-inoculation) or *Pst* (*avrRpt2*) to induce SAR (SAR-induced). After two more days the third inoculation occurs, where the upper leaves are inoculated with virulent *Pst*. Three days post inoculation (dpi) *in planta* bacterial levels of *Pst* in distant leaves are determined.

1.3.3 SAR Establishment in Distant Tissues

The establishment phase involves perception of the mobile signal in distant tissue leading to priming, which allows the plant to respond rapidly and effectively to future pathogen attack. Champigny and Cameron (2009) postulated that an unknown receptor interacts with the mobile signal(s) to initiate SAR establishment (Champigny and Cameron, 2009). Upon recognition of the SAR signal, distant leaves accumulate SA leading to PR gene expression. This is a modest response, typically in the ~2-fold range when comparing mock vs. SAR-induced *Arabidopsis* (Delaney et al., 1994; Lawton et al., 1995; Cameron et al., 1999). SA signal transduction during priming in distant leaves is mediated through several key SAR proteins. The transcription factor NPR1 is critical for SAR establishment and evidence suggests that SA may bind directly to NPR1 (Wu et al., 2012) and its paralogs (Fu et al., 2012; Wu et al., 2012) to stabilize and help activate the protein during SAR. Available evidence indicates that in naïve plants NPR1 exists as a cytosolic oligomer held together by disulfide bonds. Upon arrival of the SAR signal, elevated SA leads to NPR1 migration into the nucleus through redox elicited reduction of disulfide bonds to create an NPR1 monomer (Mou et al., 2003). NPR1 interacts with TGACG Motif-Binding Factor (TGA) (Zhou et al., 2000) and NIMIN (Weigel et al., 2001) transcription factors to coordinate SAR transcriptional reprogramming. From this stage, the SAR signal pathway appears to be complicated by feedback loops, non-linear pathways, and overlaps with several other defense pathways making the exact series of events difficult to decipher. However, using an elegantly designed microarray experiment Wang et al. identified many of the gene targets of NPR1 (Wang et al., 2005). The targets of NPR1 include small PR proteins (14-30 kDa) generally destined for the secretory system. Several of these proteins have been characterized (

β1-3 glucanase, chitinases and defensins) and act as antimicrobial compounds *in vitro*. Other downstream targets include secretory system genes (ER-related) which are believed to be important for PR protein secretion (Wang et al., 2005) and heat shock factor TL1-binding factor1 (HSF1) which is believed to be involved in a shift from active growth to defense (Pajerowska-Mukhtar et al., 2012). This is thought to occur to allow the plant to direct energy to disease resistance rather than to growth and development. Unlike wild-type plants, the *hsf1* mutant is compromised in defense and it shows no inhibition of growth during infection, demonstrating its involvement the growth-to-defense shift.

During SAR, constitutive expression of defense in distant tissues would be energetically expensive with high costs to plant fitness (van Hulten et al., 2006). This may explain why SAR response does not lead to constitutive expression of defense, but rather distant tissue becomes primed allowing the plant to respond to subsequent pathogen infection in a rapid and effective manner compared to uninduced or naïve tissue. Bekers et al. (2009) demonstrated that the defense-related Mitogen-Activated Protein Kinases (MAPK) 3 and 6 accumulate in an inactive state during SAR establishment or priming and become activated during the SAR manifestation stage (Beckers et al., 2009). During SAR initiated by *Pst* (*avrRpt2*), MAPK3 transcripts accumulate. During the manifestation stage after inoculation with virulent *Psm*, MAPK3 and 6 phosphorylation is enhanced compared to proteins from mock- inoculated plants. In addition, MAPK3 and 6 mutants are unable to establish SAR (Beckers et al., 2009). Epigenetic modifications to amplify transcriptional responses to secondary infection have also been investigated. Epigenetic modifications are known to occur post *Pst* infection or SA application

(Dowen et al., 2012). Covalent modification of histones by acetylation or methylation is known to repress or enhance gene transcription by altering the nucleosome structure reducing or enhancing access of transcription factors to chromatin. For example, *Psm* inoculation triggered chromatin modification of the promoter region of WRKY defense genes and these epigenetic changes led to more rapid induction upon secondary stress than naïve plants without WRKY chromatin modifications (Jaskiewicz et al., 2011). These are also studies providing evidence that this molecular memory is transferred to the next generation providing increased resistance to progeny plants (Luna and Ton, 2012; Luna et al., 2012; Slaughter et al., 2012). Luna et al. showed that PR1 gene expression was faster in descendents of primed plants and that this faster expression was associated with chromatin modifications in the PR1 promoter.

1.3.4 Manifestation of SAR

Lastly, SAR is manifested when the plant responds in a resistant manner to a secondary infection with a normally virulent pathogen. Primed plants respond to subsequent infections with robust SA accumulation and PR gene expression compared to non-primed plants. In the *Arabidopsis-Pst* SAR model, an initial infection with avirulent *Pst* leads to resistance to virulent *Ps pv. tomato* and virulent *Ps* pv. *maculicola* (Cameron et al., 1994).

1.4 *Arabidopsis-Pseudomonas syringae* pv *tomato* SAR Model System

Arabidopsis thaliana, a member of the *Brassicaceae* (Mustard) family, has become a model organism for plant biology. Its small fully sequenced genome (120Mb) (Theologis et al., 2000), fast generation time

(8 to 12 weeks), small size and ability to self fertilize make it very amenable to molecular and genetic research. In addition it is easily transformed by the natural genetic engineer *Agrobacterium tumefaciens*. *Arabidopsis* can be infected by a diverse set of pathogens; bacteria (*Pseudomonas syringae*, *Ralstonia solanacearum*, *Xanthamonas campestris*), fungi (*Colletotrichum destructivum, Botrytis cinerea*), an oomycete (*Hyaloperonospora arabidopsidis*), viruses (*Turnip Crinkle Virus, Cauliflower mosaic virus*), and nematodes.

Pseudomonas syringae is a gram negative bacterium that lives as an epiphyte on plant leaf surfaces before entering through wounds or stomata where it multiplies in the intercellular space (Katagiri et al., 2002). A hemibiotroph, it can proliferate in both living and dead tissue. Upon infection *Pseudomonas syringae* proliferates as a biotroph in living plant tissue but later in its life cycle the bacteria switches to necrotrophic form of growth, killing plant cells and escaping to the leaf surface for dissemination (Xin and He, 2013). *P. syringae* pv. *tomato* DC3000 (*Pst* DC3000) (Whalen et al., 1991) and *P. syringae* pv. *maculicola* ES4326 (*Psm* ES4326) (Dong et al., 1991) have become widely used to study plant-pathogen interactions including systemic acquired resistance in *Arabidopsis*. The *Arabidopsis-Pseudomonas* SAR pathosystem has become a popular model for the study of SAR (Cameron et al., 1994). To avoid a lengthy natural inoculation, *Pst* DC3000 (*avrRpt2*) is artificially pressure-inoculated through the stomata and into the intercellular space. Here *Pst* (*avrRpt2*) secretes effectors directly into the plant cell including AvrRpt2. AvrRpt2 is recognized by the plant RPS2 receptor and the HR is initiated followed by SAR. It takes 36 to 48 hours to produce, move and perceive SAR mobile signals in distant leaves (Cameron et al, 1994). Therefore after

two days distant uninoculated leaves are inoculated with virulent *Pst* and quantification of *Pst* growth *in planta* is determined three days later. SAR competence is monitored by comparing *Pst* levels in mock- versus SAR-induced plants.

1.5 Cucumber-*Pseudomonas syringae* pv *syringae* SAR Model System

In the 1980s and 90s cucumber was used as a model for SAR. Several cell death-inducing pathogens were found to induce SAR, either by pathogen-induced necrosis or plant-induced HR. These pathogens included *Pseudomonas lachrymans*, *Colletotrichum lagenarium* (Caruso and Kuc, 1979), tobacco necrosis virus (Jenns and Kuc, 1979), and *Pseudomonas syringae* pv *syringae* (Smith et al., 1991a). Work with cucumber demonstrated that the SAR signal was graft transmissible (Jenns and Kuc, 1979) and that once the signal reached distant tissues, it was not remobilized to other leaves (Dean and Kuc, 1986). Furthermore, although salicylic acid (SA) accumulated during SAR (Metraux et al., 1990), these researchers showed that SA is not the SAR mobile signal (Smith et al., 1991a). Few SAR studies in cucumber were conducted after the *Arabidopsis*-SAR model was developed because cucumber's genome was not sequenced until recently (Huang S. et al., 2009). However, with the newly available genome (Huang S. et al., 2009), the cucumber-SAR model is being used in the Cameron lab as it possesses several advantages over *Arabidopsis*. For example, concentrated phloem sap can be collected directly from the cut petiole, plus grafting this larger organism is fast and requires less skill that grafting small *Arabidopsis* plants. In addition, the study of cucumber has direct relevance, as it is a crop plant.

1.6 Research Hypotheses and Objectives

The main goal of this thesis is to contribute to understanding the roles of DIR1 and DIR1-like in long distance signaling during SAR using the *Arabidopsis* and cucumber model systems.

Hypothesis 1: If DIR1 and DIR1-like arose from a recent tandem duplication then an analysis of their phylogenetic relationship should support this hypothesis.
Objective 1: Examine evolutionary relationships between DIR1 and DIR1-like.

Hypothesis 2: If DIR1-like is responsible for the occasional SAR-competent phenotype of the *dir1-1* SAR mutant, then DIR1-like should travel from induced to distant tissues during SAR and complement the SAR defect in *dir1-1* .
Objective 2: Determine if DIR1 and DIR1-like share the ability to travel to distant tissues.

Hypothesis3: The occasional SAR-competent phenotype of *dir1-1* is due to the reduced ability of DIR1-like to move to distant leaves during SAR
Objective 3: Develop new tools to distinguish DIR1 and DIR1-like movement

Hypothesis 4: If DIR1-like is responsible for the occasional SAR-competent phenotype of the *dir1-1* SAR mutant, then a *dir1-1dir1-like* double mutant should be completely SAR defective.

Objective 4: Develop a *dir1-1dir1-like* double mutant transgenic plant line to dissect the roles of DIR1 and DIR1-like during SAR.

Hypothesis 5: If DIR1 is a conserved SAR long distant signal then DIR1 orthologs should be found in other plant species.
Objective 5: Probe the genomes of crop plants for putative DIR1 orthologs and perform phylogenic analysis.

Hypothesis 6: If the putative DIR1 orthologs identified in crop plants are orthologous to DIR1 then they will perform an equivalent function to DIR1 during SAR.
Objective 6: Test the ability of CucDIR1 to complement the *dir1-1* mutant and develop tools to investigate if other crop plant orthologs are functionally equivalent to DIR1.

Hypothesis 7: If DIR1 possesses residues that are critical for its function during SAR, then these residues should be conserved in DIR1 orthologs
Objective 7: Use knowledge of AtDIR1, AtDIR1-like and DIR1 orthologs to discover residues and motifs that are critical for AtDIR1 protein structure and participation in SAR long distance signaling.

Chapter 2 - Methods

2.1 Plant Growth Gonditions

Arabidopsis thaliana wild-type Wassilewskija (Ws-2) and *defective* in *induced resistance1-1* (*dir1-1*) (Ws-2 background) were used. *Arabidopsis* seeds were surface sterilized and allowed to stratify at 4°C for 2-3 days. Seeds were then germinated under continuous light on Murashige and Skoog (MS) media phytagar (Caisson Laboratories Phytoblend) plates for 5-7 days. Seedlings were transplanted onto soil (Sunshine Mix #1, Jack Van Klaveren) hydrated with 1 g/L 20-20-20 fertilizer. A plastic dome was placed over newly transplanted seedlings for 48 hours to maintain an initial high humidity. Plants were grown for 3-4 weeks in 65-85% relative humidity at 22°C in a 9 h photoperiod (150 μE m^{-2} s^{-1} light intensity). Cucumber Wisconsin S.M.R. 58 146B seeds (Stokes Seeds LTD., St. Catharines, Ontario) and *Nicotiana benthamiana* (Peter Moffet, Serbrooke University Quebec) were sown directly onto 1 g/L 20-20-20 fertilized soil. Cucumber and tobacco were grown for 3-4 weeks in 65-85% relative humidity at 22°C in a 16 h photoperiod (150 μE m^{-2} s^{-1} light intensity).

2.2 Pathogen Culture and Inoculation

SAR experiments employed virulent *Pseudomonas syringae* pv. *tomato* (*Pst*) DC3000 (containing pVSP1) and avirulent *Pst* (DC3000 containing pVSP1 + *avrRpt2*) described by (Whalen et al., 1991). *Pseudomonas* strains were cultured overnight at room temperature in sterile King's B medium (g/L: 20 g Proteose Peptone #3, 10 ml Glycerol, 1.5 Potassium Phosphate, 15 Agar for solid media, after autoclaving 6 ml 1 M $MgSO_4$) shaking at 200 rpm. *Pst* cultures were supplemented with 100 μg/ml rifampicin (chromosomal resistance) and 50 μg/ml kanamycin

(plasmid resistance). *Pst* cultures were diluted to either 10^5, 10^6 or $5x10^7$ cfu ml^{-1} in 10 mM $MgCl_2$ and pressure infiltrated into the abaxial side of a leaf using a needleless 1 ml syringe. *In planta* bacterial levels were quantified by dilution plating as described by (Cameron et al., 1999).

Agrobacterium tumefaciens GV3101::pMP90 strain was used in this work (Holsters et al. 1980). *Agrobacterium* was cultured overnight at 30 °C at 200 rpm in YEP (yeast extract peptone: g/L 10 Bacto-peptone, 5 NaCl, 10 Yeast Extract, 15 Agar for solid media) media supplemented with 50 μg/ml rifampicin, (chromosomal resistance), 75 μg/ml gentamycin (helper plasmid resistance) and where appropriate, 100 μg/ml kanamycin or 75 μg/ml spectinomycin. *Agrobacterium* transiently expressing 35S:*EYFP* (spectinomycin), 35S:*DIR1-EYFP*(spectinomycin) and 35S:*DIR1-like* (kanamycin) were created by Champigny et al. (2013). 35S:*CucDIR1* and all other *AtDIR1* ortholog *Agrobacterium* strains were created by this report and require kanamycin for selection.

DB3.1, DH5α (Life Science Technologies) and Rosetta Gami *Escherichia coli* competent cells (Novagen) were cultured overnight at 37 °C at 200 rpm in Luria Bertani (LB) media (g/L: 10 tryptone, 5 yeast extract, 10 NaCl, 15 Agar for solid media). *E.coli* DB3.1 containing gateway vectors were supplemented with 100 μg/ml kanamycin and 50 μg/ml chloramphenicol. Rosetta Gami *E.coli* were supplemented with 20 μg/ml tetracycline, 20 μg/ml streptomycin and 20 μg/ml chloramphenicol (pRARE2 plasmid expressing rare tRNAs to eliminate codon bias) plus the selective antibiotic for any transformed vector (ie 50 μg/ml kanamycin (pET29 selection marker)).

Bacteria were stored in -80 °C in a 1:1 mixture of culture and 40% glycerol in cryogenic tubes.

2.3 SAR and Agro-SAR Assays (modified from Champigny et al. 2013)

Due to unknown environmental factors SAR assays work poorly during the winter and therefore experiments were conducted between May-October. SAR assays were conducted on plants from 3.5-4 wpg whereas Agro-SAR assays were started a little earlier on plants 3-3.5 wpg. *Agrobacterium tumefaciens* strain GV3101 harboring 35S:EYFP or 35S:DIR1like-EYFP were diluted to an OD_{600} of 0.4, resuspended in 10 mM $MgCl_2$ and pressure infiltrated into the abaxial side of a leaf. Transient expression off of the TDNA was allowed to occur for 4 days before the SAR assay was initiated. After *Agrobacterium* inoculation the AgroSAR-assay followed a typical SAR experiment protocol where 2 or 3 lower leaves already inoculated with *Agrobacterium* were then SAR-induced with avirulent *Pst (avrRpt2)* (10^6 cfu ml^{-1}) or mock-inoculated. Distant leaves were then challenged with 10^5 cfu ml^{-1} of virulent *Pst* and *in planta* bacterial levels were determined 3 dpi. See Chapter 1, Figure 1.5 for a diagram of the assay.

2.4 Petiole Exudate Collection (modified from Champigny et al. 2013)

The *Arabidopsis* petiole exudate method was modified from King and Zeevaart (1974). Leaves were mock-inoculated or SAR-induced by inoculation with *Pst* (*avrRpt2)* (10^6 cfu ml^{-1}). To avoid HR induced tissue softening, an intermediate dose (10^6 cfu ml^{-1}) of *Pst (avrRpt2)* was used and a reduction in the number of cells undergoing HR allowed for the induced leaves to remain intact through the duration of the exudation process. Petiole exudates were collected at different times after induction by cutting one petiole at a time just above the stem, followed by surface

sterilization for 10 seconds (50% ethanol, 0.0006% bleach), rinsing in sterile 1 mM EDTA and submerging petioles in ~1.5 ml 1 mM EDTA (must be done quickly to prevent sieve element clogging) and 50 μg ml^{-1} ampicillin (to kill any remaining surface bacteria). The sterilization step must be long enough to kill *Pst* clinging to leaf surfaces, but not long enough to kill the *Pst* in the plant intercellular spaces. The petioles of seven to ten leaves per microfuge tube (depending on size) were allowed to exude phloem sap from 12-24 and 24-48 hpi in a humid environment (90-100%) on the lab bench. Petiole exudate samples (~1.5 ml) contained between 5 to 50 μg total protein (Biorad Protein Assay Kit) and were stored at -20 °C until concentration by lyophillzation, followed by protein gel blot analysis. Leaf weight could not be used to normalize exudate amounts loaded per lane as cut petioles must be immersed immediately in EDTA, allowing no time for weighing. In some experiments, exudate total protein levels were in the lower range (3 to 10 μg/exudate) but a DIR1 antibody signal could still be detected. For each experiment the same number of lyophilized exudates were loaded per lane and probed with our DIR1 antibody signal.

2.5 Protein Gel Blot Analysis (modified from Champigny et al. 2013)

Protein samples (crude protein extract, purified protein or petiole exudates concentrated by lyophillization) were mixed with 5X SDS loading buffer (350 mM Tris-HCl pH 6.8, 30% glycerol, 10% SDS, 0.01% bromophenol blue and 0, 5, 200 mM DTT) followed by boiling for 5 minutes. Two individual lyophilized exudates were reconstituted in loading buffer and loaded per lane. Samples were loaded onto 4-12% NuPAGE Bis-Tris polyacrylamide gels (Life Science Technologies) and subjected to electrophoresis in denaturing MES running buffer (g/L: 9.7 g MES, 6.0 g Tris,

1 g SDS, 0.37 g EDTA). Proteins were transferred to nitrocellulose membranes (Schleicher and Schuel) in Towbin transfer buffer (25 mM Tris base, 192 mM glycine, 20% methanol). Membranes were probed with anti-DIR1 antisera (Maldonado et al., 2002) at a 1:20,000 dilution in 5% non-fat milk in 1X TBST. Antibody binding was detected with a goat anti-rabbit horseradish peroxidase conjugate and WestFemto reagents (Pierce) as described by the manufacturer.

2.6 Phylogenetic Analyses (modified from Champigny et al. 2013)

A rooted phylogenetic Maximum Likelihood tree was created for AtDIR1 (AT5G48485) Brassicaceae ortholog family members and another for Brassicaceae family plus additional crop plant DIR1 orthologs. Phylogenies used protein sequences lacking the divergent ER signal sequence. Signal P 4.0 was used to determine where the signal sequence cleavage site was located (Perterson et al., 2011). The sequences were aligned in MEGA 5 using Muscle (Tamura et al., 2011). The evolutionary history was inferred using the Maximum Likelihood method based on the Kimura 2-parameter (Kimura, 1980) model with discrete Gamma distribution using MEGA 5 (Tamura et al., 2011). 10,000 bootstrap replicates were conducted and percent bootstrap values were placed on the branches (Felsenstein, 1985). Branches were drawn to scale, measured in number of substitutions per site and were labeled by species name followed by The *Arabidopsis* Information Resource (TAIR) (http://www.arabidopsis.org) gene number or Phytozome 8.0 accession. For the Brassicaceae plus additional crop plant AtDIR1 ortholog phylogeny, branches with less than 50% bootstrap values were collapsed

using Archaeopteryx software (Han and Zmasek, 2009). Phylogeny was viewed in FigTree v1.4 (Drummond et al., 2012).

2.7 Bioinformatics (modified from Champigny et al. 2013)

Coding sequence and amino acid sequences of DIR1 (AT5G48485) and DIR1-like (AT5G48490), LTP2sw (AT5G38170), were retrieved from (TAIR). Tobacco AtDIR1 ortholog sequences were retrieved from National Center for Biotechnology Information (NCBI) (http://www.ncbi.nlm.nih.gov/). Cucumber, tomato, and soybean AtDIR1 ortholog sequences were retrieved using Phytozome (phytozome.net). Sequences were compared using the EMBOSS Needleman-Wunsch pairwise alignment algorithm (http://www.ebi.ac.uk/emboss/align). Signal peptides were deduced using the SignalP 3.0 prediction server (http://www.cbs.dtu.dk/services/SignalP) (Perterson et al., 2011). A SWISS-MODEL homology models of AtDIR1-like, CucDIR1 and CucDIR2 were produced using the Lascombe *et al.*, (2008) AtDIR1-phospholipid crystal structure as a template (Peitsch, 1995; Guex and Peitsch, 1997; Schwede et al., 2003; Arnold et al., 2006; Kiefer et al., 2009). The Swiss-pdf viewer 4.0.1 and ICM browser were used to compare the AtDIR1 structure and the AtDIR1-like, CucDIR1, and CucDIR2 protein models (http:/www.expasy.org/spdbv/) (Guex and Peitsch, 1997). Sequence Logo plot was created by submitting the Muscle aligned mature DIR1 orthologs protein sequences in FASTA format to the Web logo program (Web logo application http://weblogo.berkeley.edu).

2.8 Quantitative Real Time PCR to Determine DIR1 and DIR1-like Transcript Abundance

Total RNA was extracted from frozen and ground *Arabidopsis* leaf tissue (100-200 μg) using the Trizol (Sigma) method followed by DNA removal using Turbo DNase Free (Ambion). First strand cDNA synthesis was performed using 2 μg of total RNA as template which was reverse transcribed into cDNA by MMLV reverse transcriptase (Life Science Technologies) using manufacturer instructions and diluted 3-fold in water before use. qRT-PCR was performed in a 10 μl reaction consisting of 2 μl of diluted cDNA, 1x LuminoCT SYBR Green qPCR ready mix (Sigma) and 200 or 400 nM of each primer. The mixture was loaded into low profile optical 96-well plates. qRT-PCR was performed in the Bio-Rad CFX96 touch™ Real-Time PCR Detection System and analyzed using BioRad CFX manager 2.0 software. Gene specific primers (Table 2.1) were validated for specificity and efficiency using an 8-point standard curve and purified products were Sanger sequenced to confirm identity (See appendix for summary of primer validation Figure 7.1-7.4). Primer secondary structure was evaluated using MFOLD (http://mfold.rna.albany.edu/). All primers were run at a final concentration of 400 nM with the exception of DIR1-like, which was run at a lower concentration (200 nM) in an effort to decrease the efficiency. To avoid measuring both DIR1-like sense transcript and DIR1-like antisense transcripts, DIR1-like primers had to be designed so that at least one of the primer pairs was outside the range of the antisense construct (See Figure 2.2). Genevestigator was used to choose the 5FCL and AT3G25800 reference genes based on the transcript stability with biotic challenge and a similar expression range to our genes of interest. All samples were analyzed in three biological and technical replicates. A no template control, as well as a no reverse transcriptase control were run simultaneously with the samples.

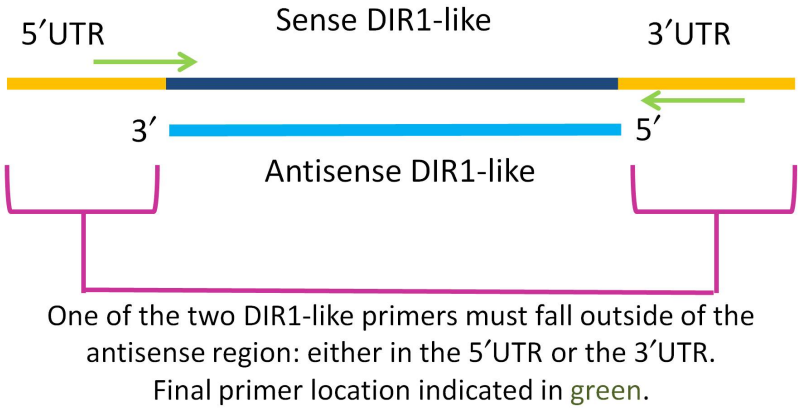

Figure 2.1: Diagram illustrating DIR1-like primer design. Special consideration had to be given to DIR1-like primer design to avoid amplifying the antisense transcript.

Table 2.1: Gene specific qRT-PCR primers for DIR1, DIR1-like, and reference genes AT3G25800 and 5FCL.

qRT-PCR Target	Primers	Efficiency	Concentration Used
DIR1	F5′ TCG TGA TAA TGG CTA TGT TGG TC R5′ ACT GTT TGG GGA GAG CAG AAG	100%	400nM
DIR1-like	F5′ AATAAAGAGGATAAAATGACAA GC R5′ CTGGTAAGCATTCATTCAACTC	115%	200nM
AT3G25800	F5′ GATGAGTTCCCGGATGTACG R5′ AGCTGGCAACAAGGATTGTG	103%	400nM
5FCL	F5′ TGTCCGCAAATCCCTAAAAG R5′ CCAGGGAGCTTCAAGAACAG	99%	400nM

2.9 Confocal Microscopy to Visualize iLOV Fluorescent Protein

N. tabacum plants (3 wpg) were inoculated with *Agrobacterium* expressing 35S:SS-HA-DIR1-iLOV for transient expression analysis essentially as described by (Moffett, 2011). *Agrobacterium* was grown overnight at 30 °C shaking at 200 rpm. *Agrobacterium* was then spun down at 4000 rpm for 15 minutes and the pellet was resuspend in infiltration buffer (10 mM $MgCl_2$, 10 mM MES pH 5.6, 100 mM acetosyringone (added fresh from a 100 mM stock in DMSO)). This mixture was allowed to sit at room temperature for 6 hours. After 6 hours, *Agrobacterium* cultures were diluted to an OD_{600} of 0.4 and infiltrated into the abaxial side of the Tobacco leaf using a needleless syringe. Mock inoculations with infiltration buffer alone were used as a control. *Agrobacterium* was allowed to transiently express for 3 days. Leaf discs were taken 3 dpi and fluorescence was examined on a Leica confocal microscope at excitation wavelength of 476 nm and emission was collected between 510-550 nm. All images were captured under the same conditions.

2.10 Purification of Rosetta Gami Expressed Recombinant Proteins

AtDIR1, AtDIR1-like, AtLTP2sw, CucDIR1, CucDIR2, and the AtDIR1 variants (L43D, NPH, D39Q, AxxA, F40Y, AAxxAA See Chapter 5, Table 5.5 for a description of these variants) lacking their ER signal sequence were cloned into pET29b (with N-terminal S-tag and C-terminal His tag) expression vector (Novagen) with an isopropyl β-D-1-thiogalactopyranoside (IPTG) inducible promoter (See Table 2.2 for primers). These constructs were transformed into Rosetta Gami *E.coli* (Novagen) cells, which are modified to encourage cytosolic disulfide

bond formation required for proper LTP2 folding. Transformed cells were plated on LB plates supplemented with 50 μg/ml kanamycin (pET29 seletion marker), 20 μg/ml tetracycline, 20 μg/ml streptomycin and 20 μg/ml chloramphenicol (pRARE2 plasmid expressing rare tRNA to eliminate codon bias). Next, 250 ml and 500 ml Rosetta Gami *E.coli* cultures were grown overnight in LB at 30 °C with shaking at 200 rpm. At an OD_{600} of 0.6, 100 ml of culture was poured into a new flask and 1 mM IPTG was added to induce expression. Cultures were shaken for another 4 hours at 30 °C. Cells were harvested by centrifugation in two sterile 50 ml falcon tubes at 4000x g for 20 minutes at 4°C. A single 1 ml eppendorf tube was also collected for crude protein extraction. LB was poured out and the pellet was dried. The pellet was then placed in the -80 °C freezer and either a crude total protein extraction or S-Tag thrombin protein purification (Novagen) was performed (described in more detail in section 2.12).

Table 2.2: pET29b cloning primers.

Organism	**Insert**	**Made By**	**RE - Primers**
Arabidopsis thaliana	AtDIR1		Champigny et al. (2013)
	AtDlike	This work	BamHI F5' TCGGGATCCGGCGATTGACCTTTGTGGCATG XhoI R5' AGCCTCGAGACAAGTTGGGGCGTTGGTTAGG
	AtLTP2 sw	This work	BamHI F5' TCGGGATCCGACTGAGGTCAAACTTTCTGGAGG XhoI R5' AGCCTCGAGACAAGTAGGATAAGGAACACCAC
***Cucumis Sativus* (Cucumber)**	CucDIR1	This work	BamHI F5' TCGGGATCCGATGGAAGTTTGCGGCGTCGACG XhoI R5' GCCTCGAGAGCAGAGCAAGTGGGAGTGTTA

			GG
	CucDI R2	This work	BamHI F5' TCGGGATCCGCAATCCATTTGCAACATGCC XhoI R5'AGCCTCGAGGCAATTTGGAGACTTAGAAATG
DIR1 Variants	No Cysteines	This work	BamHI F5' TCGGGATCCGGCGATAGATCTCGCTGGCATG XhoI R5' AGCCTCGAGAGCAGTTGGGGCGTTGGCTAGA
	L43D, PxxP, NPH, D59Q, F40T, AD, LAxxLP	This work	BamHI F5'CGGGATCCGGCGATAGATCTCTGCGGCATGAGC XhoI R5'AGCCTCGAGACAAGTTGGGGCGTTGGCTAGACC

2.11 Crude Protein Extraction

To ensure that proteins were successfully expressed a crude protein extraction followed by protein gel blot analysis was performed before pellets were purified using the S-tag Thrombin purification kit (Novagen). Pellets collected from 1 ml of culture were resuspended in 100 μl of lysis buffer (140 mM NaCl, 2.7 mM KCl, 1.8 mM KH_2PO_4, PBS pH 7.3, 1 mM PMSF (protease inhibitor-Sigma), 0.1% TritonX-100). This mixture was sonicated on medium for 10 seconds and repeated three times with cooling on ice in between. After lysis the cells were centrifuged for 5 minutes at 13000 rpm to separate the soluble and insoluble proteins. Next, 20 μl of soluble protein was then denatured and used directly for protein gel blot analysis to measure protein expression.

2.12 S-Tag Thrombin Purification (Novagen)

An S-Tag thrombin purification kit was used to purify recombinant Rosetta Gami expressed proteins. S-Tag and S-peptide are derived by

cleavage of a modified mammalian RNase A protein. The two halfs of the protein (S-Tag and S-peptide) have high affinity for one another and are therefore used for protein purification. Manufacturer's instructions were followed and therefore the general concept will be outlined. Frozen pellets were thawed on ice and resuspended in the bind/wash buffer. Cells were then lysed using sonication and soluble and insoluble fractions were separated by centrifugation. S-protein agarose beads were then added. Our proteins of interest were tagged with His as well as an S-tag. The S-tag binds to the S-protein with high affinity. Bound to agarose beads, the protein of interest was washed, spun down and impurities were removed with the supernatant. This was repeated twice. A thrombin cleavage site between the protein and S-tag allows the protein to be cut from the S-protein agarose beads using thrombin cleavage enzyme. After cleavage streptavidin agarose was applied to remove the thrombin cleavage enzyme. The mixture then contained free recombinant protein, Stag/S-protein beads and streptavidin/Thrombin cleavage enzyme beads. To separate the purified protein from the beads, the protein was run through a purifying column with a resin designed to collect the agarose beads. The flow through then contained highly purified recombinant protein. Protein concentrations were determined by Bradford assay (Biorad manufacturer's instructions) and ranged from 40-80 ng/μl for our proteins. Next, 50 μl aliquots of protein were stored directly in the -80 °C freezer.

2.13 TNS Folding Assay & TNS Inhibition/Displacement Ligand Binding Experiments

Proteins were engineered to resemble mature protein lacking the ER signal sequence and were expressed in Rosetta Gami *E.coli*. To test protein folding increasing amounts (0-30 uM) of 6,P-toluidinylnaphthalene-2-sulfonate (TNS) were added to ~1 μg of each Rosetta Gami *E.coli* (Novagen) purified protein. Plates were loaded with 60 μl of protein, 182 μl of measurement buffer (0.5 mM K_2SO_4, 0.5 mM $CaCl_2$, 0.175 M Mannitol, 5 mM MES) and TNS concentrations were increased 5 μM at a time by adding 3.8 μl of a 0.3 mM stock. As a negative control, protein samples were denatured by boiling in 6 M urea for 10 minutes. Samples were loaded into Thermofisher microflor two black bottom 96 well microtiter plates and read using the Gen5 bioTek Synergy 4 plate reader at Cornell University, Ithaca New York. Samples were excited with 320 nm and emission was collected at 437 nm and the change in fluorescence (x μM TNS – no TNS) was calculated for three technical replicates. Error bars represent the standard deviation of the technical variation.

The TNS inhibition/displacement ligand binding assay was performed using the same plates and instrument. Fluoresecence was first measured when TNS (5 μm) and putative ligands (Azelaic acid, pipecolic acid, glycerol-3-phosphate) (16 μm) were inclubated together for 3 minutes in a 96 well plate, then a second reading was recorded after purified proteins were added. Plates were loaded with 60 μl of protein (~1 μg), 182 μl of measurement buffer (0.5 mM K_2SO_4, 0.5 mM $CaCl_2$, 0.175 M mannitol, 5 mM MES) and 5 μM TNS (3.8 μl of a 0.3 mM stock). Azelaic acid was prepared in 5 mM MES, while all other ligands were prepared in water. Fluorescence was measured at excitation wavelength of 320 nm and emission was collected at 437 nm in technical triplicate. Ligand binding was represented by the percent of TNS fluorescence that was inhibited by

the addition of the purified proteins. Error bars represent the standard deviation of the technical variation.

1.14 DNA Extraction

The same DNA extraction protocol was used to extract DNA from *Arabidopsis*, tobacco, soybean cucumber and tomato. Tissue was harvested and flash frozen in liquid nitrogen and stored at -80 °C until use. Frozen tissue (100-200 μg) was then placed in crushed dry ice and tissue was then ground into a powder using a blue tip attached to a drill. Next, 200 μl of DNA extraction buffer (200 mM Tris-HCl pH7.5, 250 mM NaCl, 25 mM EDTA, 0.5% SDS) was then added and samples were vortexed to homogenize the mixture. They were then placed in a water bath for 15 minutes at 37 °C. 200 μl of phenol-chloroform mix (phenol/chloroform/isoamyl alcohol (25:24:1)) was added and then the mixture was vortexed. Tubes were then centrifuged at 10000x g for 5 minutes at 4°C. The aqueous (top) layer was transferred to a new tube and the phenol chloroform purification was repeated. Once the top layer was in a new tube, an equal volume of isopropanol was added and the mixture was centrifuged for 15 minutes. Isopropanol was discarded and the pellet washed with 70% ethanol followed by centrifugation for 2 minutes, 10000x g at 4°C. The ethanol wash was repeated to remove impurities. The pellet was allowed to dry for 5-10 minutes on a heating block at 55°C, then dissolved in 30-50 μl of RNase DNase free water. DNA was stored at -20°C until used as a PCR template.

2.15 DNA Amplification PCR

Phusion High-Fidelity *Taq* DNA polymerase (New England Biolabs) was used to amplify target sequences from *Arabidopsis*, cucumber, tomato, tobacco and soybean. General PCR conditions used were: 98°C, 30 sec initial denaturation; 98°C 5 sec, 60°C 15 sec, 72°C 15 sec repeated 30-34 times; 72°C 5 min final extension; 4°C hold. 2μl of DNA was used as template. If a PCR amplicon is to be used for downstream cloning, six 25 μl reactions were typically run and the PCR product was run on a gel and gel purified (Qiagen Gel Purification Kit). For gel purification the DNA binding column was eluted twice with 13 μl of RNase DNase free water.

2.16 Digestion of Insert DNA and Plasmid Backbone

New England BioLabs (NEB) restriction enzymes were used to digest the insert DNA and plasmid backbone following NEB instructions. To increase the chances of successful cloning a ration of at least 3:1 insert to vector was used. This was estimated using the molecular standards on the DNA ladder. Typically three reactions of PCR digests and four vector reactions were purified and used in the ligation reaction. For the insert reation 30 μl of the following was used: 3 μl of NEB buffer (1,2,3, or 4) 1 μl enzyme 1, 1 μl enzyme 2, 0.3 μl of BSA (Bovine serm albumim) (10ug/ul stock, if required), 4.7 μl H_20, 20 μl of gel purified insert (Qiagen Gel Purification Kit). For the plasmid reaction 30 μl of the following was used: 3 μl of NEB buffer (1,2,3, or 4) 1 μl/enzyme, 0.3 μl of BSA (10 ug/ul stock, if required), 8 μl of miniprep plasmid and the remaining volume was made up with water (to 30 μl). These reactions were then digest overnight (~14 hours) at the recommended temperature (usually 37°C), and held at 4 °C. The digests were then run on a gel and purified (Qiagen gel purification kit) and eluted twice with 13 μl of RNase DNase free water.

2.17 Ligations

After obtaining gel purified plasmid backbone and insert that have been digested with the appropriate enzymes the insert and plasmid backbone were ligated using T4 ligase (Life Science Technologies). The following components were added for a 10 μl ligation reaction: 2 μl 5x T4 ligase buffer, 1 μl T4 DNA Ligase (High Concentration), 2.5 μl digested vector, 4.5 μl digested insert. A negative control reaction where the digested insert was replaced with RNase DNase free water determined the amount of background plasmids that have not incorporated the insert, either due to the fact that they were never cut in the first place or the digested overhangs had reattached. This mixture is ligated overnight (12-16 hours) at 16°C. If a thermocycler was being used then the hot lid option was turned off.

2.18 Transformations:

For transformations, 50 μl aliquots of *E.coli* DH5a sub-cloning efficiency chemically competent cells (Life Science Technologies) were transformed with 2.5 μl of the ligation mix according to manufacturer's instructions. After shaking for 1 hour, bacteria were plated onto selection plates that were incubated overnight at 37°C. Transformation efficiency was accessed by transforming bacteria with a plasmid of known concentration.

2.19 Construct Verification

After 24 hours the *E.coli* cells grew on the selection plates and cloning success was then assessed. To ensure successful cloning, negative

control plates were checked to ensure that they had a low number of colonies compared to ligation plates. If the number of colonies on the negative control was the same as the ligation plates then cloning was considered unsuccessful. The number of colonies picked depended on the background levels, however, typically 5-10 colonies per plate were picked. These colonies were placed in liquid LB media with appropriate antibiotics, grown overnight and plasmids were isolated using a miniprep kit (Qiagen) the next day. The isolated plasmids were then diagnosed by enzyme digest, usually with the same enzyme used for cloning. For diagnostic purposes smaller reactions were used. For a 20μl reaction the following components were added: 2 μl of NEB buffer (1,2,3, or 4) 0.75 μl enzyme 1, 0.75 μl enzyme 2, 0.2 μl of BSA (if required), 12.3 μl H_20, 4 μl of purified plasmid (Qiagen Miniprep Kit). Plasmids were digested for 3-5 hours at the recommended temperature (usually 37°C) and then they were run on a gel. If the digest revealed that the insert of predicted size was present then the miniprep was sent for sequencing to ensure that no errors were introduced during the cloning process. Sequencing primers (Table 2.3) were designed to be at least 50 bp away from the insert start site.

Table 2.3: Sequencing Primers for pMDC32, pHannibal, pER8 and pET29b vectors.

Plasmid	Primer name	Squence
pMDC32	NosR	R 5′ ATATGATAATCATCGCAAGACCGG 3′
pHannibal	Forward Reverse Intron primer Reverse	F 5′ CGCACAATCCCACTATCCTT 3′ R 5′ CAAGCAGATTGGAATTTCTAAC 3′ R 5′ GGGTACAATCAGTAAATTGAACG 3′
pER8	Pea3A-R	R 5′ ATGCCATAATACTCAAACTTAGTAGG 3′

pET29b	T7 promoter	F 5' TAATACGACTCACTATAGGG 3'

2.20 *Agrobacterium* Transformation:

2.20.1 Making Freeze/Thaw Competent *Agrobacterium:*

Freeze/thaw competent *Agrobacterium tumefaciens* GV3101 were created for rapid freeze thaw transformation. In brief, *Agrobacterium* GV3101 was grown overnight shaking at 200 rpm at 30°C in YEP supplemented with 50 μg/ml rifampicin, (chromosomal resistance), 75 μg/ml gentamycin (helper plasmid resistance). When cultures reach an OD_{600} of 0.3 the cells were chilled on ice for 15 minutes. Cells were then centrifuged 4000xg for 5 minutes at 4°C. Supernatant was discarded and cells were resuspended in 10 ml of cold sterile 100 mM $MgCl_2$ and incubated for 1 hour. Cells were centrifuged again with the same conditions. Supernatant was discarded and cells were resuspended in 2 ml of cold sterile 20 mM $CaCl_2$ and incubated on ice for 6 hours. Sterile glycerol was then added to a final concentration of 20% and the cells were aliquoted (100 μl/tube). Tubes were then dropped in liquid nitrogen to freeze the cells and tubes were transferred to -80°C for storage.

2.20.2 Freeze/Thaw Transformation of *Agrobacterium*:

Tubes of frozen cells were removed from -80°C, placed on ice, and 1-2 μg of miniprep plasmid DNA was added to the top of the frozen cells. Cells were allowed to thaw on ice for 10 minutes until the bacterial pellet was liquid. Contents were mixed gently and dropped into liquid nitrogen for 10 minutes. Tubes were removed and allowed to thaw at 37°C for 5 minutes. Next, 1 ml of sterile YEP was added to the tubes which were then

shaken at 180rpm for 2 hours at 30°C. Cells were then plated onto selective plates. *Agrobacterium* takes a minimum of 2 days to grow at 30°C.

2.21 Making Antisense Constructs

Three different DIR1-like antisense constructs were designed to increase our chances of success (Table2.4).

Table 2.4: DIR1-like antisense contruct primers for insertion into 35S pMDC32 plant transformation vector.

Antisense Construct spMDC32	**DIR1-like cDNA antisense (D)**	F5′ GGGGACAAGTTTGTACAAAAAAGCAGGCTCG AAACAAACAAAGGAAAACACCA R5′ GGGGACCACTTTGTACAAGAAAGCTGGGTT ACAAGCAAGAAGGTGGCAAT
	Antisense with small region where DIR1 and DIR1-like are the same (C)	F5′ GGGGACAAGTTTGTACAAAAAAGCAGGCTTC TAACAAGTTGGGGCGTTG R5′ GGGGACCACTTTGTACAAGAAAGCTGGGTT GGCTCGGTTCTTTTGGTGTA
	Antisense with small region unique to DIR1-like (B)	F5′ GGGGACAAGTTTGTACAAAAAAGCAGGCTTC AAGCGAATCCATTAAAATATCCTT R5′ GGGGACCACTTTGTACAAGAAAGCTGGGTT TGGTGTTTTCCTTTGTTTGTTT

*AttB recombination sequence highlighted in grey.

Gateway vector pMDC32 (Curtis and Grossniklaus, 2003) was maintained in *E.coli* DB3.1 (Life Science Technologies) cells which are resistant to the *ccdB* death gene targeting DNA gyrase. *ccdB* is a positive marker for recombination of a insert DNA into the Gateway vector as in

the process *ccdB* should recombine out. After recombination the gateway vector was transformed into regular DH5α *E.coli* (Life Science Technologies) cells. If the *ccdB* gene has not been recombined out and replaced with the insert then DH5α *E.coli* growth will be prevented. Antisense segments were PCR amplified using Phusion High-Fidelity *taq* (NEB). To avoid amplifying the highly similar *DIR1* gene, *dir1-1* cDNA was used as a template. Amplicons were sequenced to confirm identity. The antisense constructs were first recombined into pDONR221 entry clone using BP clonase (Life Science Technologies). The insert was then transferred from pDONR221 into pMDC32 35S expression vector using LR clonase (Life Science Technologies). pMDC32 containing the antisense constructs were sequenced and then transformed into *Agrobacterium* GV3101 and *Arabidopsis* were transformed with the construct using the floral dip protocol (Clough and Bent, 1998; Zhang et al., 2006). T_1 seeds collected from the dipped T_0 generation were then MS supplemented with 20 μg/ml hygromycin (transgene selection) and 200 μg/ml timentin (antibiotic resistance to prevent residual *Agrobacterium* contamination). Hygromycin resistant T_1 plants were allowed to self fertilize. The T_2 generation was examined for single copy insertions based on the seedling hygromycin resistance ratio which should be 1 (homozygous no insertion) to 2 (heterozygous insertion) to 1 (homozygous insertion). T2 plants lines deviating from this ratio were considered to have multiple copies of the insertion and the lines were not carried to the T3 generation.

2.22 Making RNAi Constructs

DIR1-like sense and antisense strands were amplified using Phusion High-Fidelity *Taq* (NEB) using gene specific primers (Table 2.5). To avoid

amplifying the highly similar *DIR1* gene, *dir1-1* cDNA was used as a template. pHannibal plasmid (Wesley et al., 2001) was used to create the DIR1-like hairpin RNAi cassette which would then be transferred into 35S pMDC32 curtis vector (Curtis and Grossniklaus, 2003) or the estrogen inducible (XVE) pER8 (Zuo et al., 2000) plant transformation vectors (Figure 2.2). Restriction enzymes for transfer to pMDC32 or pER8 were included during the construction of pHannibal DIR1-like RNAi.

DIR1-like sense and antisense strands were inserted into the pHannibal vector sequentially. A pHannibal DIR1-likeRNAi plasmid with pMDC32 restriction sites and a pHannibal DIR1-like RNAi plasmid with pER8 restriction sites were created and confirmed by sequencing. The DIR1-likeRNAi cassette was then transferred to pMDC32 and pER8, sequenced and transformed into *Agrobacterium*. *Arabidopsis* plants were transformed with the construct using the floral dip protocol (Clough and Bent, 1998; Zhang et al., 2006). T_1 seeds collected from the dipped T_0 generation are currently being screened on MS supplemented with 20 μg/ml hygromycin (transgene selection) and 200 μg/ml timentin (antibiotic resistance to prevent residual *Agrobacterium* contamination).

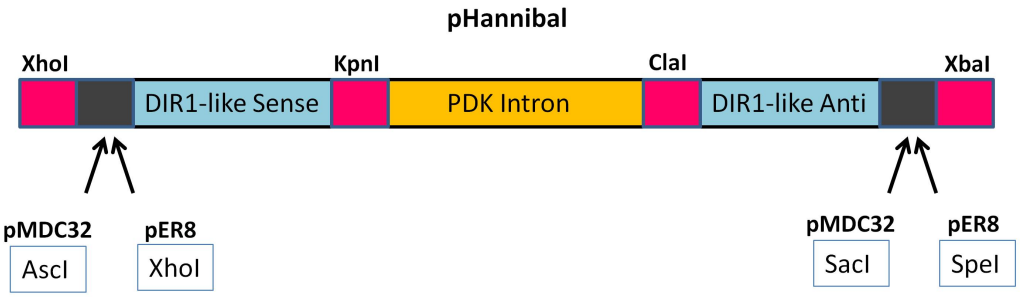

Figure 2.2: pHannibal DIR1-like RNAi cassette with restriction enzyme sites. pHannibal DIR1-like RNAi was designed to be easily cloned from pHannibal into either 35S pMDC32 or the estrogen inducible (XVE) pER8 plant transformation vectors.

Table 2.5: pHannibal DIR1-like RNAi primers for easy transfer to pMDC32 and pER8 plant expression vectors.

pHannibal construct	**RE**	**Primers**
Sense PER8	XhoI	F5′ TCGCTCGAGATTGACCTTTGTGGCATGACTC
	KpnI	R5′ TCGGGTACCTTAACAAGTTGGGGCGTTG
Anti PER8	ClaI	F5′ CTGATCGATTTAACAAGTTGGGGCGTTG
	XbaI/SpeI	R5′ CTGTCTAGA ACTAGTATTGACCTTTGTGGCATGAC
Sense pMDC32	XhoI/AscI	F5′ TCGCTCGAGGGCGCGCCATTGACCTTTGTGGCATGACTC
	KpnI	R5′ TCGGGTACCTTAACAAGTTGGGGCGTTG
Anti pMDC32	ClaI	F5′ CTGATCGATTTAACAAGTTGGGGCGTTG
	XbaI/SacI	R5′ CTGTCTAGA GAGCTCATTGACCTTTGTGGCATGAC

***** RE= restriction enzyme

2.23 Construction of SS-HA-DIR1-iLOV and SS-FLAG-DIR1-like-phiLOV

The SS-HA-DIR1-iLOV and SS-HA-DIR1-like-phiLOV constructs were created by a gene synthesis company (Biobasic) and cloned out using gene specific primers (Table 2.5). These were cloned into pMDC32 plant transformation vector (Curtis and Grossniklaus, 2003) with and without the iLOV or phiLOV fluorescent tag (Chapman et al., 2008; Christie et al., 2012). Constructs were sequenced and then transformed into *Agrobacterium*. *Arabidopsis* plants were transformed with the construct using the floral dip protocol (Clough and Bent, 1998; Zhang et al., 2006). T_1

seeds collected from the dipped T_0 generation were screened on MS supplemented with 20 μg/ml hygromycin (transgene selection) and 200 μg/ml timentin (antibiotic resistance to prevent residual *Agrobacterium* contamination). Hygromycin resistant T_1 plants were allowed to self fertilize. The T_2 generation is currently being examined for single copy insertions based on the seedling hygromycin resistance ratio which should be 1(homozygous no insertion) to 2(heterozygous insertion) to 1(homozygous insertion). T2 plants lines deviating from this ratio will be considered to have multiple copies of the insertion and the lines will not be carried to the T3 generation.

Table 2.6: Primers for insertion of SS-HA-DIR1-iLOV and SS-HA-DIR1-like-phiLOV with and without the fluorescent tag into 35S pMDC32 plant transformation vector.

pMDC32 construct	**RE Primer**
SS-HA-DIR1-iLOV	AscI F5′ AGCGGCGCGCCATGGCGAGCAAGAAAGCAGC SacI R5′ AGCGAGCTCTTAAACATGATCAGATCCATCAAG
SS-HA-DIR1	AscI F5′ AGCGGCGCGCCATGGCGAGCAAGAAAGCAGC SacI R5′ AGCGAGCTCTTAACAAGTTGGGGCGTTGGCTAGACC
SS-FLAG-Dlike-phiLOV	AscI F5′ AGCGGCGCGCCATGACAAGCAAGAAGGTGGC SacI R5′ AGCGAGCTCTTAAACATGATCAGATCCAACAAG
SS-FLAG-Dlike	AscI F5′ AGCGGCGCGCCATGACAAGCAAGAAGGTGGC SacI R5′ AGCGAGCTCTTAACAAGTTGGGGCGTTGGTTAGG

*RE= restriction enzyme.

2.24 *Arabidopsis* AtDIR1 Ortholog Constructs

Arabidopsis DIR1 orthologs were PCR amplified out of their native species and cloned into 35S pMDC32 plant transformation vector (Curtis and Grossniklaus, 2003) for use in transient Agro-SAR assay (See Chapter 1 Figure 1.5 for Review). Each construct was confirmed by sequencing. See Table 2.6 for primers

Table 2.7: Primers used to amplify AtDIR1 and DIR1 orthologs.

Organism	Insert	Vector	Made By	RE	Primers
Arabidopsis thaliana	AtDIR1 EYFP	pCambia			Champigny et al. 2013
	At Dlike	pCambia			Champigny et al. 2013
	AtLTP2sw	pMDC32	Phil	AscI SacI	F5'CACACG*GGCGCGCC*accA*TGAAGTTCACGGCGCTTGTG* R5'GGAACA*GAGCTC*TCAACAAGTAGGATAAGGAACACC
***Cucumis sativus* (Cucumber)**	Cuc DIR1	pMDC32	Phil	AscI SacI	F5'CACACGGGCGCGCCACCATGGAGATGGCTCAAAAGGTG R5'GGAACAGAGCTCTTAAAGGTTTAAGCAGAGCAAG
	Cuc DIR2	pMDC32	This work	KpnI SpeI	F5'AGCGGTACCTTAGCAGTTGGGAGGATGAGG R5'AGCACTAGTCTAGCAATTTGGAGACTTAGAAATG
***Glycine Max* (Soybean)**	Soy DIR1	pMDC32		**KpnI SacI**	F5'TCGGGTACCATGGAACAAAAGAAGTTTGTGGC R5'AGCGAGCTCTCAGCAATTATCTGGAGGAGTGAG
	Soy DIR2	pMDC32		**KpnI SacI**	F5'TCGGGTACCATGGAACAAAAGAAGTTTGTGGC R5'AGCGAGCTCTTATGAGCAATTATCTGGGGGAG
	Soy DIR3	pMDC32		**KpnI SacI**	F5'TCGGGTACCATGATAGTGGGTGTGGCATTGG R5'AGCGAGCTCTTAGCAGTTGGGAGGATGAGG

***Solanum lycopersicum* (Tomato)**	Tom DIR1	pMDC32	PhiI	AscI SacI	F5'CACACGGGCGCGCCACCATGCCTATGAAAGGAAGCAAAG 3' R5'GGAACAGAGCTCTTAACAATTAGAAGGAGAAGTG 3'
	Tom DIR2	pMDC32	PhiI	AscI SacI	F5'CACACGGGCGCGCCACCATGGAGCATTATAACTTTGCCC 3' R5'GGAACAGAGCTCTTAGCAACGGGGAGGATTAGGTAG3'
	Tom DIR3	pMDC32	PhiI	AscI SacI	F5'CACACGGGCGCGCCACCATGGAAGCAAAGCAAAACTTGG 3' R5'GGAACAGAGCTCTTAAGCGGAGCAATTAGGTGAG 3'
***Nicotiana tabacum* (Tobacco)**	Tob DIR1	pMDC32	This work	KpnI SacI	F5'TCGGGTACCATGCATATGATAGGAAACAAAGTG R5'AGCGAGCTCTTAACAATTAGCAGGAGAAGTGAG
	Tob DIR2	pMDC32	This work	KpnI SacI	F5'TCGGGTACCATGGAAGCAAAGCAAAAGCTTG R5'AGCGAGCTCTTAAGCGGCGCAGTTTGGAG
	TobDIR3L (Klessig version)	pMDC32	This work	KpnI SacI	F5'TCGGGTACCATGCTGGATCCGCCCCTG R5'AGCGAGCTCTTAGCAATGGGGAGGATTAGG
	Tob DIR3s (shorter)	pMDC32	This work	KpnI SacI	F5'TCGGGTACCATGGAGCATTACTTGGCCAAAAAACC R5' AGCGAGCTCTTAGCAATGGGGAGGATTAGG

*RE = restriction enzymes

Chapter 3: Examining the role of DIR1 and DIR1-like during SAR and creation of key tools for future dissection of DIR1 and DIR1-like SAR involvement

Preface

Sections 3.2.1, 3.2.3 in this chapter have been modified from the publication Champigny et al. (2013) which appeared in Frontiers in Plant Science, 4:230. Figure 3.1 in section 3.2.1 was reproduced unmodified from the manuscript. This is possible because authors maintain copy right to their images from publications in Frontiers in Plant Science. Figure 3.3 in section 3.2.3 was modified from the original manuscript image. Phylogeny studies were conducted with advice from Yifei Huang and Wilson Sung, bioinformaticians in the Golding Lab at McMaster University. Section 3.2.3 experiments were conducted with the help of Philip Carella, a member of the Cameron lab. The Agro-SAR assay was created by Dr. Robin Cameron and Dr. Marc Champigny.

3.1 Introduction

The occasional SAR competent phenotype observed in *dir1-1* mutants led to the discovery of a highly similar DIR1-like protein (At5g48485; 88% sequence similarity to mature DIR1 protein). It was hypothesized that DIR1-like may occasionally compensate for reduced DIR1 levels in *dir1-1* by acting in a partially redundant manner, which could explain the occasional SAR^+ phenotype of *dir1-1*. Using the Agro-SAR assay (Reviewed in Figure 1.5 Chapter 1) the SAR defect in the *dir1-1* mutant was rescued by transiently expressing DIR1 or DIR1-like (Champigny et al., 2013). This experiment suggests that DIR1-like is functionally equivalent to DIR1 and thus can contribute to SAR in *Arabidopsis*. However, in the absence of ectopic *Agrobacterium*-mediated expression of DIR1-like, native DIR1-like does not reliably complement the SAR defect in *dir1-1*. This suggests that a threshold level of DIR1-like is necessary for DIR1-like participation in SAR, such that higher

levels produced by *Agrobacterium*-mediated expression of DIR1-like can reliably complementent *dir1-1,* while endogenous DIR1-like alone rarely meets this threshold. It is also possible that transient expression of DIR1-like by *Agrobacterium* is higher in certain cell types important for SAR and this may explain why transiently expressing *DIR1-like* rescues the SAR defect in *dir1-1*. Based on these observations, the idea emerged that DIR1-like is less effective in contributing to a functional SAR response compared to DIR1. Many questions remain about DIR1-like's contribution to SAR.

The overall goal of this chapter was to provide a better understanding of the DIR1-like protein and how it might be compensating for the *dir1-1* SAR defect. If DIR1-like was responsible for the occasional SAR competent phenotype of *dir1-1* then it should possess the characteristics of a SAR long distance signal. An additional aim of this chapter was to provide tools to support future research that dissects the role of DIR1 and DIR1-like during SAR.

3.2 Results

3.2.1 Examination of the evolutionary relationship between DIR1 and DIR1-like

DIR1-like and DIR1 likely arose through a tandem gene duplication as suggested by Boutrot et al. (2008). This hypothesis is supported by the 88% amino acid sequence similarity of DIR1 and DIR1-like (EMBOSS Needleman-Wunsch pairwise alignment EMBL-EBI) and their tandem location on chromosome 5. A BLAST search of the *Arabidopsis* genome did not reveal other highly similar genes such that all other LTP2s proteins share less than 52% amino acid sequence similarity compared to DIR1 (Needleman-Wunsch pair wise global alignment using EMBL-EBI). Using

various *Brassicaceae* family members, a phylogeny of putative DIR1 orthologs was constructed to add support to the hypothesis of tandem duplication as well as to determine the evolutionary node where DIR1 duplication occurred (Figures 3.1). *Arabidopsis* LTP2 (At5g38170) was used as an outgroup based on its low sequence similarity to DIR1 (37%) and because its ortholog is studied in wheat (hereafter referred to as LTP2sw for similar to wheat LTP2). Using phylogenetic analysis, two distinct groups were revealed, those with two DIR1 orthologs (*Arabidopsis thaliana* and *lyrata*) and those with one (*Thellungiella salsuginea* and *Brassica rapa*). Because only a single "DIR1-type" gene is present in *T. salsuginea* and *B. rapa,* a tandem duplication event occurring in the last common ancestor of *A. thaliana* and *A. lyrata* likely resulted in the DIR1 and DIR1-like paralogs. *A. thaliana* and *A. lyrata* speciation occurred approximately 13 million years ago (Beilstein et al., 2010) suggesting the duplication event occurred sometime before this split. The prediction that DIR1 and DIR1-like are orthologous to *lyrata* genes is strengthened by the finding that the *lyrata* genes are also tandemly located on scaffold 8 of the *A. lyrata* genome. Recent species phylogenies of the Brassicaceae family (Schranz et al., 2007) and the DIR1 gene phylogeny presented here share a similar pattern where the species tree organization mirrors the protein relatedness, providing further support for the DIR1 phylogeny. These results are consistent with Boutrot et al. (2008), and provide further information on the timing of DIR1 and DIR1-like duplication in the mustard family.

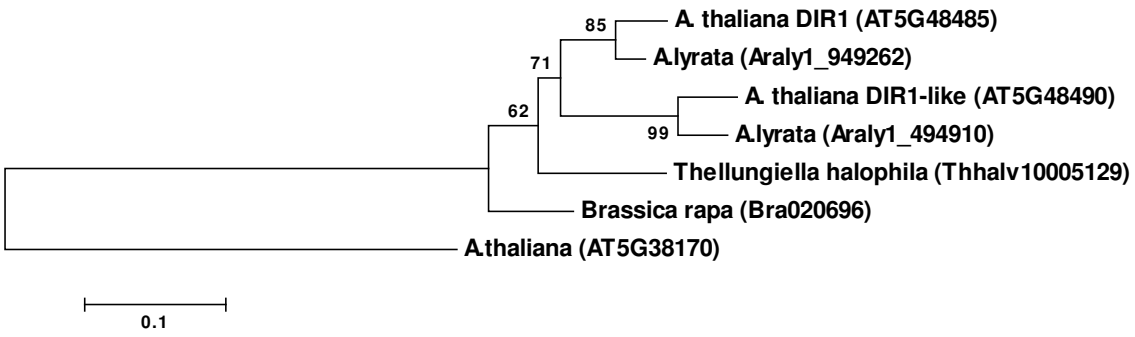

Figure 3.1: Rooted Phylogenetic Maximum Likelihood tree of DIR1 and DIR1-like proteins. Protein sequences lacking the divergent ER signal sequence were aligned using Muscle. The evolutionary history was inferred using the Maximum Likelihood method based on the Kimura 2-parameter (Kimura, 1980) model with discrete Gamma distribution using MEGA 5 (Tamura et al., 2011). 10000 bootstrap replicates were conducted and percent bootstrap values were placed on the branches (Felsenstein, 1985). Branches were drawn to scale, measured in number of substitutions

per site and were labeled by species name followed by TAIR gene number or Phytozome 8.0 accession.

3.2.2 The occasional SAR-competent phenotype of *dir1-1* cannot be explained by changes in *DIR1* or *DIR1-like* expression

One hypothesis for the occasional SAR-competent phenotype of *dir1-1* is that under certain environmental conditions expression of *DIR1* or *DIR1-like* is enhanced leading to rescue of the SAR defect in the *dir1-1* mutant. To test this hypothesis, expression of *DIR1* and *DIR1-like* was examined in *dir1-1* during an experiment in which *dir1-1* displayed a SAR-competent phenotype. Expression in SAR-competent *dir1-1* leaves was measured using quantitative RT-PCR analysis. Wild-type Ws plants exhibited a typical SAR response in which plants induced for SAR with *Pst* (*avrRpt2*) supported 27-fold lower bacterial levels in distant leaves compared to mock-induced plants (Figure 3.2). The *dir1-1* mutant displayed a less robust SAR response, such that SAR-induced plants supported 10-fold lower bacterial levels compared to mock-induced plants. Untreated leaf tissue was collected from the same set of plants and qRT-PCR analysis confirmed that little *DIR1* was expressed in the *dir1-1* mutant providing evidence that the SAR-competent phenotype of *dir1-1* was not due to expression of *DIR1* (Figure 3.2 B). Another possibility to

explain the occasional SAR-competent phenotype of *dir1-1*, is that *DIR1-like* expression is elevated in the *dir1-1* mutant thereby compensating for the lack of DIR1. qRT-PCR results suggest that *DIR1-like* is not elevated in the mutant since *DIR1-like* transcript levels were similar in wild-type and *dir1-1* plants. Together this data suggests that the occasional SAR-competent phenotype of the *dir1-1* mutant cannot be explained by modifications to *DIR1* or *DIR1-like* expression.

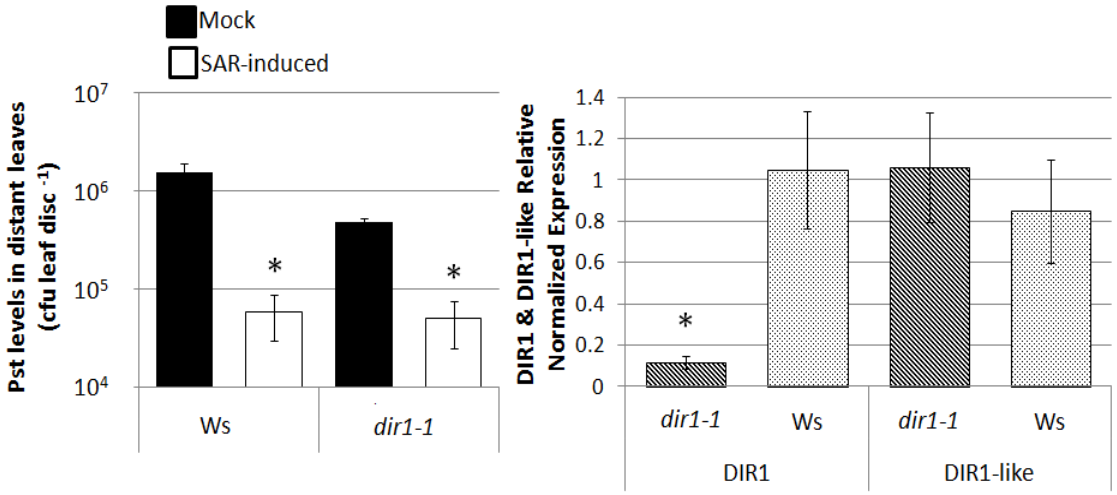

Figure 3.2: Quantitative Real Time PCR (qRT-PCR) analysis of *DIR1* and *DIR1-like* transcript abundance relative to wild-type Ws plants in untreated tissue provides evidence that *DIR1* and *DIR1-like* expression levels are not altered when *dir1-1* is SAR competent . (A) SAR assays were performed on three weeks post germination (wpg) Ws and *dir1-1* plants which were inoculated in one-two lower leaves with either 10mM $MgCl_2$ (mock-inoculated) or SAR-inducing *Pst* (*avrRpt2*) (SAR-induced). Two days later distant leaves were inoculated with virulent *Pst* and *in planta* bacterial levels were measured three days post inoculation (dpi). Asterisks (*) denote a significant difference (student t-test $p<0.05$) between distant leaf *Pst* levels in mock versus SAR-induced plants. (B) Quantitative Real Time PCR (qRT-PCR) analysis of *DIR1* and *DIR1-like* transcript abundance relative to wild-type Ws plants performed on untreated tissue of plants from the same experiment as A. A Students T-test was used to identify significant differences ($p<0.05$) compared to Ws plants and is denoted by (*).

3.2.3 Does DIR1-*like* move to distant tissues during SAR?

Despite its high sequence similarity to DIR1, DIR1-like rarely compensates for the loss of DIR1 in the *dir1-1* mutant. DIR1 has been shown to move from SAR-induced tissue to distant leaves during the SAR response (Champigny et al., 2013). Perhaps the inability of DIR1-like to compensate for lack of DIR1 lies in a compromised ability to travel to distant tissues during SAR. To address this question, the Agro-SAR assay was used to monitor DIR1-like movement during SAR

In the Agro-SAR assay *DIR1* is transiently expressed in one leaf of *dir1-1* using *Agrobacterium tumefaciens,* followed by a SAR assay (Reviewed in Figure 1.5, Chapter 1). The *Agrobacterium*-treated and SAR-induced leaf is the only source of DIR1 since *dir1-1* expresses insignificant levels of DIR1. Thus, DIR1 protein detected in petiole exudates from local or distant

leaves traveled there from the site of SAR induction in the inoculated leaf. Protein gel blot analysis indicates that the DIR1 antibody recognizes DIR1 and DIR1-like but not a similar LTP2sw protein (Champigny et al., 2013), providing a tool to monitor DIR1-like movement. Therefore, probing exudates of the *dir1-1* mutant with the DIR1 antibody should detect DIR1-like.

We employed the Agro-SAR assay and collected petiole exudates to monitor DIR1 or DIR1-like movement. *Agrobacterium*-expression of *DIR1-EYFP* in *dir1-1* followed by a SAR assay resulted in a robust SAR response in SAR-induced with *Pst* (*avrRpt2*) compared to mock-inoculated plants, indicating that ectopically expressed DIR1 complements the *dir1-1* mutant (Figure 3.3 A). *Agrobacterium*-expression of EYFP in *dir1-1* did not complement the mutant, where bacterial density of distant leaves inoculated with virulent *Pst* was similar in SAR-induced and mock-inoculated plants. Protein gel blots of petiole exudates collected from distant leaves show a DIR1-sized signal in SAR-induced DIR1-EYFP expressing plants by 24 hours post inoculation (hpi) (Figure 3.3 B). Interestingly, bands appear in both DIR1-EYFP SAR-induced and EYFP expressing plants by 48 hpi. Since DIR1 expression is severely reduced in the EYFP expressing *dir1-1* plants and our DIR1 antibody detects recombinant DIR1-like, this suggests that DIR1-like moves to distant tissue during SAR but it is only detected at the 24-48 hour timepoint compared to DIR1 which is detected at 14-24 hours. This suggests that similar to DIR1, DIR1-like has the capacity to move from induced to distant tissues, which supports the hypothesis that DIR1-like may occasionally compensate for the lack of DIR1 in the *dir1-1* mutant.

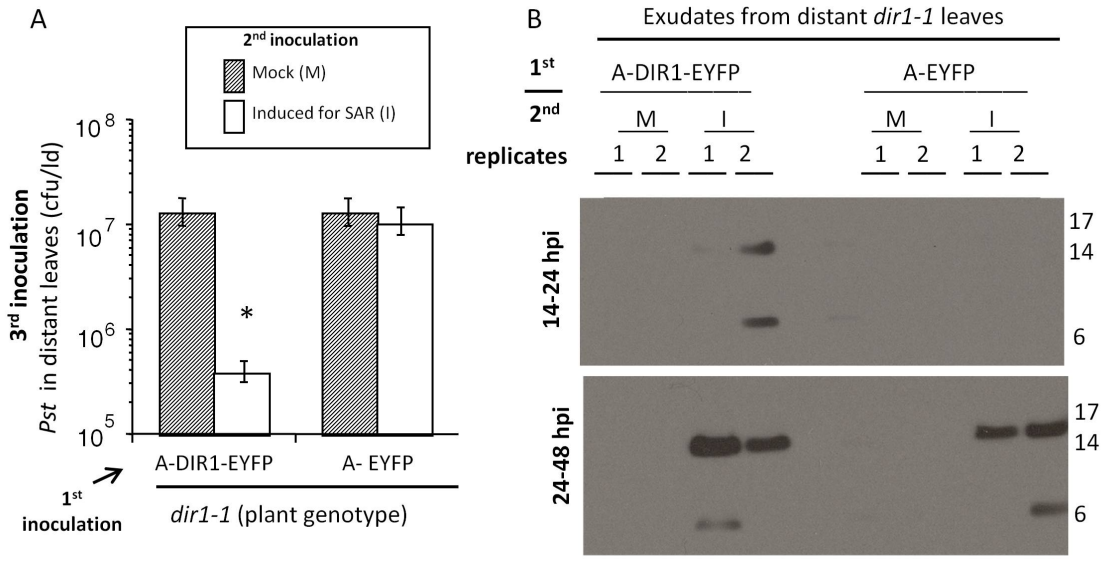

Figure 3.3. DIR1-EYFP Agro-SAR assay and DIR1-antibody signals in *dir1-1* distant leaf exudates.
(A) The Agro-SAR assay involves three inoculations. First, *Agrobacterium* is inoculated into two lower leaves. Second, after four days, the same leaves are inoculated with either 10 mM $MgCl_2$ (Mock-inoculation) or *Pst* (*avrRpt2*) to induce SAR (SAR-induced). After two more days, the upper leaves are inoculated with virulent *Pst*. Three dpi *in planta* bacterial levels of *Pst* in distant leaves were determined. Asterisks (*) denote a significant difference (student t-test $p<0.05$) between distant leaf bacterial levels of mock vs SAR-induced plants. (B) Petiole exudates were collected (14 to 48 hpi) from distant leaves (Dis) of plants which received a 1st inoculation with either *Agrobacterium* expressing EYFP or DIR1-EYFP, followed by a 2nd inoculation with either mock (M) or SAR-inducing *Pst*(*avrRpt2*). Petiole exudates were lyophilized and subjected to protein gel blot analysis with DIR1 antibodies. This experiment was repeated twice with similar results.

3.2.4 Tools to monitor DIR1-like movement

The polyclonal DIR1 antibody does not distinguish between the highly similar DIR1 and DIR1-like proteins. To circumvent this issue we designed DIR1 and DIR1-like fusion proteins with different epitope tags. Previous attempts to generate stable DIR1-fusion proteins, DIR1-GUS (Champigny et al., 2011) and DIR1-GFP (Champigny et al., 2013) in stably expressing transgenic lines resulted in the cleavage of the tag *in planta*. Both GFP and GUS encode fairly large proteins (28 and 75 kDa) which may alter DIR1 function/stability *in planta.* Furthermore, both proteins were fused to the C-terminal end of DIR1, which encodes a cysteine residue that participates in a disulphide bond. The attachment of the tag to this cysteine residue may interfere with protein folding/stability which may lead to cleavage. To increase the probability of producing a stable fusion protein, a smaller fusion protein or an alternative attachment location was pursued.

To generate stable epitope-tagged DIR1- and DIR1-like *in planta,* we designed constructs encoding a dual fusion at both the N- and C-terminal end of DIR1/DIR1-like (Figure 3.4). Since both DIR1 and DIR1-like harbour an ER signal sequence (SS), all N-terminal fusions were sandwiched between the SS and the mature protein to ensure proper localization/targeting *in planta*. We chose two tags, the first being a small epitope tag (HA/FLAG) at the N-terminal region after the SS, and the second a small fluorescent protein at the C-terminal end (iLOV/phiLOV). The iLOV (Light, oxygen or voltage sensing domain) (Chapman et al., 2008) and phiLOV (Christie et al., 2012) tags are small fluorescent proteins (~10 kDa) derived from photoreceptors and have been shown to outperform GFP in tobacco (Chapman et al., 2008). To aid in the future characterization of DIR1/DIR1-like movement during SAR, we designed SS-

HA-DIR1-iLOV and SS-Flag-DIR1-like-phiLOV constructs. We predict the use of smaller tags and their presence on the N terminus of DIR1 or DIR1-like will eliminate *in planta* cleavage of the tags. Rare restriction enzymes not present in the vectors used for creating transgenic lines were included on either side of the N-terminal tags (designed by P. Carella and M. Isaacs) making it possible to easily switch in new tags in the future.

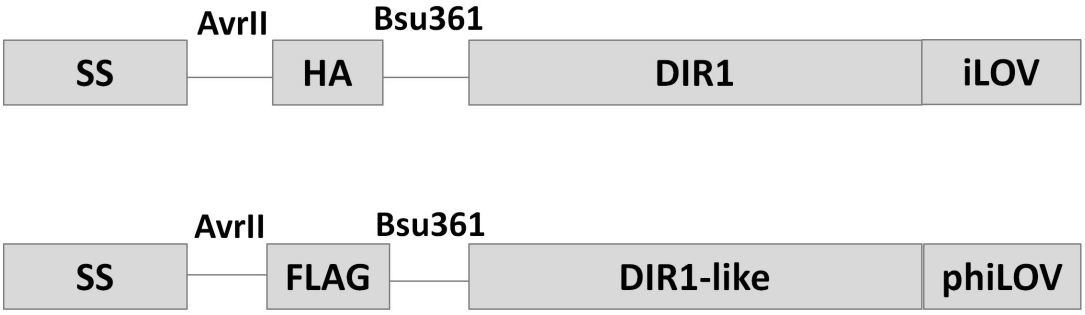

Figure 3.4: Illustration of SS-HA-DIR1-iLOV and SS-FLAG-DIR1-like-phiLOV constructs where AvrII and Bsu361 restriction sites were included to facilitate easy swapping of the N-terminal tags.

The SS-HA-DIR1-iLOV and SS-FLAG-DIR1-like-phiLOV constructs were manufactured by a gene synthesis company (Biobasic) and then I cloned them into pMDC32 plasmid (Curtis and Grossniklaus, 2003) with a 2x35S promoter. These constructs were transformed into *Agrobacterium* (GV3101) and used to transform *Arabidopsis dir1-1* plants using the floral dip protocol (Clough and Bent, 1998; Zhang et al., 2006). T_1 seeds collected from the dipped T_0 generation are currently being screened on MS media supplemented with hygromycin (transgene selection) and cefotaxime (antibiotic to eliminate residual *Agrobacterium* contamination).

To check for *in planta* stability and to validate the constructs before stably transforming *Arabidopsis, Agrobacterium* was used to transiently express SS-HA-DIR1-iLOV in *Nicotiana benthamiana.* iLov expression was examined by monitoring fluorescence using confocal microscopy three days after *Agrobacterium* inoculation (SS-HA-DIR1-iLOV) (Figure 3.5). Enhanced fluorescence was observed in leaves inoculated with *Agrobacterium* (SS-HA-DIR1-iLOV) compared to the mock-inoculated leaves. This suggests that the SS-HA-DIR1-iLOV fusion protein is being expressed. However, a protein gel blot of leaf protein extracts is necessary to see whether or not iLOV is still attached to DIR1.

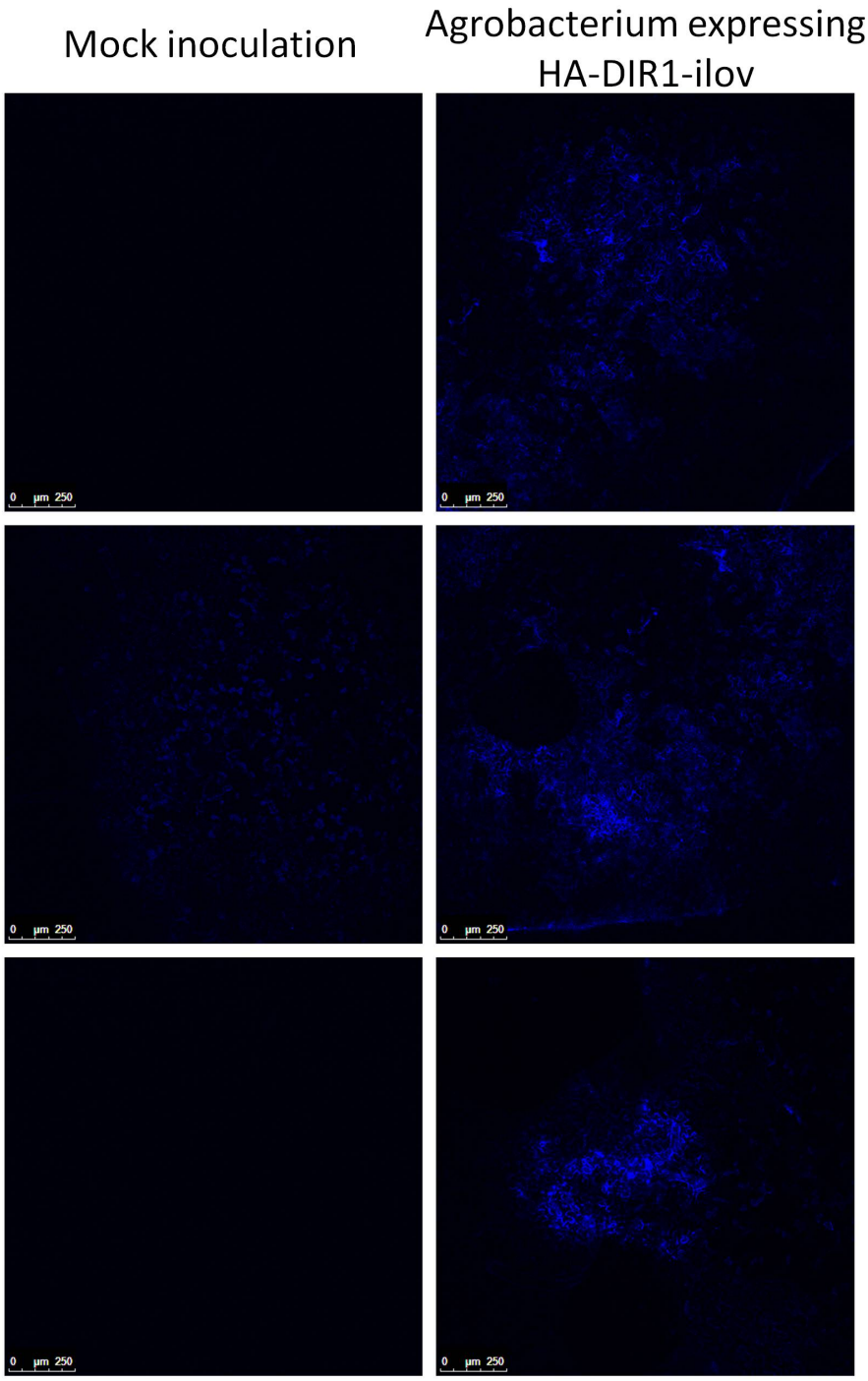

Figure 3.5: Transient expression of SS-HA-DIR1-iLOV in tobacco (*Nicotiana benthamiana)*. Tobacco plants (3 wpg) were inoculated with *Agrobacterium* expressing SS-HA-DIR1-iLOV and fluorescence was examined using a confocal microscope three dpi at an excitation

wavelength of 476nm and emission was collected between 510-550nm. Scale 0-240 μm.

3.2.5 Creation of a *dir1-1 dir1-like* double mutant for elucidating the importance of DIR1-like during SAR

3.2.5.1 Antisense Lines

If DIR1 and DIR1-like are both involved in SAR and if no other functionally redundant proteins exist, then a double *dir1-1dir1-like* mutant should result in complete loss of SAR while a *dir1-like* single mutant should be compromised in SAR. The LTP1 protein AZI1 is required for SAR and therefore could be a candidate for functional redundancy. Currently, there are no T-DNA insertional mutants available for *DIR1-like*. The creation of double and single mutants would be an extremely useful tool to dissect the role of highly similar DIR1 and DIR1-like during SAR. Furthermore, a *dir1-1 dir1-like* double mutant may provide a more robust system for SAR studies since the *dir1-1* mutant is occasionally SAR competent.

Using antisense technology, *DIR1-like* antisense DNA was transformed into the *dir1-1* (T-DNA mutant) line and wild-type Ws plants, thereby creating a single and double mutant respectively (35S:antisenseDIR1-like/*dir1-1* and 35S:antisenseDIR1-like/Ws). Several antisense segments were used to maximize the likelihood of success (Table 3.1).

Table 3.1: Antisense constructs created and the predicted mutants generated after transformation into the wild-type Ws or *dir1-1* mutant background.

Constructs	**Predicted Transgenic Mutants**	
	Ws	***dir1-1***
DIR1-like cDNA antisense (D)[a]	*dir1-like*	*dir1-1 dir1-like*
Antisense with small region where DIR1 and DIR1-like are the same (C) [a]	*dir1-1 dir1-like*	*dir1-1 dir1-like*

Antisense with small region unique to DIR1-like (B) [a]	*dir1-like*	*dir1-1 dir1-like*

[a] D,C,B are designators of the construct used and appear in the qRT-PCR screens.

Antisense constructs were generated in the plant transformation vector pMDC32 (Curtis and Grossniklaus, 2003) containing a 35S promoter using Invitrogen Gateway technology and transformed into *Agrobacterium tumefaciens* (GV3101). *Arabidopsis* was transformed using *Agrobacterium* containing the antisense vector using the floral dip protocol (Clough and Bent, 1998; Zhang et al., 2006). T_1 seeds were collected from the T_0 generation and screened on MS media supplemented with hygromycin (transgene selection) and cefotaxime (antibiotic to eliminate Agro contamination). Hygromycin resistant T_1 plants were allowed to self fertilize. The T_2 generation was examined for single copy insertions based on hygromycin resistance ratios in entire seedling population which should be 1 (homozygous no insertion, hygromycin sensitive) to 2 (heterozygous insertion, hygromycin resistant) to 1 (homozygous insertion, hygromycin resistant). Therefore T2 plants lines whose population deviated from this ~75% resistance ratio were considered to have multiple copies of the insertion and the lines were not carried to the T3 generation.

T2 lines were screened for *DIR1* and *DIR1-like* expression using qRT-PCR. Genevestigator (plant biology) identified two reference genes with similar transcript abundance to our target genes and displayed expression stability with biotic challenge (5FCL- AT5G13050 and AT5G25800). In accordance with the MIQE qRT-PCR guidelines, primers were validated before use. See appendix figure 6.1, 6.2, 6.3, 6.4 for a summary of the primer validation. Briefly, gene specific primers with low secondary

structure (confirmed by mfold http://mfold.rna.albany.edu/) were validated for specificity and efficiency using an 8-point standard curve and purified products were Sanger sequenced to confirm identity. The sequence available for creation of *DIR1-like* primers was limited because detection of endogenous transcript rather than antisense transcript requires one of the two primers to be outside of the antisense construct (See Figure 2.1). Out of the 5 different primers assayed only one had an acceptable efficiency (116%). Because the efficiency was 6% higher than suggested (90-110%), the efficiency was included in the normalization calculations which adjusted the values to compensate for the higher efficiency (Figure 3.6).

DIR1 and *DIR1-like* transcript abundance was measured in T2 *DIR1-like* antisense *dir1-1* transgenic plants. If *DIR1-like* expression levels were lower than the wild-type Ws control then these potential *dir1-1 dir1-like* double knockdown T2 lines were taken to the T3 generation. The corresponding T3 plants were then analyzed for DIR1 and DIR1-like expression to identify stable *dir1-1 dir1*-like double knockdowns. Figure 3.6 depicts transcript abundance of *DIR1* and *DIR1-like* in T2 & T3 generation plants normalized to the reference 5FCL and At3g25800. Fold-expression was calculated relative to the wild-type Ws control. As expected, the T2 antisense lines displayed reduced *DIR1* expression similar to the parental *dir1-1* plant, whereas wild-type *DIR1* levels were observed in Ws. The abundance of *DIR1-like* was similar in the Ws and *dir1-1* controls, but varied among the T2 lines. Several plant lines of interest were identified in the T2 generation (highlighted in Figure 3.6) and were examined in the T3 generation. The plant line CT2-27(1) (where C = the type of construct used as outlined in table 3.1) had the greatest reduction in *DIR1-like* levels at 4-

fold less than wild-type. CT2-27(2) had 2-fold less *DIR1-like* expression compared to wild-type. It is difficult to test T2 plant lines because the antisense transgene is segregating and therefore 67% of the plants will be heterozygous for the insertion and 33% will be homozygous. It is therefore not possible to analyze T2 plants in biological triplicate because each plant must be tested individually. Therefore no statistical analysis could be performed on the T2s.

The plant lines that looked promising in the T2 generation displayed wild-type *DIR1-like* expression in the T3 generation. This trend occurred in every line pursued (See appendix for additional screens Figure 7.5). The inability to find *dir1-like* or *dir1-1dir1-like* mutants in the T3 generation along with an absence of seed production in three promising putative double mutant lines suggested that perhaps a *dir1-1dir1-like* double mutant is lethal. This hypothesis is strengthened by the fact that *dir1-1* mutant seed germinates poorly on soil (unpublished). Both *DIR1* and *DIR1-like* are expressed during seed development (Toronto BAR) (Winter et al., 2007), however their function during seed development has not been previously examined. The inability to collect seed from several antisense lines as well as the germination phenotype of *dir1-1* leads to the hypothesis that DIR1 and DIR1-like may play an important role during seed development.

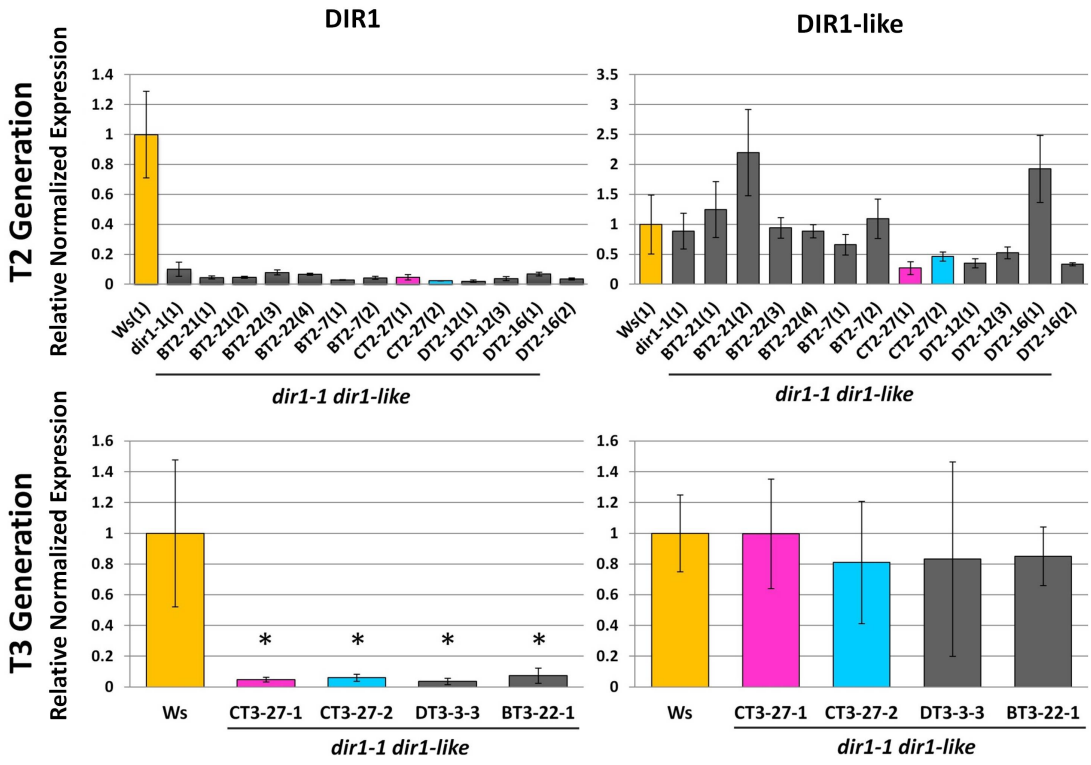

Figure 3.6: Quantitative Real Time PCR (qRT-PCR) analysis of *DIR1* and *DIR1-like* transcript abundance relative to wild-type Ws plants in untreated T2 and T3 plants collected at three wpg. Values were normalized to 5CFL and AT5G25800 reference genes. Fold-expression was calculated relative to the wild-type Ws control. Ws wild type plants are highlighted in yellow and two plant lines of interest are highlighted in pink and blue. T2 tissue was collected from a single plant and analyzed in three technical replicates. T2 error bars represent the standard deviation of the technical variation. Homozygous T3 tissue was collected in biological triplicate and analyzed in technical triplicates. T3 error bars represent the standard deviation of the biological variation. A Students T-test was used to identify significant differences ($p<0.05$) compared to Ws plants and is denoted by (*). B,C,D abbreviations indicate the type of antisense construct used (See table 3.1). Expected mutation is identified below the construct identifier.

Table 3.2 highlights the large number of plant lines screened. A total of 100 plants were screened to identify *dir1-1dir1-like* double mutants and 36 plants were screened for single *dir1-like* mutants in the T2 generation. The insertion site of a transgene can make a big difference in its expression. The T-DNA may insert into a transcriptionally active or inactive location in the genome and therefore it is important to screen seeds from more than a signal insertion event. Therefore 52 unique T2 insertions were screened. Due to the inability to isolate T3s with reduced DIR1-like expression work on the antisense lines was terminated.

Table 3.2: Outline of transgenic antisense lines tested.

	Ws		
CONSTRUCTS	**Predicted mutation**	**# of T2 Insertions[a] Screened**	**# of T3s with ½ DIR1-like expression**
DIR1-like cDNA antisense (D)	*dir1-like*	6 insertions (6 plants)	0
Antisense with small region where DIR1 and DIR1-like are the same (B)	*dir1-1 dir1-like*	0	0
Antisense with small region unique to DIR1-like (C)	*dir1-like*	8 insertions (32 plants)	0
	dir1-1		
CONSTRUCTS	**Predicted mutation**	**# of T2 Insertions Screened**	**# of T3s with ½ DIR1-like expression**
DIR1-like cDNA antisense (D)	*dir1-1 dir1-like*	13 insertions (43 plants)	0
Antisense with small region where DIR1 and DIR1-like are the same (B)	*dir1-1 dir1-like*	15 insertions (25 plants)	0
Antisense with small region unique to DIR1-like	*dir1-1 dir1-like*	11 insertions (32 plants)	0

(C)

[a]Insertions indicate a descendent of a unique T1 insertion screened.

3.2.5.2 DIR1-like RNAi lines

Antisense technology was chosen for single and double *dir1-1 dir1-like* and *dir1-like* mutant construction because of the earlier success in creating DIR1 antisense lines (Maldonado et al., 2002). It is unclear if DIR1-like reduced expression mutants were not identified due to lethality issues associated with DIR1 and DIR1-like or due to silencing of the antisense construct in the T3 generation. Silencing of transgenes is a recurring problem in transgenic plant production. Transgenes can be silenced through transcriptional gene silencing (TGS) where the foreign transgene DNA becomes methylated reducing transcription (Reviewed in Stam et al., 1997).

Others have observed transgene silencing between the heterozygote and homozygous generations (Reviewed in Stam et al., 1997). Although both antisense and RNAi forms of post translational gene silencing (PTGS) have been used effectively in plants, there is evidence in *C.elegans* (Fire et al., 1998) and *Arabidopsis* (Wesley et al., 2001) that RNAi is more effective and specific than antisense technology.

To avoid possible antisense and lethality issues, DIR1-like RNAi constructs have been inserted into *dir1-1* and Ws background plants (double and single mutants respectively) under the control of a constitutive promoter (35S) or an estrogen inducible promoter (XVE). It is predicted that these RNAi lines may be more effective at silencing DIR1 and DIR1-like expression. To avoid the possible seed lethality issue, estrogen inducible lines will also be created to reduce expression of DIR1-

like only in adult plants and not during seed production, maturation or germination. T2 plants are currently being screened.

Chapter 4: Examination of Cucumber DIR1 ortholog structure and its ability to rescue the SAR defect in *Arabidopsis dir1-1*

Preface

Section 4.2.1.2 homology modeling was conducted in consultation with protein modeling expert Dr. Dan Yang (McMaster, Department of Biochemistry). Cucumber DIR1 complementation and cucumber expression profiles (section 4.2.2 & 4.2.3) were completed with the help of Philip Carella. Preliminary TNS inhibition binding assays were performed at McMaster University by Philip Carella to standardize the protocol for our lab.

4.1 Introduction

If the mechanisms responsible for the SAR response are conserved in commercially important crop species then these plants may possess DIR1 orthologs. Cucumber DIR1 orthologs were of initial interest because like *Arabidopsis,* cucumber (*Cucumis sativus*) has been used as a SAR model

organism. Cucumber was rarely used in SAR studies once the *Arabidopsis-Pst* SAR model system was developed (Cameron et al., 1994). Recently the genome sequence of cucumber has become available (November 2009) (Huang S. et al., 2009). Moreover, cucumber displays a very robust SAR response and concentrated highly pure phloem samples can be collected from cucumber. For all these reasons cucumber has once again become a very attractive model for SAR studies.

Evidence for the conservation of mobile SAR signals across diverse species has been obtained in number of studies. For example petiole exudates from SAR-induced *Arabidopsis* were shown to promote SAR in both a dicot (tomato) and a monocot (wheat) (Chaturvedi et al., 2008). Several DIR1 orthologs have been identified including a putative DIR1 ortholog, LeDIR1 (TomDIR1) in tomato and western analysis confirmed its presence in the phloem of untreated plants (Mitton et al., 2009). Transgenic *Arabidopsis* plants expressing two different tobacco DIR1 orthologs complemented the SAR-defect in *dir1-1* (Liu et al., 2011). Moreover, petiole exudates collected from SAR-induced cucumber restored SAR in the *Arabidopsis* SAR-defective mutant *dir1-1* and western blots using *Arabidopsis* AtDIR1 antibodies on cucumber petiole exudates produced a 7 kDa AtDIR1 antibody signal (Cameron Lab, unpublished). Taken together, these studies suggest that SAR mobile signals and DIR1 are involved in SAR in diverse plant families.

The goal of this chapter is to discover putative DIR1 orthologs, obtain evidence that they are in fact orthologous to AtDIR1 and provide support for the hypothesis that these orthologs participate in SAR.

4.2 Results

4.2.1 Cucumber DIR1 orthologs are similar to *Arabidopsis* AtDIR1

4.2.1.1 Sequence similarity and phylogeny of putative DIR1 orthologs

Using Phytozome (phytozome.net) the mature AtDIR1 protein sequence was used in a blast search (tBLASTn) against the cucumber genome along with several other plant genomes (Table 4.1). Several putative orthologs were identified and share higher than 50% sequence similarity suggesting that the sequences have a common ancestry. In other words they likely originated from a single ancestral gene but were separated by several speciation events (vertical descent). However, sequence similarity alone is not enough to definitively say that these proteins are orthologs, as sequences often share similar motifs due to convergent evolution. Additional evidence of their shared ancestry is required, such as their ability to perform the same or equivalent function, which can be tested through complementation (Reviewed in Koonin, 2005). In *Arabidopsis thaliana* the highest sequence similarity to AtDIR1 is with AtDIR1-like and all other *Arabidopsis* proteins share less than 51% sequence similarity. AtLTP2sw (similar to wheat LTP2) is an *Arabidopsis* LTP2 protein that was selected as an outgroup for the AtDIR1 phylogenetic study as its wheat ortholog has been characterized and crystallized and it shares a lower sequence similarity with AtDIR1 (38%) than all other putative orthologs from this study. By sharing a common ancestor with the other members of the tree but being the most distantly related, the outgroup provides a direction of evolution to the phylogenetic tree. In other words the outgroup allows the location of the root of the tree to be identified.

Without a root, the relationship among nodes is provided but there is no information about ancestry or the direction of time.

Table 4.1: Sequence similarity and identity of putative DIR1 orthologs.

Organism	**Protein**	**Amino Acid Sequence Similarity** [a]	**Amino Acid Sequence Identity** [a]
Arabidopsis thaliana	AtDIR1-like	88%	80%
	AtwLTP2	38%	27%
	AT5G55410 (Best hit after DIR1-like)	51%	28%
Arabidopsis lyrata	LyrDIR1	96%	93%
	LyrDIR1-like	87%	80%
Brassica rapa	RapaDIR1	83%	72%
Thellungiella salsuginea (Eutrema salsugineum)	ThellDIR1	86%	77%
Nicotiana tabacum Tobacco	TobDIR1	62%	52%
	TobDIR2	57%	44%
	TobDIR3	67%	51%
Solanum lycopersicum Tomato	TomDIR1	63%	50%
	TomDIR2	63%	47%
	TomDIR3	58%	46%
Cucumis sativus Cucumber	CucDIR1	61%	48%
	CucDIR2	65%	47%
Glycine max Soybean	SoyDIR1	59%	47%
	SoyDIR2	57%	46%
	SoyDIR3	61%	49%

[a] The EMBOSS Needleman-Wunsch algorithm was used to determine percent sequence similarity and identity.

Using the sequences of putative DIR1 orthologs from table 4.1 a phylogenetic tree of DIR1 orthologs was created (Figure 4.1). If this phylogeny is compared to the *Brassicaceae* phylogeny from Chapter 3 (Figure 3.1), this tree still supports a tandem duplication of AtDIR1 in an ancestor of *Arabidopsis lyrata* and *thaliana,* despite the addition of new sequence information. However, this new phylogeny predicts independent DIR1 duplications in tomato, cucumber, tobacco, and soybean that may be lineage specific. If these duplication events are determined to be lineage-specific then they are referred to as inparalogs. If these duplication events occurred in a common ancestor, they are referred to as outparalogs. It appears that the only lineage-specific duplication event in this phylogeny is in soybean (*Glycine max*) where SoyDIR1 and SoyDIR2 are inparalogs. All other duplication events appear to have occurred in a common ancestor. The phylogeny suggests that in tomato and tobacco two duplication events produced three outparalogs.

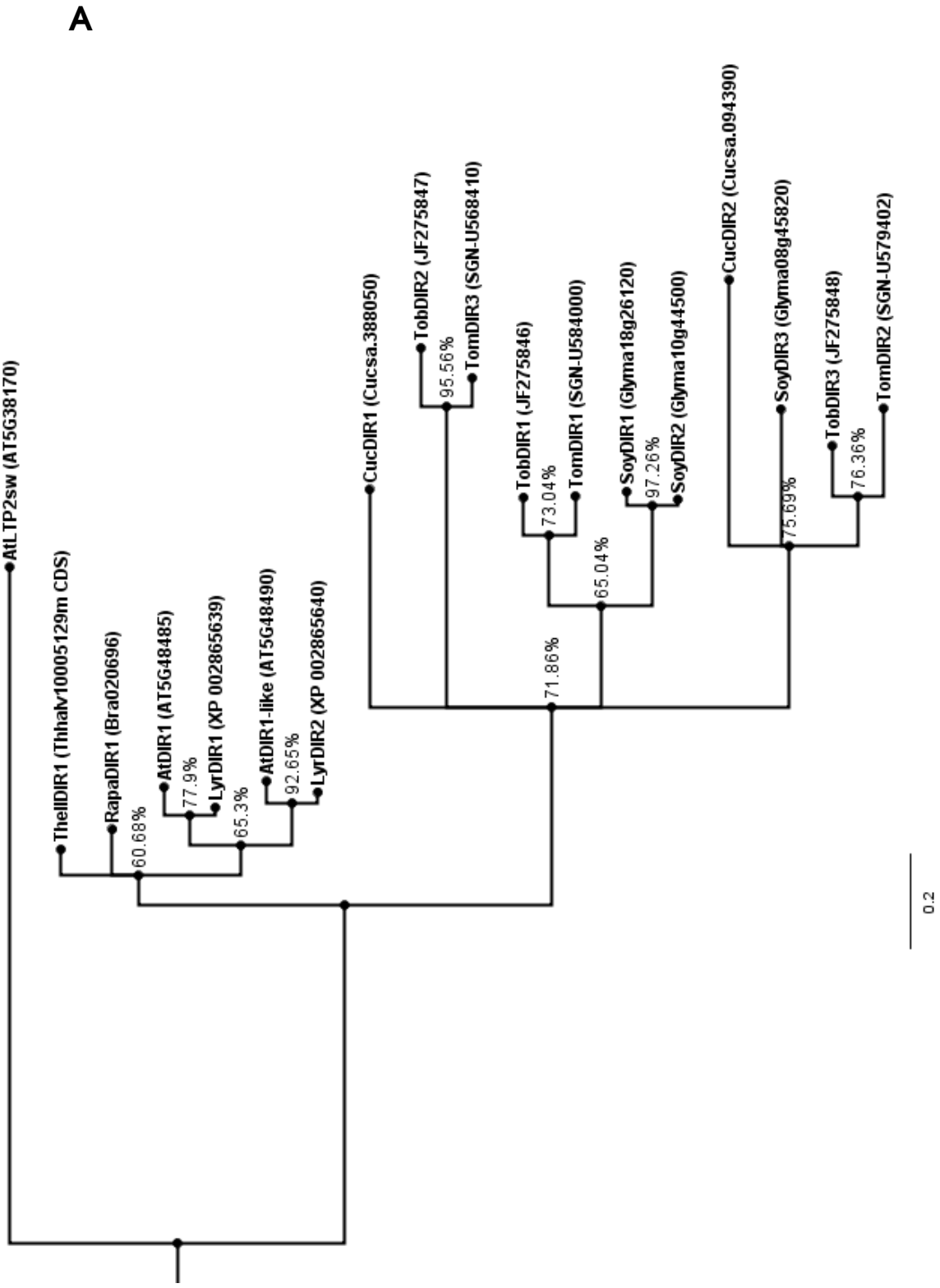
A
AtLTP2sw (AT5G38170)
ThellDIR1 (Thhalv10005129m CDS)
RapaDIR1 (Bra020696)
AtDIR1 (AT5G48485)
LyrDIR1 (XP 002865639)
AtDIR1-like (AT5G48490)
LyrDIR2 (XP 002865640)
CucDIR1 (Cucsa.388050)
TobDIR2 (JF275847)
TomDIR3 (SGN-U568410)
TobDIR1 (JF275846)
TomDIR1 (SGN-U584000)
SoyDIR1 (Glyma18g26120)
SoyDIR2 (Glyma10g44500)
CucDIR2 (Cucsa.094390)
SoyDIR3 (Glyma08g45820)
TobDIR3 (JF275848)
TomDIR2 (SGN-U579402)
60.68%
77.9%
65.3%
92.65%
95.56%
73.04%
71.86%
65.04%
97.26%
75.69%
76.36%
0.2

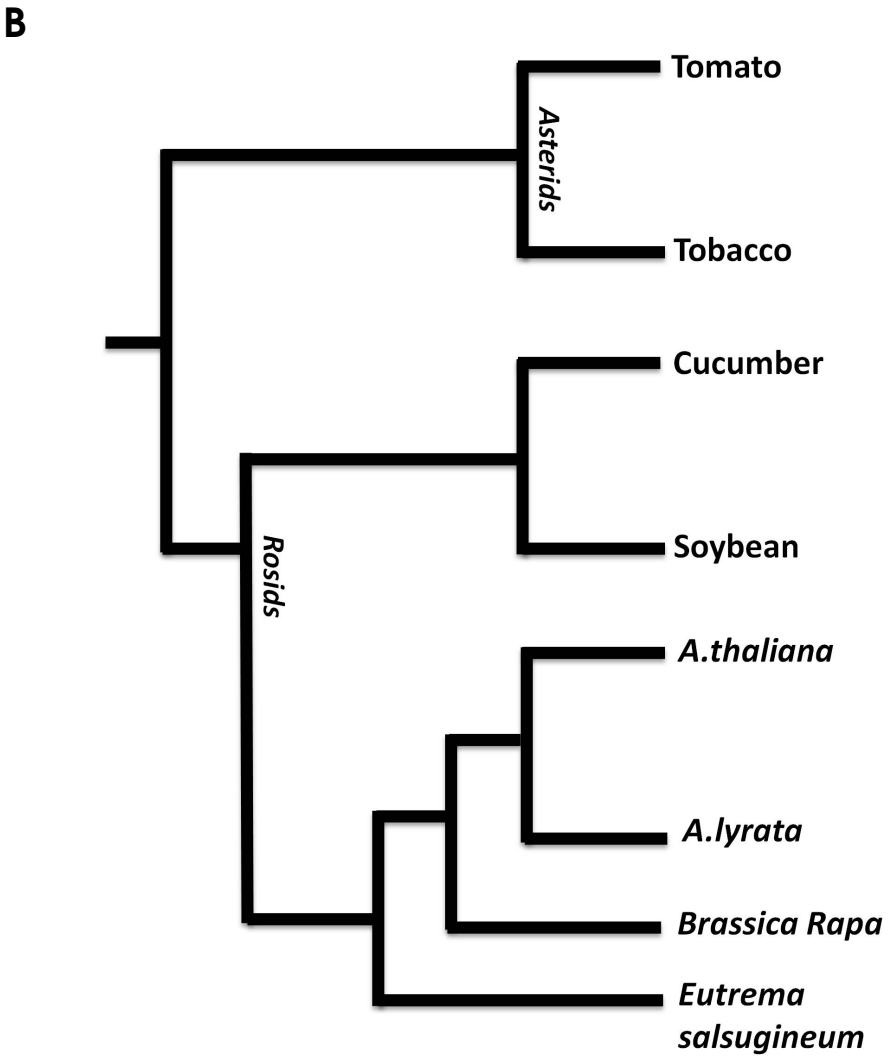

Figure 4.1: Phylogeny of DIR1 orthologs and Cladogram of organism relationships. A) Rooted Phylogenetic Maximum Likelihood tree of putative DIR1 orthologs. Protein sequences lacking the divergent ER signal sequence were aligned using MUSCLE. The evolutionary history was inferred using the Maximum Likelihood method based on the Kimura 2-parameter (Kimura, 1980) model with discrete Gamma distribution using MEGA 5 (Tamura et al., 2011). 10,000 bootstrap replicates were conducted and percent bootstrap values were placed on the branches (Felsenstein, 1985). Nodes with bootstrap values below 50% were collapsed using Archaeopteryx software (Han and Zmasek, 2009). Phylogeny was viewed in FigTree v1.4 (Drummond et al., 2012). Branches were drawn to scale, measured in number of substitutions per site and branches were labeled by species name followed by TAIR gene number

or Phytozome 8.0 accession. B) Species cladistic tree show general relationships between the species studied and was created based on the phytozome tree (Goodstein et al., 2012).

4.2.1.2 Homology modeling of cucumber orthologs

Homology modeling was used to compare the protein structure of *Arabidopsis* AtDIR1 and the putative cucumber orthologs, CucDIR1 and CucDIR2. Using the AtDIR1-phospholipid crystal structure (Lascombe et al., 2006; Lascombe et al., 2008) as a template, a homology model of each cucumber ortholog was computed using the SWISS-MODEL server (Figure 4.2) (Peitsch, 1995; Guex and Peitsch, 1997; Schwede et al., 2003; Arnold et al., 2006; Kiefer et al., 2009). AtDIR1 and both the cucumber orthologs share a similar hydrophobic cavity into which the hydrophobic tails of the phospholipids extend (Figure 4.2A). Interestingly, the AtDIR1 PxxPxxP (where P is proline and x is any amino acid) motif that was highlighted by Lascombe et al. (2008) as a potential site of protein-protein interaction is different in the cucumber orthologs. CucDIR1 and CucDIR2 possess a proline rich region that is offset by 2 and 10 residues respectively compared to the AtDIR1 PxxPxxP motif location. CucDIR1 contains a PxPxxxPP motif while CucDIR2 contains a PPxPxPP motif (Figure 4.2B). Another region considered to be important for phospholipid docking is the hydrophilic residues at the cavity entrance. Lascombe et al. (2008) postulated that these charged residues may interact with the hydrophilic region of a putative ligand while the hydrophobic portion is bound in the cavity. AtDIR1 possesses three hydrophilic residues within 5 Å of the phospholipids (GLN9, ASN13, LYS16) while CucDIR1 and CucDIR2 both possess two (TYR7, ARG10 and GLU8, THR12 respectively) (Figure 4.2C). Based on this homology modeling, it appears that the cucumber orthologs are very similar to AtDIR1 in structure.

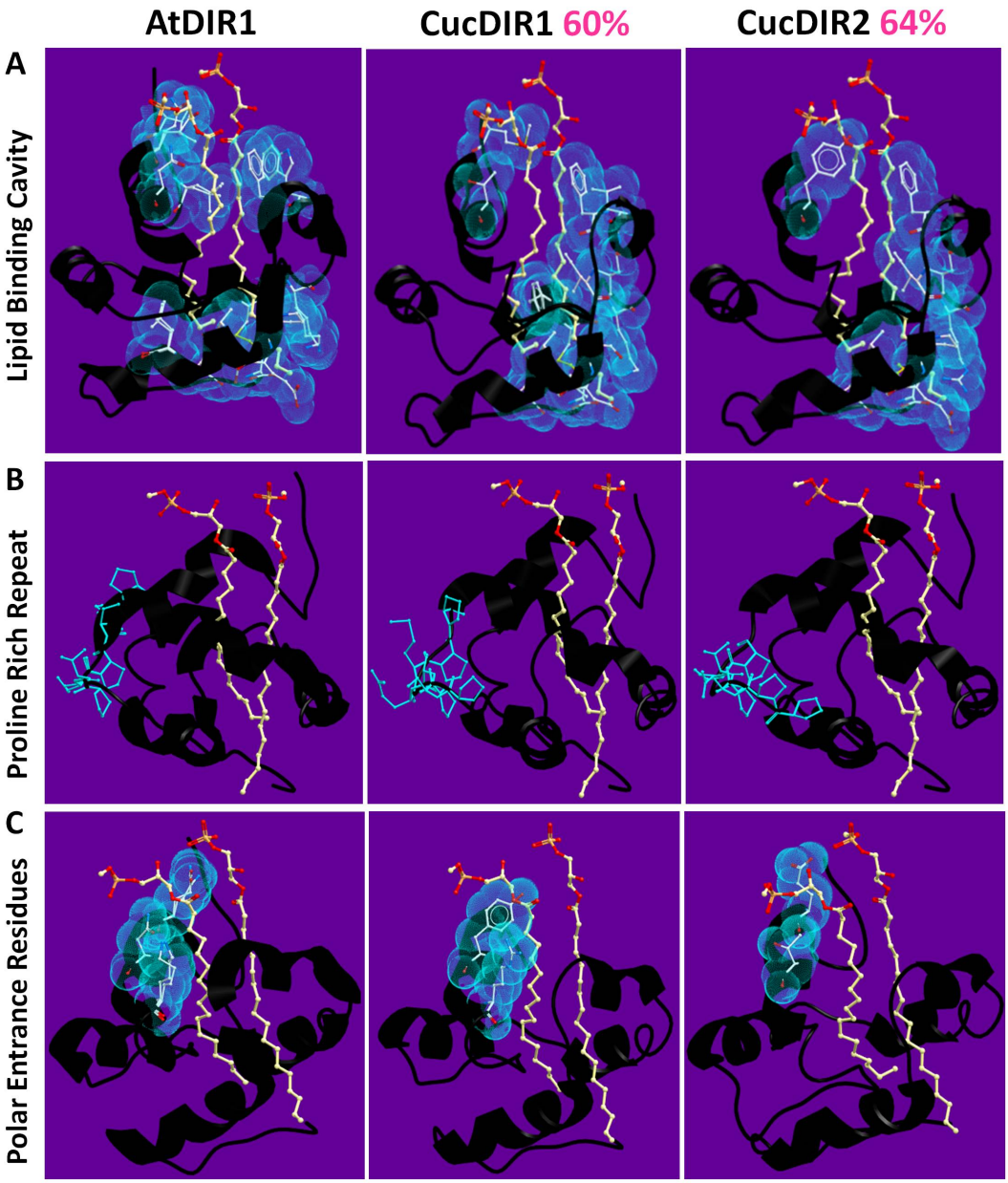

Figure 4.2: Homology models of CucDIR1 and CucDIR2 using AtDIR1-phospholipid crystal structure (Lascombe et al., 2006; Lascombe et al., 2008) as a template and modeled with SWISS-MODEL 4.0.1 server (Peitsch, 1995; Guex and Peitsch, 1997; Schwede et al., 2003; Arnold et al., 2006; Kiefer et al., 2009) and viewed using Molsoft ICM browser. Percent sequence similarity compared to AtDIR1 is identified in pink. (A-C) phospholipids in orange (phosphate), red (oxygen) and white (carbon). (A) The hydrophobic residues (blue) that are within 5 Angstroms of the

phospholipids highlight the inner hydrophobic cavity of these LTP2 proteins. (B) The proline rich repeats are highlighted in blue. (C) The polar residues at the cavity entrance are highlighted in blue.

4.2.2 Can Cucumber DIR1 orthologs rescue the *dir1-1* SAR defect?

If cucumber DIR1 orthologs perform a similar function during SAR as *Arabidopsis* AtDIR1 then it should be possible to complement the *dir1-1* mutant with CucDIR1 or CucDIR2. This would also provide additional evidence that these proteins are functionally conserved orthologs of AtDIR1. CucDIR1 was cloned into plant transformation vector pMDC32 (Curtis and Grossniklaus, 2003) under the control of a 35S promoter, followed by transformation into *Agrobacterium* strain GV3101 for use in transient Agro-SAR transformation experiments (Reviewed in Chapter1, Figure 1.5). CucDIR1 was transiently expressed in one leaf of the *Arabidopsis dir1-1* mutant followed by induction of SAR in the same leaf. The SAR response was monitored by inoculation of two to three distant leaves with virulent *Pst* (Figure 4.3). As expected, transient expression of DIR1-EYFP complemented the *dir1-1* mutation as indicated by a significant 4.6-fold reduction in bacterial density in distant leaves of SAR-induced plants compared to mock-inoculated control plants. Expression of EYFP alone did not complement the SAR defect in *dir1-1*, confirming that *Agrobacterium* infection or expression of EYFP alone is not capable of inducing a SAR response. Expression of CucDIR1 in one leaf of the *dir1-1* mutant resulted in a significant 11.6-fold reduction in *Pst* levels in SAR-induced versus mock-inoculated plants. Therefore CucDIR1 complemented the *dir1-1* mutation and performed an equivalent function as AtDIR1 providing additional evidence that CucDIR1 and AtDIR1 are orthologs.

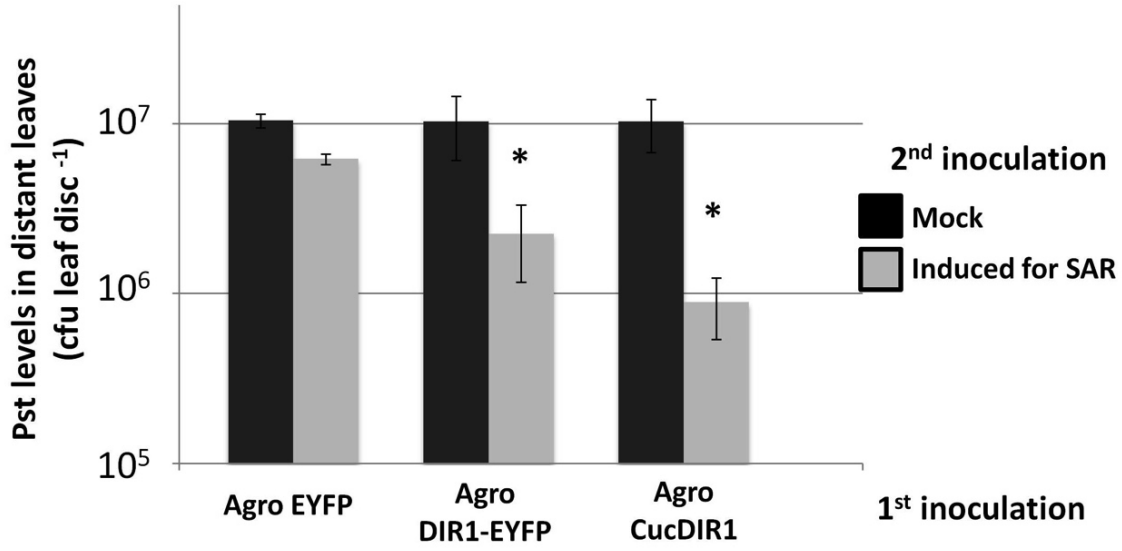

Figure 4.3: CucDIR1 Agro-SAR assay. 1st inoculation: two leaves of *dir1-1* were inoculated with *Agrobacterium* expressing EYFP, DIR1-EYFP or CucDIR1. 2nd inoculation: four days later the same two leaves were either mock-induced with 10 mM $MgCl_2$ or induced for SAR with 10^6 cfu ml^{-1} *Pst* (*avrRpt2*). 3rd inoculation: two days later two to three distant leaves were inoculated with virulent *Pst* (10^5 cfu ml^{-1}) and *in planta* bacterial levels were determined 3dpi. Statistically significant differences between mock-induced and SAR-induced plants (Student t-test $p < 0.01$) are indicated with asterisks (*). This experiment was repeated three times with similar results.

Future experiments will include determining if the second CucDIR2 protein rescues the SAR defect in *dir1-1*. In addition, the tobacco, tomato, and cucumber putative DIR1 orthologs identified in Table 4.1, have been cloned into pMDC32 and transformed into *Agrobacterium* for future *dir1-1* rescue experiments (to be completed by Philip Carella).

4.2.3 Cucumber ortholog TNS inhibition/displacement ligand binding experiments

The data presented thus far suggests that CucDIR1 and CucDIR2 perform equivalent functions as AtDIR1 during SAR. If this is true these proteins should bind similar ligands as AtDIR1, especially if the ligand(s) is crucial for SAR. It is hypothesized that AtDIR1 may bind a putative SAR ligand within its lipid binding cavity and carry this signal to distant tissues during SAR (Maldonado et al., 2002). The identity if the DIR1 *in vivo* ligand is unknown but several candidates have been identified. These include the SA conjugate methyl salicylate (MeSA) (Park et al., 2007; Vlot et al., 2008; Liu et al., 2011), a lipid derived molecule (Chaturvedi et al., 2008), azelaic acid (AA) (Jung et al., 2009), pipecolic acid (PA) (Navarova et al., 2012), dehydroabietinal (DA) (Chaturvedi et al., 2012), and glycerol-3-phosphate (G3P) (Chanda et al., 2011) (Signals reviewed in (Dempsey

and Klessig, 2012; Fu and Dong, 2013; Shah and Zeier, 2013)). Interestingly, MeSA, AA, DA and G3P all require AtDIR1 to induce SAR.

To investigate if AtDIR1 can bind these ligands *in vitro* and to see if cucumber DIR1 orthologs can bind the same molecules, TNS (6,P-toluidinylnaphthalene-2-sulfonate) inhibition/displacement binding studies were conducted with several of these putative ligands. The ligands chosen for this study were AA, PA and G3P which are small molecules that could fit in the hydrophobic cavity of AtDIR1. AtDIR1 has been shown to bind two monoacylated phospholipids *in vitro* (Lascombe et al., 2006) and therefore lysophosphatidylcholine (LPC) was planned to be our positive control for DIR1-ligand binding. Unfortunately, LPC caused TNS to fluoresce making analysis impossible and thus LPC was removed from the study. Our inability to produce or buy DA, and the fluorescence of MeSA at the same wavelength as TNS were deciding factors in excluding these molecules from the study. Recombinant proteins were produced by cloning *AtDIR1, AtLTP2sw* and the two cucumber orthologs into the pET29b expression vector and then transformed into Rosetta Gami *E.coli* (Novagen) cells. AtLTP2sw is a random LTP2 protein control that will provide information on whether the ligands tested bind specifically to AtDIR1 and orthologs or if the ligands might bind to all LTP2 proteins. Rosetta Gami *E. coli* promote disulfide bond formation in the cytoplasm because of mutations in both the thioredoxin reductase and glutathione reductase genes (enzymes responsible for disulfide bond reduction). This is an ideal strain to produce correctly folded AtDIR1 and cucumber DIR1 orthologs as the four disulfide bonds essential for LTP2 folding should form in this *E.coli* strain. Proteins were purified using an S-Tag Thrombin purification kit (Novagen).

Ligand binding was tested *in vitro* using the TNS (2-p-Toluidinylnaphthalene-6-sulfonate) inhibition/displacement test. TNS is a small fluorescent probe with negligible fluorescence in aqueous solution, however, in hydrophobic environments TNS fluoresces significantly. TNS fluoresces in the hydrophobic cavities of proteins, thus TNS is ideal for LTP proteins which produce a characteristic hydrophobic cavity (McClure and Edelman, 1966). First, TNS can be used to determine if recombinant proteins contain a hydrophobic cavity and thus have folded properly. If fluorescence increases with increasing TNS concentration it suggests that the hydrophobic cavity is accommodating additional TNS molecules until the pocket is saturated and a plateau is reached. Each protein was denatured to unfold the protein and act as a negative control for TNS-hydrophobic pocket binding. To test folding, each protein was incubated with increasing amounts of TNS. As expected, denatured proteins lacking a hydrophobic cavity had baseline fluorescence (Figure 4.4). Fluorescence increased with increasing concentrations of TNS in reactions containing the purified proteins, AtDIR1, AtLTP2sw, CucDIR1 and CucDIR2. The elevated fluorescence levels in wells containing TNS and purified proteins suggest that Rosetta Gami *E.coli* cells produced properly folded LTP proteins.

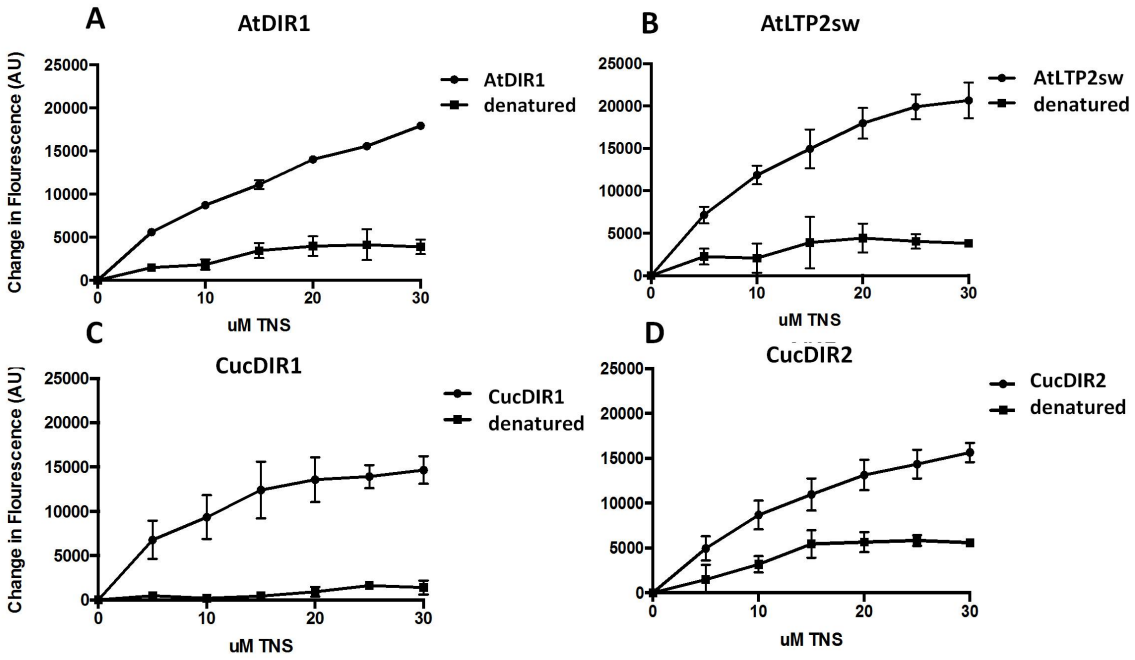

Figure 4.4: TNS folding assay of AtDIR1, AtLTP2sw, CucDIR1, and CucDIR2. Increasing concentrations of TNS were added to ~1 μg of each Rosetta Gami *E.coli* purified protein. Proteins were engineered to resemble the mature protein lacking the ER signal sequence. Proteins were denatured by boiling in 6 M Urea. Samples were excited with 320 nm and emission was collected at 437 nm and the change in fluorescence was calculated for three technical replicates. Error bars represent the standard deviation of the technical variation.

Next, putative ligands AA, PA and G3P were added to the TNS-protein solution and if the ligand competed with TNS for the protein hydrophobic cavity, then TNS would be displaced and TNS fluorescence

would be reduced (inhibition). If the protein did not bind the ligands the TNS fluorescence would remain at 100%, no inhibition of TNS fluorescence. Thus TNS fluorescence inhibition or quenching by the ligand-protein interaction is a measure of ligand binding. This technique has been used to test ligand binding for several elicitins (Krasikov et al., 2011) and LTPs (Buhot et al., 2004; Girault et al., 2008; DeBono et al., 2009; Krasikov et al., 2011). In these studies TNS displacement leading to fluorescence inhibition above 75% is considered high, inhibition 50%-75% is moderate and inhibition between 30-50% is considered low (Buhot et al., 2004; Krasikov et al., 2011). Philip Carella and I performed this experiment in collaboration with the Rose lab at Cornell University. Data for AtLTP2sw and AtDIR1 was collected and compared to data for CucDIR1 and CucDIR2.

TNS fluorescence was measured after purified protein addition and this represents the maximum fluorescence (100% fluorescence). Each ligand was then added and the fluorescence was measured again. If the ligand binds the protein then TNS does not have access to the hydrophobic cavity and will not fluoresce to the same extent as the control (TNS+protein). The data is represented as the percent fluorescence level of assays containing protein-ligand-TNS compared to assays with TNS and protein alone. As a control the MES buffer used to dissolve the ligands was also tested to make sure that the buffer did not affect TNS fluorescence inhibition. As expected, in the absence of protein there was no interaction between the TNS probe and the ligands or ligand buffer as indicated by baseline fluorescence (See appendix Table 7.1 for data). The addition of MES did not inhibit TNS fluorescence levels as they maintained the same fluorescence as the control (100%). AtDIR1+TNS+ligand resulted in fluorescence levels that were the same

compared to the TNS + protein control (95-115%). When AtLTP2sw was incubated with the ligands there was a 23% and 12% reduction in TNS fluorescence with G3P and PA respectively, compared to the control (TNS + protein). TNS displacement was higher in assays containing CucDIR1 plus AA and PA, with a 23% and 24% reduction in TNS fluorescence respectively, compared to the control. While a 30% reduction in TNS fluorescence compared to the control was observered in assays where CucDIR2 was incubased with AA. In this *in vitro* assay AtDIR1 did not interact with any of the putative ligands, whereas AtLTP2sw and CucDIR1 interacted very weakly with AA and PA and there was a weak but significant interaction was between CucDIR2 and AA.

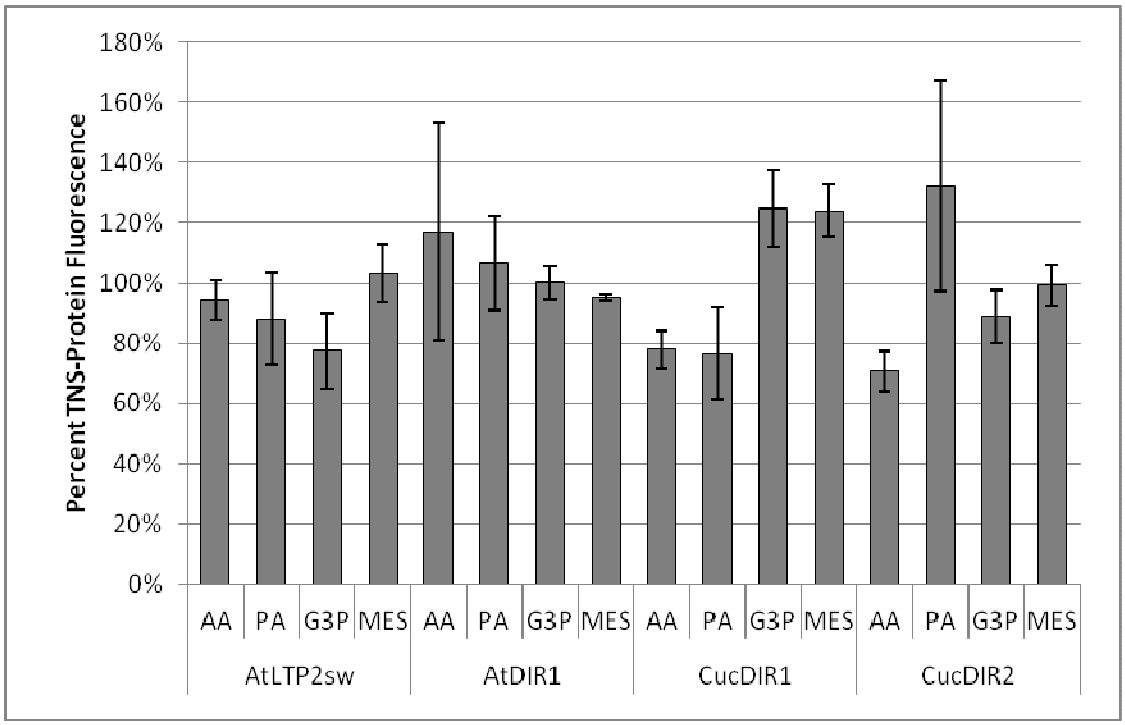

Figure 4.5: TNS inhibition/displacement ligand binding assay testing AtDIR1, AtLTP2sw, CucDIR1, and CucDIR2 binding of AA, PA, and G3P. Fluoresecence was measured when TNS (3 μm) and putative ligands (16 μm) were inclubated together for three minutes in a 96 well plate, followed by a second reading after purified proteins were added. Fluorescence was measured at excitation wavelength of 320 nm and emission was collected at 437 nm in technical triplicate. The data is represented as the percent fluorescence level of protein-ligand-TNS compared to TNS-protein alone (100%). Error bars represent the standard

deviation of the technical variation. AA = azelaic acid, PA = pipecolic acid ,G3P = glycerol-3-phosphate, MES = ligand buffer.

Chapter 5: Identification of motifs important for DIR1 function during SAR

Preface

Section 5.2.1, in this chapter has been modified from the publication Champigny et al. 2013 which appeared in Frontiers in Plant Science, 4:230. The 5.2.1 section figure was reproduced unmodified from the manuscript. This is possible because authors maintain copy right of their images in publications in Frontiers in Plant Science. Section 5.2.1 Homology modeling was conducted in consultation with protein expert Dr. Dan Yang (McMaster University, Biochemistry). Preliminary TNS inhibition binding assays were performed at McMaster University by Philip Carella to standardize the protocol for our lab.

5.1 Introduction

DIR1 has been shown to move from SAR-induced tissue to distant leaves to initiate priming during SAR (Champigny et al., 2013), however, the mechanism by which DIR1 establishes SAR in distant tissue remains unclear. The DIR1 protein has a number of regions which may be important for its function during SAR. DIR1 possesses a hydrophobic cavity which may be involved in chaperoning a molecule to distant tissues. Polar residues at the entrance of the cavity are hypothesized to stabilize or provide ligand specificity to DIR1 (Lascombe et al., 2008). Lastly, a PxxP

protein-protein interaction motif may allow DIR1 to participate in transient protein interactions (Lascombe et al., 2008). Despite having high sequence similarity to DIR1, our data suggests that the homologous DIR1-like protein only occasionally participates in SAR by compensating for the *dir1-1* SAR mutant. We hypothesize that comparisons between DIR1 and DIR1-like structure, along with identifying conserved residues between orthologs may provide clues as to which amino acids are critical for DIR1 function. The ultimate goal of this chapter is to use homology modeling to identify potentially important regions and residues that are important for DIR1 function and provide tools for future research to test the importance of these regions or residues during the SAR response.

5.2 Results

5.2.1 Homology modeling of DIR1 and DIR1-like. *Can structural differences in DIR1-like explain its occasional participation in SAR?*

DIR1 and DIR1-like are 88% similar at the amino acid level and yet only the *dir1-1* mutant was identified in a forward genetic mutant screen (Maldonado et al., 2002). Since *dir1-1* is rarely SAR-competent, we hypothesize that DIR1-like has a reduced capacity to participate in SAR. A homology model of DIR1-like was produced by the SWISS-MODEL server (Peitsch, 1995; Schwede et al., 2003; Arnold et al., 2006; Kiefer et al., 2009) to obtain clues as to why *dir1-1* is sometimes SAR competent. The DIR1 protein bound to two phospholipids was crystallized and the structure was solved (Lascombe et al., 2006; Lascombe et al., 2008). The DIR1 crystal structure was used as a template for the DIR1-like homology model. The Swiss-pdb viewer 4.0.1 (Guex and Peitsch, 1997) was used to compare the

solved DIR1-phospholipid structure and the DIR1-like protein model. The backbones of both proteins were overlapped to observe vicinity information for conserved versus non-conserved residues. Both proteins are very similar in terms of the arrangement of the five α-helices and four disulphide bonds that produce the internal cavity of DIR1 (Figure 5.1A). A number of differences were observed between DIR1 and the DIR1-like model. Within the binding pocket, thirteen hydrophobic residues were within 3.8 Å of the two phospholipids found in the internal cavity of the DIR1 crystal (Figure 5.1B). A phenylalanine is present at residue 40 in the internal cavity of DIR1, whereas a tyrosine residue was observed in DIR1-like (Figure 5.1C,D). The polar hydroxyl group present on DIR1-like's tyrosine may reduce the interaction with the phospholipid acyl chains at the bottom of the internal cavity or change the shape of the cavity through the attraction to polar water molecules in the solution. Additionally, DIR1 has three polar amino acids (GLN9, ASN13, LYS16) located at the entrance of the internal cavity, while DIR1-like has only two (GLN9, ASN13) (Figure 5.1E,F). Lascombe *et al.* (2008) postulate that these three polar amino acids create a favourable environment for interaction with hydrophilic phospholipid head groups. Loss of lysine at the cavity entrance in DIR1-like may affect its ability to form a stable interaction with a signal molecule(s) and reduce its capacity to contribute to SAR. Finally, DIR1-like possesses a putative SH3 interaction domain, PXXP, while DIR1 contains PXXPXXP at the same location on the protein surface (Figure 5.1G,H). SH3 interaction domains act as protein docking sites for transient protein-protein interactions and repeated PXXP motifs are hypothesized to strengthen these interactions (Williamson, 1994). Therefore it is possible that DIR1-like interacts less strongly with a binding partner and this may provide

evidence to support the hypothesis that DIR1 has a reduced capacity to participate in SAR.

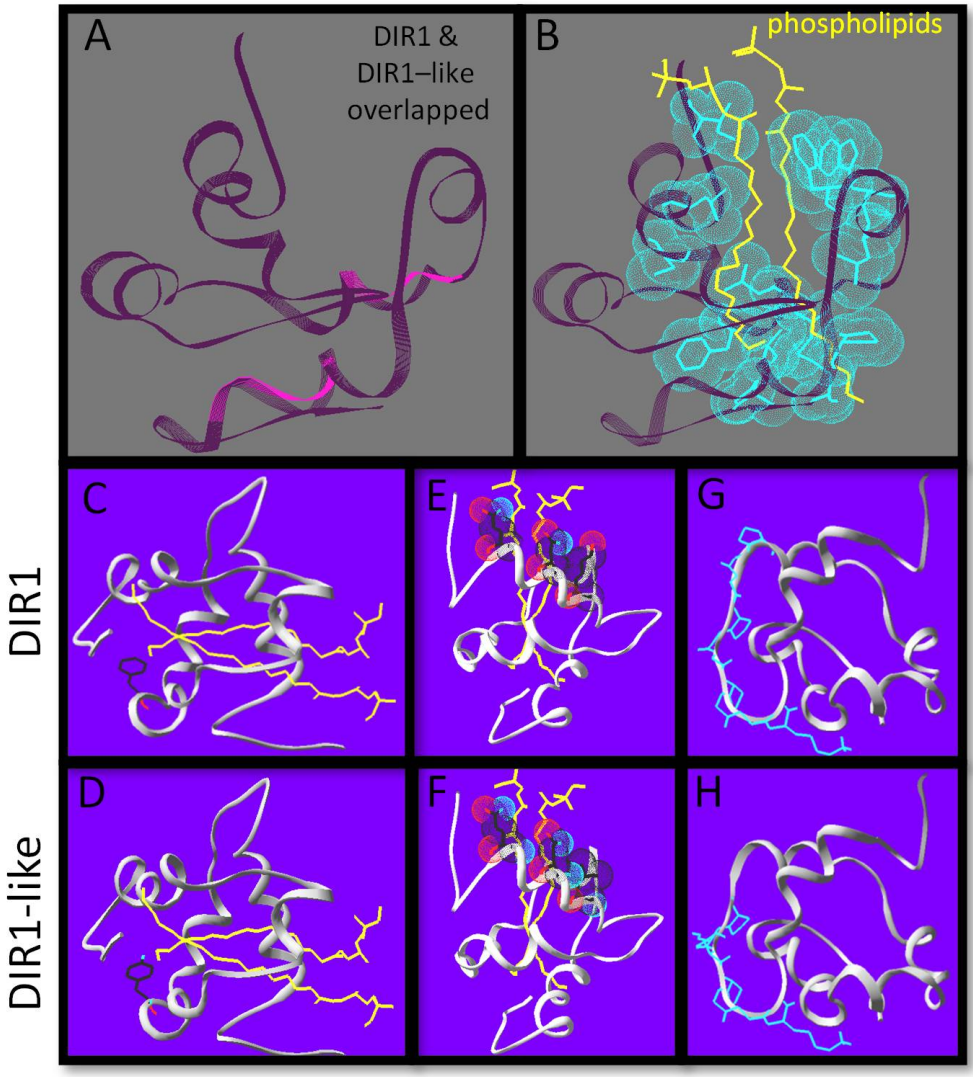

Figure 5.1. Homology modeling reveals differences between DIR1 and DIR1-like protein structure. Homology modeling of DIR1-like protein using the DIR1 crystal structure as a template using the Swiss-pdb viewer 4.0.1 to compare the DIR1 structure and the DIR1-like protein model. **A.** DIR1 protein backbone in dark purple is over-laid on the DIR1-like protein backbone in pink. **B.** The two yellow phospholipids extend into the internal lipid binding pocket of DIR1. The 13 hydrophobic residues that make up the lipid binding pocket are highlighted with light blue van der waals forces. **C-F.** Phospholipids in yellow, oxygen in light blue, nitrogen in red. DIR1 has a hydrophobic non-polar phenylalanine residue **C.** while DIR1-like has a polar tyrosine residue at the same position **D.** at the bottom of the internal lipid binding pocket. **E,D.** The amino acids at the cavity entrance are shown with their van der waals forces. Three polar residues of DIR1 **D.**

compared to two of DIR1-like **E.** cup the polar phosphate groups of the phospholipids. The putative SH3 binding motifs of DIR1 and DIR1-like are illustrated in light blue **G,H.**

5.2.2 In vitro TNS inhibition/displacement ligand binding assay with purified recombinant DIR1 & DIR1-like protein to investigate DIR1 and DIR1-like ligand binding

As discussed in Chapter 4, TNS inhibition/displacement binding assays can be used to examine LTP-ligand binding *in vitro*. DIR1 and DIR1-like proteins were expressed in Rosetta Gami *E.coli* cells and purified using an S-Tag thrombin purification kit (Novagen). Before ligand binding assays could be performed it was necessary to determine if the proteins had folded to form the characteristic LTP hydrophobic cavity. In the protein folding assay increasing amounts of TNS were added to ~1 μg of protein. Folded LTP proteins should accommodate additional TNS molecules in their hydrophobic cavity as the concentration increases until the pocket is saturated and a plateau is reached. Each protein was denatured by boiling in 6M Urea to unfold the protein and act as a negative control for TNS-hydrophobic pocket binding. As expected, denatured proteins lacking a hydrophobic cavity had baseline fluorescence (Figure 5.2). Fluorescence increased with increasing concentrations of TNS in reactions containing the purified proteins, DIR1, DIR1-like (1), DIR1-like(2) and LTP2sw. The elevated fluorescence levels in wells containing TNS and purified proteins suggest that Rosetta Gami *E.coli* cells produced properly folded LTP proteins.

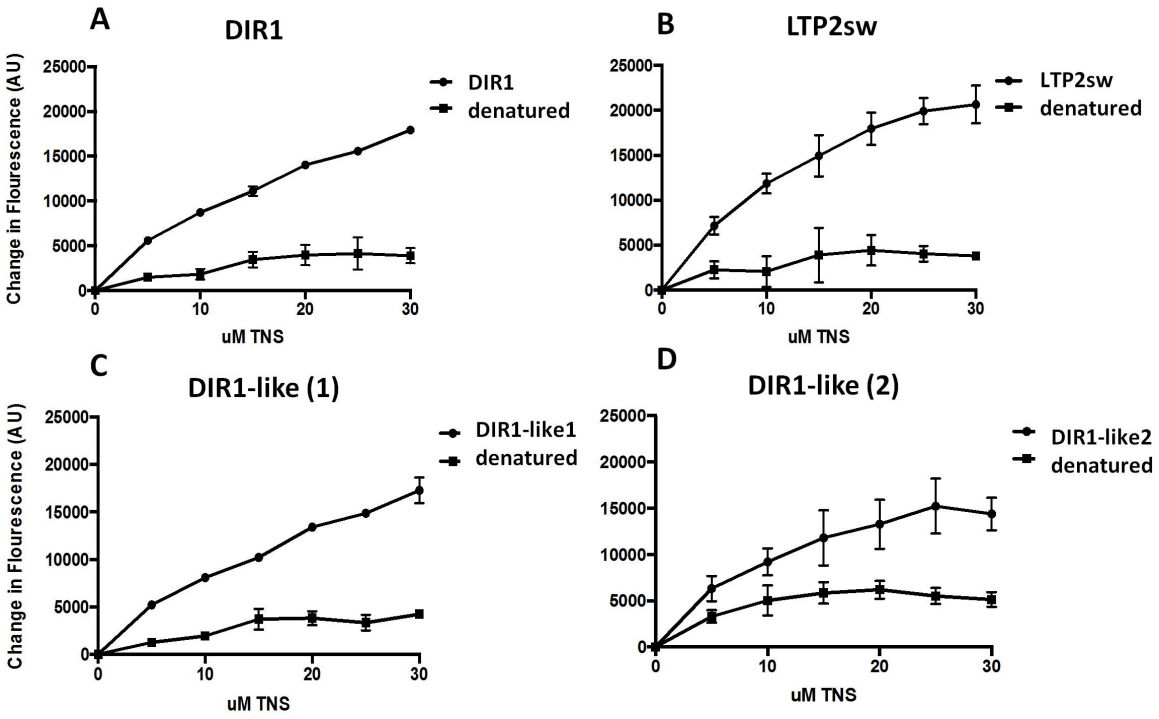

Figure 5.2: TNS folding assay looking at recombinant DIR1, LTP2sw, DIR1-like(1) and DIR1-like(2) protein folding. Increasing amounts of TNS were added to ~1μg of Rosetta Gami *E.coli* purified proteins. Proteins were expressed as the mature protein lacking the ER signal sequence. Proteins were denatured by boiling in 6 M Urea. Samples were excited at 320nm and emitted light was detected at 437nm. The change in fluorescence

was calculated for three technical replicates. DIR1-like (1) and DIR1-like (2) were obtained from two independent protein purifications. Error bars represent the standard deviation of the technical variation.

Based on homology modeling and the fact that *Agrobacterium*-mediated expression of DIR1-like rescues the SAR defect in *dir1-1*, it was predicted that DIR1-like has a reduced capacity to bind and/or transport a ligand to distant tissues during SAR. To test this hypothesis, *in vitro* TNS inhibition/displacement binding assays were conducted to see if DIR1 and DIR1-like bind the putative SAR mobile signals, azelaic acid (AA), glycerol-3-phosphate (G3P) and pipecolic acid (PA) with equal affinity. These putative signals were chosen because they are small molecules capable of fitting in the hydrophobic pocket of DIR1. The *in vitro* DIR1 ligand, lysophosphatidylcholine (LPC) could not be used as a positive control for binding because this molecule fluoresced in the presence of TNS. Previous studies indicated that TNS fluorescence inhibition above 75% was considered high, inhibition 50%-75% was moderate and inhibition between 30-50% was considered low (Buhot et al., 2004; Krasikov et al., 2011). Philip Carella and I performed these experiments in collaboration with the Rose lab at Cornell University. Data for LTP2sw and DIR1 was compared to data for two separate purifications of DIR1-like (1) and (2).

TNS fluorescence was measured after purified protein addition and this represents the maximum fluorescence (100% fluorescence). Each ligand was then added and the fluorescence was measured again. If the ligand binds the protein then TNS does not have access to the

hydrophobic cavity and will not fluoresce to the same extent as the control (TNS+protein). The data is represented as the percent fluorescence level of assays containing protein-ligand-TNS compared to assays with TNS and protein alone. As a control the MES buffer used to dissolve the ligands was also tested to make sure that the buffer did not affect TNS fluorescence inhibition. As expected, in the absence of protein there was no interaction between the TNS probe and the ligands or ligand buffer as indicated by baseline fluorescence (See appendix Table 7.1 for data). The addition of MES did not inhibit TNS fluorescence levels as they maintained the same fluorescence as the control (100%).

When LTP2sw was incubated with the ligands there was a 23% and 12% reduction in TNS fluorescence with G3P and PA respectively, compared to the control (TNS + protein). The TNS fluorescence with DIR1, DIR1-like (1), and DIR1-like (2) did not change in the presence of the three ligands compared to the control (TNS + protein) with fluorescence values between 95%-115%. This data indicates that these ligands do not bind in the hydrophobic cavities of DIR1 or DIR1-like *in vitro* as previous LTP TNS studies have indicated that inhibition below 30% could be due to random chance alone.

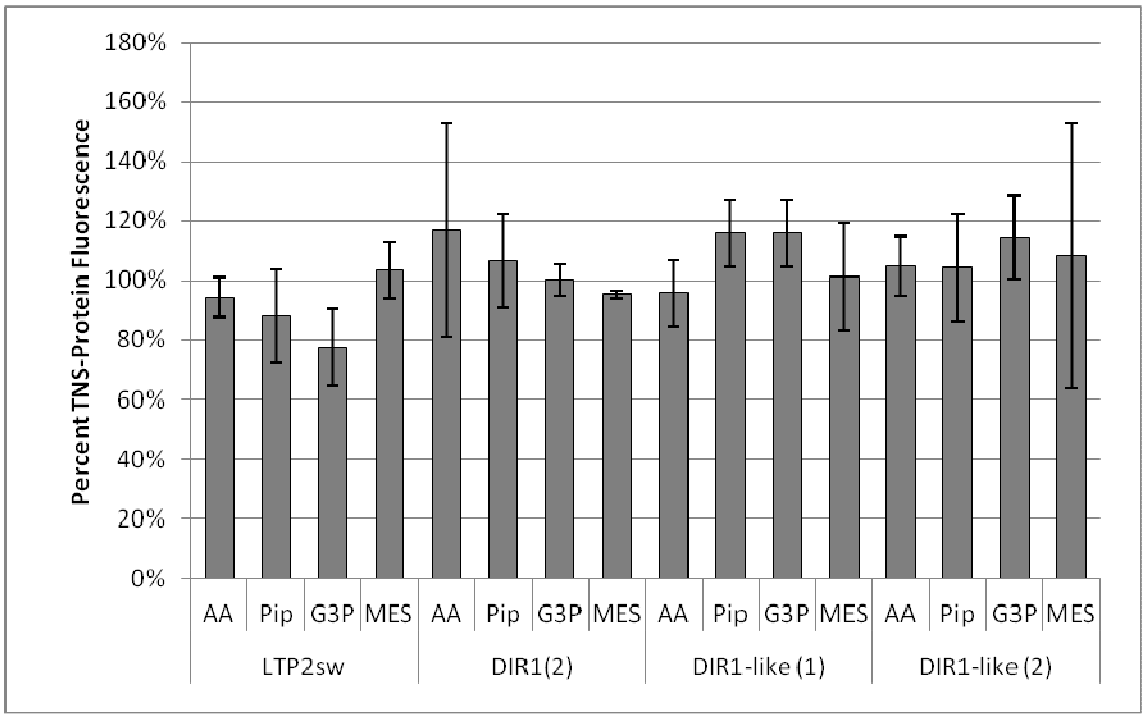
Percent TNS-Protein Fluorescence
180%
160%
140%
120%
100%
80%
60%
40%
20%
0%
AA
Pip
G3P
MES
LTP2sw
DIR1(2)
DIR1-like (1)
DIR1-like (2)

Figure 5.3: TNS inhibition ligand binding assay testing DIR1, LTP2sw, DIR1-like(1) and DIR1-like(2) binding of AA, PA, and G3P. Fluoresecence was measured when TNS (3 μm) and putative ligands (16 μm) were inclubated together for three minutes in a 96 well plate, then a second reading was recorded after purified proteins were added. Fluorescence was measured at excitation wavelength of 320 nm and emission at 437 nm in technical triplicate. The data is represented as the percent fluorescence level of protein-ligand-TNS compared to TNS-protein alone (100%). Error bars represent the standard deviation of the technical variation. AA = azelaic acid, PA= pipecolic acid ,G3P = glycerol-3-phosphate, MES = ligand buffer.

5.2.3 Are highly conserved residues/motifs across the DIR1 orthologs essential for AtDIR1 ligand binding and SAR function?

In Chapter 4 section 4.2.1.1, several DIR1 orthologs were identified including CucDIR1. Our data suggests that CucDIR1 performs an equivalent function to AtDIR1 during SAR as CucDIR1 complemented the *dir1-1* mutant in Agro-SAR assays. If the putative DIR1 orthologs function like AtDIR1 during SAR then key protein features important for function during SAR should be conserved in these species. To identify putative motifs that are essential for AtDIR1 function a Sequence Logo was created using the online Web Logo algorithm (Schneider and Stephens, 1990; Crooks et al., 2004). Sequence Logos provide a visual output of multiple sequence alignments where residues are stacked on top of one another and their frequency determines the height of the residue letter, allowing fast and easy identification of conserved regions. The size of the total

stack is measured in bits which represents the information content at that position in the sequence. In other words, bits are a representation of the number of possible residues for that site and the fewer the possibilities the higher the bits and the higher the likelihood of conservation.

An alignment of DIR1 and orthologs was first performed using Mega. This alignment was submitted to the Sequence Logo online application. Figure 5.4 shows the Sequence Logo output and several areas of interest are highlighted. As expected, the eight cysteine residues which form the four disulfide bonds essential to LTP protein structure are conserved in all orthologs and can be seen as large green C residues throughout the Sequence Logo plot. The proline rich region, a possible site of protein-protein interaction is common to all orthologs. New putative motifs, AD and LAxxLP were identified as they are conserved among the orthologs. Interestingly, the polar tyrosine residue indentified in AtDIR1-like's internal lipid cavity which was hypothesized to negatively affect AtDIR1-like ligand binding is only present in AtDIR1-like and the ortholog of AtDIR1-like in *Arabidopsis lyrata*. All DIR1 orthologs have various non-polar residues at this location, strengthening the hypothesis that this change in amino acid may affect AtDIR1-like's ability to function during SAR.

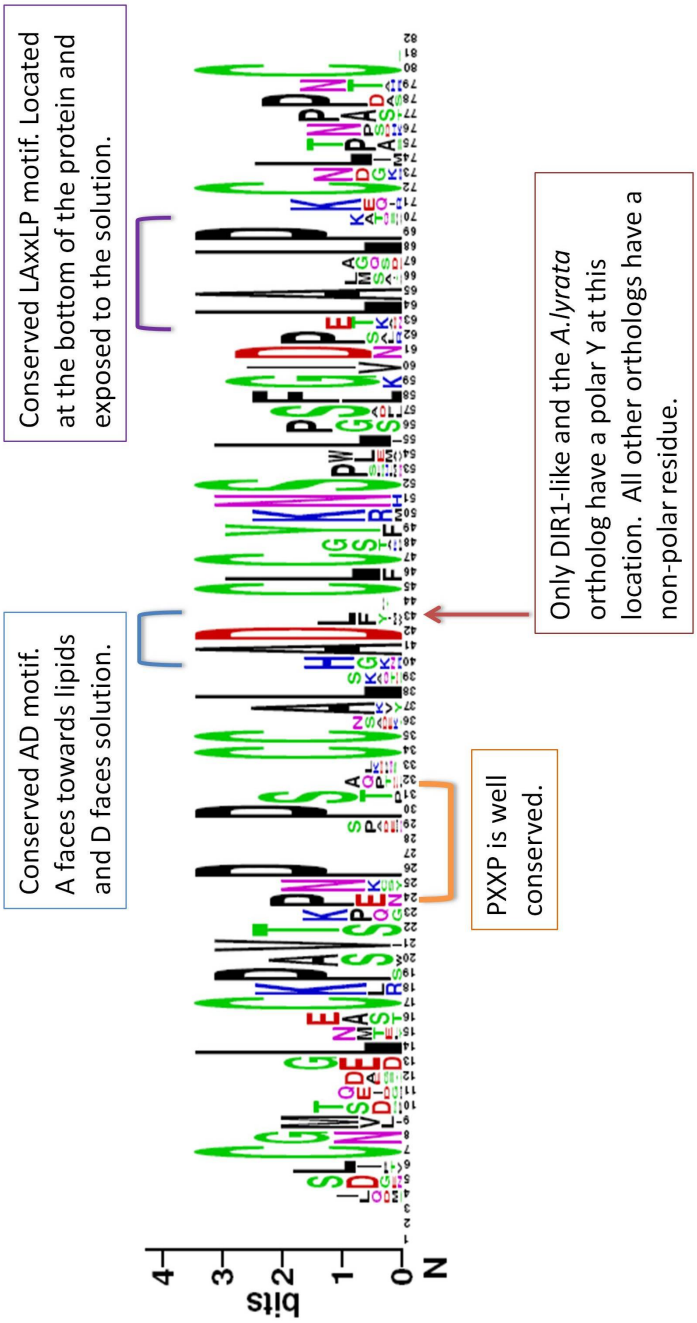

Figure 5.4: Sequence Logo plot of Muscle aligned mature DIR1 orthologs protein sequences (Web logo application http://weblogo.berkeley.edu). Residues of the orthologs are stacked on top of one another and their frequency determines the height of the residue letter in the plot. Bits is a measure of the information content at that position in the sequence. Higher Bit values represent lower number of residue possibilities for a particular site. Areas of particular interest are highlighted in the plot.

To better visualize the locations of the areas of putative importance, the DIR1-phospholipid crystal structure (Lascombe et al., 2006; Lascombe et al., 2008) was manipulated using MolSoft ICM browser to provide vicinity information on these motifs (Figure 5.5). The areas of putative importance are highlighted in blue relative to the black DIR1 backbone.

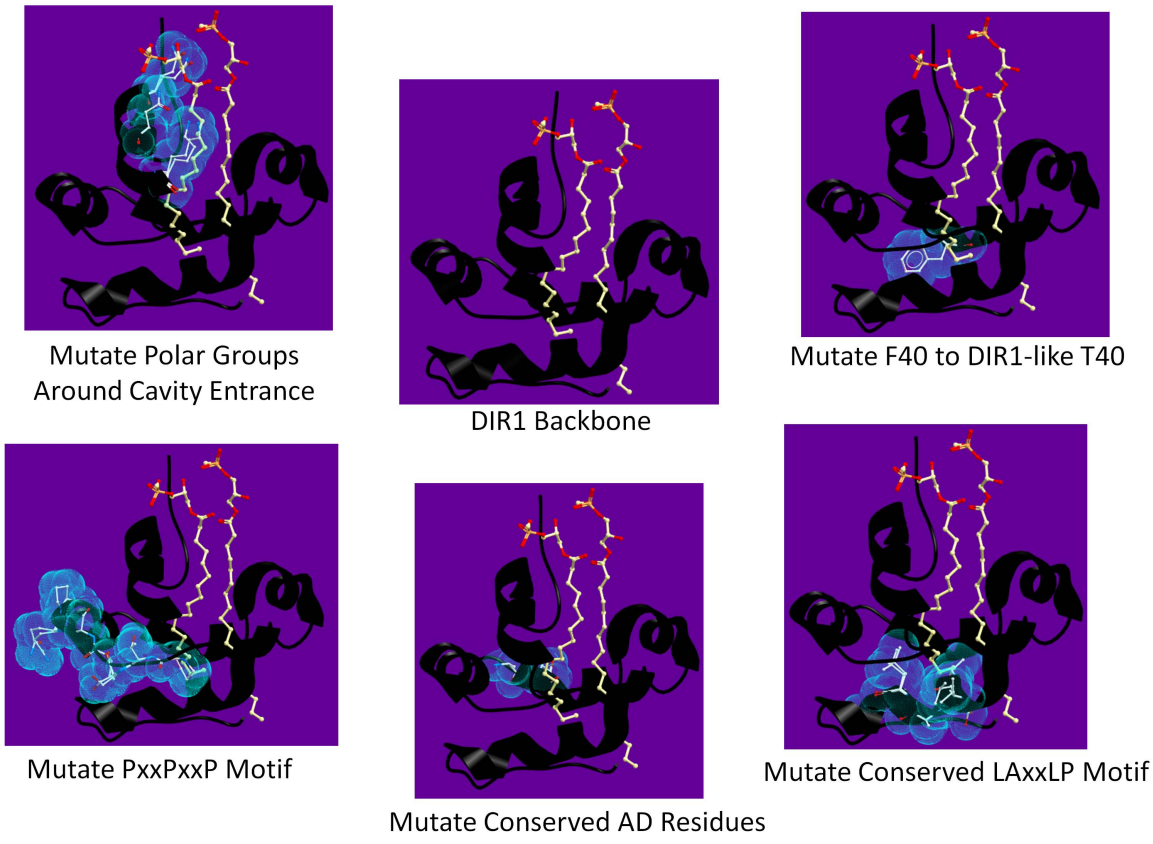

Figure 5.5: Model of DIR1 to highlight location of motifs of putative importance. DIR1-phospholipid crystal structure (Lascombe et al., 2006; Lascombe et al., 2008) was manipulated using MolSoft ICM browser to allow visualization of the various motifs that were highly conserved among the putative DIR1 orthologs. These residues are highlighted in light blue relative to the black DIR1 backbone. Phospholipids in orange (phosphate), red (oxygen) and white (carbon), extend into the DIR1 hydrophobic cavity.

5.2.4 DIR1 mutagenesis Design

Seven mutations were made in residues of putative importance to DIR1 function by providing new DIR1 variant sequences to a gene synthesis company (Biobasic Inc). Three possible experiments motivated the construction of these DIR1 variants. First, *in vitro* TNS inhibition ligand binding experiments could be performed on the purified protein to see if any of the motifs are critical for ligand binding. Second, these DIR1 variants could be cloned into a plant expression vector for use in the Agro-SAR assay. By assaying the ability to rescue the *dir1-1* SAR defect, we could determine if any of the motifs are critical for DIR1 function during SAR. Lastly, these recombinant protein variants could be infiltrated directly into *dir1-1* plant tissue to test their ability to rescue the *dir1-1* SAR defect.

Two negative controls were designed. The first negative control was a DIR1 protein that is missing all eight of its cysteine residues. The cysteine residues in DIR1 are essential for disulfide bond formation which determines DIR1 structure and cavity formation. Without them it is hypothesized that the protein would not fold correctly nor would it possess a lipid binding cavity. The second negative control was a DIR1 protein with a mutation in a hydrophobic residue Leu43 within the lipid binding pocket. Residue Leu43 rests directly between two cysteine residues where it is hypothesized to be critical for cysteine bond pairing (Samuel et al., 2002). Mutating this residue from Phe to Ala in a rice LTP2 protein resulted in an unfolded protein lacking the characteristic binding pocket as determined by circular dichroism and a TNS-like assay (Cheng et al., 2008).

To ensure pocket disruption, the DIR1 Leu residue was changed to a polar Asp (L43D) where the change from a non-polar hydrophobic leucine to a negatively charged hydrophilic aspartic acid residue will reduce cysteine bond formation and pocket folding.

The five most conserved motifs identified in the ortholog sequence comparison were changed. The PxxPxxP motif in DIR1 was chosen because of its high conservation among the orthologs and because it was suggested to be a site of possible protein-protein interactions by Lascombe et al (2008). Since we were unsure which proline residue was important and because it has been suggested that multiple PxxPxxP residues strengthen protein-protein interactions (Williamson, 1994), all proline residues were changed to alanine changing the motif from PxxPxxP to AxxAxxA.

The next region of interest was the polar head groups at the cavity entrance which may be essential for stabilizing ligand binding, especially if the ligand possess a hydrophilic moiety that remains exterior to the cavity. An example of this is the phospholipid binding observed in the DIR1 crystal structure where the hydrophobic tails extend downward into the hydrophobic cavity while the hydrophilic head groups remain in solution possibly cupped by the polar DIR1 residues, Gln9, Asn13 , Lys16. To test the importance of these residues all three were changed to Ala.

The sequence logo indentifies a putative AD motif that was completely conserved among the orthologs tested. This motif is found at the bottom of the cavity with alanine facing inwards towards the hydrophobic cavity and aspartic acid reaching outwards towards the solution. Although the role of this AD motif is unclear in DIR1, a barley LTP1 protein has been shown to carry a lipid (oxylipin) covalently bonded to an

aspartic acid residue (Lindorff-Larsen et al., 2001; Bakan et al., 2006). It is possible that the DIR1 aspartic acid may participate in some kind of covalent bond with a ligand.

The last motif is the LAxxLP motif, also of unknown function. This motif is exposed to the solution at the bottom of the cavity. To investigate its importance it was changed from LAxxLP to AAxxAA.

Another region that will be investigated is the hydrophobic pocket residue Phe40 in DIR1. In DIR1-like this residue is a tyrosine and the change from a non-polar Phe to a polar Tyr has been hypothesized to affect DIR1-like's ability to participate in SAR. Perhaps this residue disrupts the integrity of the pocket or causes a reduced interaction with the ligand. This hypothesis is strengthened by the sequence logo, which shows that other than the ortholog of DIR1-like in *Arabidopsis lyrata*, all DIR1 orthologs possess a non-polar hydrophobic residue at this location. It is difficult to tell which differences in DIR1-like alter its function, therefore to specifically examine the effect of the DIR1-like tyrosine residue in the hydrophobic cavity, DIR1 was mutagenized to contain the same residue, tyrosine instead of phenylalanine (F40Y).

Table5.1: Mutation abbreviations with a summary of the hypothesized effects of each protein modification.

Mutation Name	Predicted effects of mutant versions of DIR1
L43D	Hydrophobic cavity mutant. Cys-Leu-Cys replaced by Cys-Asp-Cys. Replacement of non-polar with polar in the hydrophobic cavity should disrupt the cavity formation.
NPH	No polar head (NPH) groups at the cavity entrance. Replacing all polar head groups with Ala may interfere with stability of ligand binding.
D39Q	AD motif is highly conserved in all orthologs. Replace

	polar Asp(D) with similarly shaped but non-polar Glu(Q) (D39Q), hard to predict how this will alter DIR1 function
AxxA	Changing all prolines in the PxxPxxP motif to Ala may interfere with protein-protein interactions and possibly ligand binding.
F40Y	Changing the nonpolar hydrophobic cavity residue Phe(F) to the polar Tyr (Y) as seen in DIR1-like may affect ligand binding.
AAxxAA	Highly conserved LAxxLP motif will be changed to AAxxAA, hard to predict how this will alter DIR1 function.

* L43D, D39Q, and F40Y the number in the middle is the position of the residue in the protein. The starting letter is the wild type residue and the letter at the end is the mutant residue.

5.2.5 Do DIR1 mutants have a reduced capacity to bind putative DIR1 ligands?

As discussed in Chapter 4, TNS inhibition/displacement binding assays can be used to examine ligand binding *in vitro*. The DIR1 variant genes were produced by a gene synthesis company (Biobasic Inc) and were cloned into a pET29b expression vector followed by expression in Rosetta Gami *E.coli* cells and purification using S-Tag thrombin purification kit (Novagen). Before ligand binding assays could be performed it was necessary to see if the proteins folded forming the characteristic LTP hydrophobic cavity. In the protein folding assay increasing amounts of TNS were added to ~1μg of protein. Each protein was denatured to unfold the protein and act as a negative control for TNS-hydrophobic pocket binding. As expected, denatured proteins lacking a hydrophobic cavity had baseline fluorescence (Figure 5.2). Both DIR1, DIR1-like, LTP2sw control and all the variant proteins exhibited increasing levels of TNS fluorescence as TNS concentration increased. This is expected for folded proteins which should accommodate additional TNS molecules in their

hydrophobic cavity as the concentration increases. The DIR1 variants proteins did not bind TNS with the same affinity as DIR1. A representative graph showing wLTP2, DIR1 and L43D mutant illustrates the lower fluorescence level of the variants.

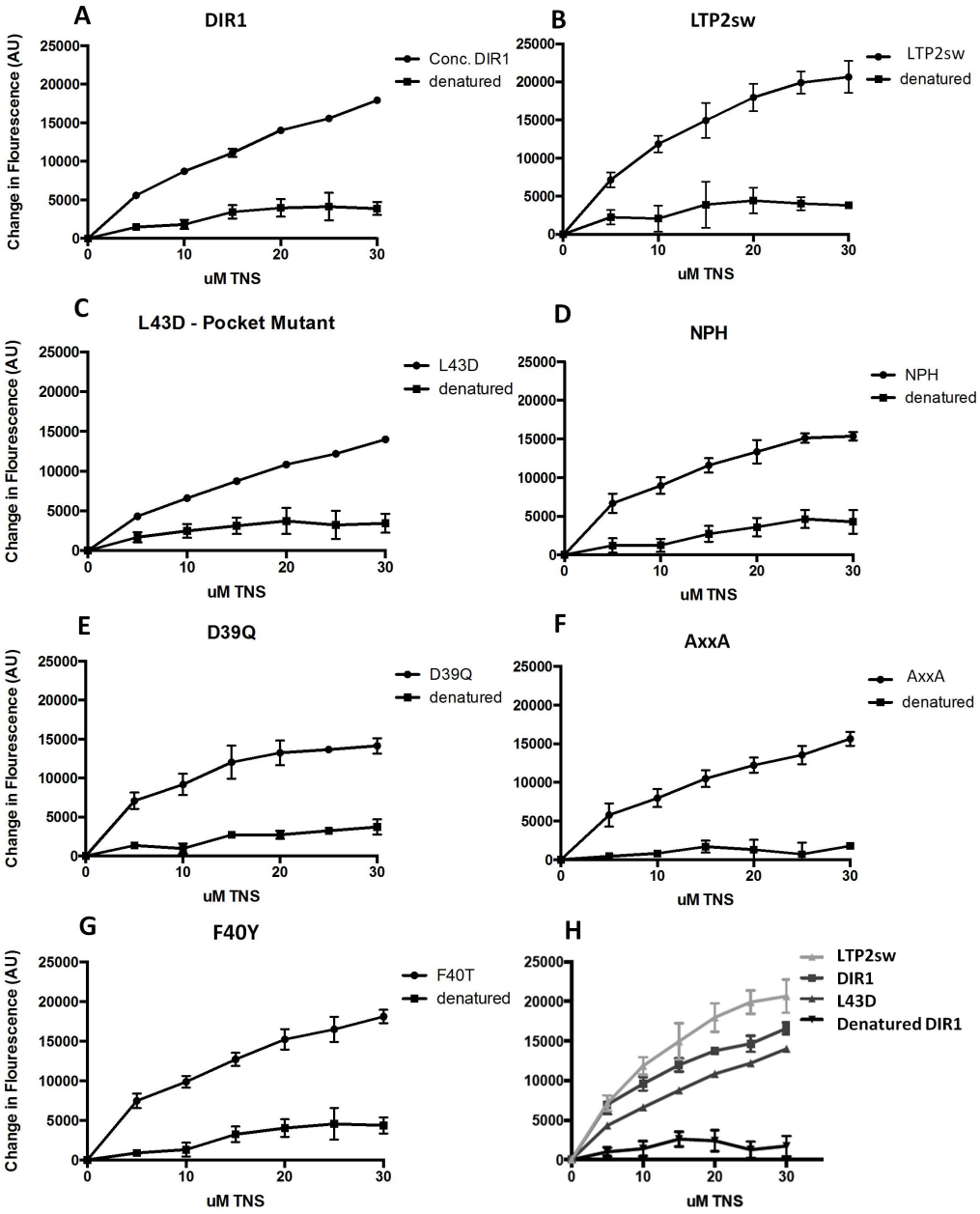

Figure 5.6: TNS folding assay looking at recombinant DIR1, LTP2sw, and DIR1 variant protein folding. Please see table 5.1 for list of DIR1 variant abbreviations. Increasing amounts of TNS were added to ~1 μg of each Rosetta Gami *E.coli* purified protein. Proteins expressed the mature protein lacking the ER signal sequence. Proteins were denatured by boiling in 6 M Urea. Samples were excited at 320 nm and emission at 437 nm and the change in fluorescence was calculated for three technical replicates. Error bars represent the standard deviation of the technical variation.

Next TNS inhibition/displacement binding assays were performed. Philip Carella and I performed these experiments in collaboration with the Rose lab at Cornell University. Data for LTP2sw and DIR1 was compared to data for the DIR1 variants. TNS fluorescence was measured after purified protein addition and this represents the maximum fluorescence (100% fluorescence). Each ligand was then added and the fluorescence was measured again. If the ligand binds the protein then TNS does not have access to the hydrophobic cavity and will not fluoresce to the same extent as the control (TNS+protein). The data is represented as the percent fluorescence level of assays containing protein-ligand-TNS compared to assays with TNS and protein alone. As a control the MES buffer used to dissolve the ligands was also tested to make sure that the buffer did not affect TNS fluorescence inhibition. As expected, in the absence of protein there was no interaction between the TNS probe and the ligands or ligand buffer as indicated by baseline fluorescence (See appendix Table 7.1 for data). The addition of MES did not inhibit TNS fluorescence levels as they maintained the same fluorescence as the control (100%).

When LTP2sw was incubated with the ligands there was a 23% and 12% reduction in TNS fluorescence with G3P and PA respectively, compared to the control (TNS + protein). DIR1, NPH and F40T TNS fluorescence in the presence of the three ligands did not change compared to the control (TNS + protein) exhibiting TNS fluorescence values between 95%-135%. A 20% reduction in TNS fluorescence intensity was observed when L43D was incubated with AA compared to the control (TNS + protein). Interestingly, AxxA mutations resulted in lower fluorescence intensities than wild-type DIR1 where AxxA had a 24%

reduction when incubated with AA and PA and a 15% reduction when incubated with G3P compared to the control (TNS + protein). Unfortunately, the AxxA variant also displayed a 35% reduction in fluorescence when incubated with MES alone control suggesting that the reduction in fluorescence in this group may have been due to plate specific variation. This may have been caused by an error in loading that section of the plate and therefore this variant should be retested. D39Q exhibited a 30% reduction in fluorescence when incubated with PA, compared to the control (TNS + protein). This data indicates that these ligands do not bind in the hydrophobic cavities of DIR1, DIR1-like or DIR1 variants *in vitro* as previous LTP TNS studies have indicated that inhibition below 30% could be due to chance alone.

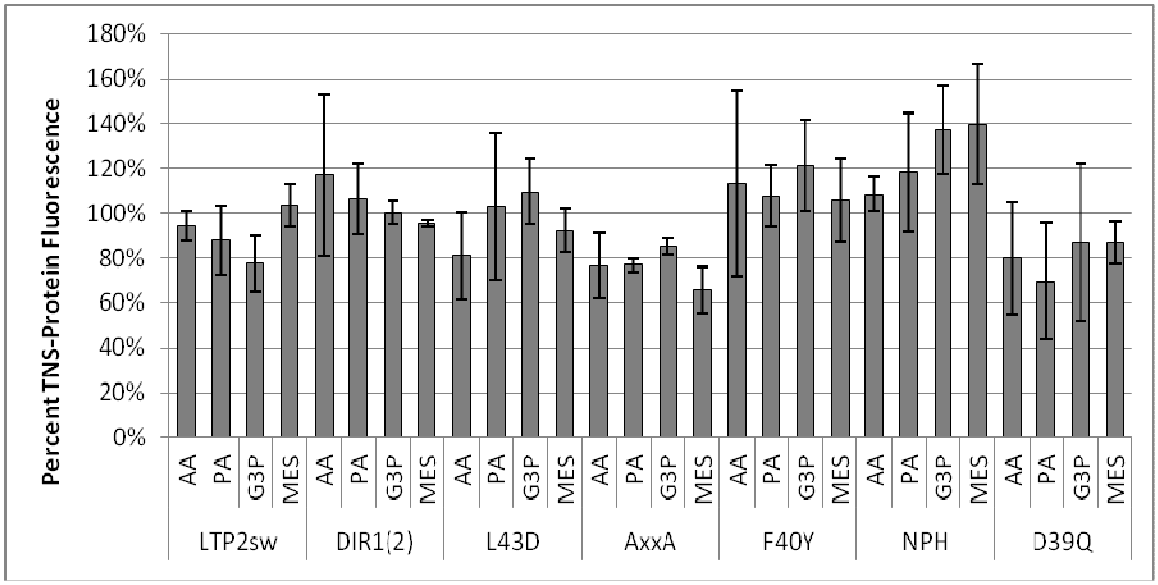

Figure 5.7: TNS inhibition/displacement ligand binding assay testing DIR1, LTP2sw, and DIR1 variant binding of AA, PA, and G3P. Fluoresecence was first measured when TNS (3 μm) and putative ligands (16 μm) were inclubated together for three minutes in a 96 well plate, then a second reading was recorded after purified proteins were added. Please see table 5.1 for a list of DIR1 variant abbreviations. Fluorescence was measured at excitation wavelength of 320 nm and emission was collected at 437 nm in technical triplicate. The data is represented as the percent fluorescence level of protein-ligand-TNS compared to TNS-protein alone

(100%). Error bars represent the standard deviation of the technical variation. AA = azelaic acid, PA = pipecolic acid ,G3P = glycerol-3-phosphate, MES = ligand buffer.

Chapter 6: Discussion

6.1 Examining DIR1 and DIR1-like and Tools for Future Analysis

A phylogeny of DIR1 orthologs of the *Brassicaceae* was created to investigate the evolutionary relationship between DIR1 and DIR1-like (Chapter 3, Figure 3.1). The *Brassicaceae* DIR1 ortholog phylogeny supports a DIR1/DIR1-like duplication event which was predicted because these genes are tightly linked genomic neighbours with high sequence similarity (88%). *A.lyrata* possesses a similar tandem duplication while *B.rapa* and *T.halophila* do not, placing the duplication event after *B.rapa* and *E. salsgineum* speciation and in a common ancestor of *A.lyrata* and *A.thaliana*. Gene duplication is thought to play an important role in the plant-pathogen arms race as a source of novel plant defense genes with new resistance specificity. This adaptive specialization strategy is hypothesized to occur in the diversification of R genes where the *Arabidopsis* gene family is estimated to have ~140 members (Leister, 2004).

Paralogs rapidly diverge from the original gene as the presence of a redundant locus creates a situation of relaxed selection where the duplicated gene can evolve without affecting the fitness of the organism

(Blanc and Wolfe, 2004). One theory is that the paralog either takes on a new function and is then subjected to selective pressure (neo-functionalization) or accumulates enough deleterious mutations that it becomes a pseudogene. However, the high percentage of duplications maintained in genomes supports an alternative theory: a gene possessing multiple functions, duplicates and splits up the functions between its duplicates instead of the paralog gaining a novel function (sub-functionalization). Both theories are reviewed in (Prince and Pickett, 2002). Our data suggests that although DIR1-like maintains some of its ancestral function in SAR it is not as effective as DIR1 and this may suggest that it has evolved a novel function. Alternatively, DIR1 may have originally had two functions but after duplication these functions were split up between the two genes. For example, the *dir1-1* mutant is not only defective in SAR but it also has a seed phenotype where *dir1-1* seeds can only germinate on media, but not on soil. Thus, DIR1 may have originally been involved in seed production as well as acting as a SAR long distance signal, but after duplication the seed development function was carried out by DIR1-like while DIR1 maintained its role in SAR. An alternative theory is that the seed phenotype of *dir1-1* mutant is due to another mutation in the genome that has not been identified. However, DIR1 and DIR1-like have similar expression profiles (Champigny et al., 2013). Immediately after duplication, the duplicated genes are completely functionally redundant with similar expression profiles. Therefore the more recent the duplication the more likely it is that functions and expression profiles between paralogs are conserved. Thus, the ability of DIR1-like to complement the *dir1-1* mutation in Agro-SAR assays, the conservation in expression profiles and

the DIR1 phylogeny, support the theory that this duplication event occurred recently in evolutionary history.

An interesting feature of *dir1-1* is its occasional SAR phenotype. *DIR1* and *DIR1-like* expression profiles were investigated in the *dir1-1* mutant to see if their expression remains constant regardless of the variability in the *dir1-1* SAR defect (Chapter 3, Figure 3.2). The hypothesis that under certain environmental conditions expression of *DIR1* or *DIR1-like* is enhanced leading to rescue of the SAR defect in the *dir1-1* mutant is incorrect. *DIR1-like* expression is maintained at wild-type levels while *DIR1* expression was negligible in an experiment where the *dir1-1* mutant was SAR competent. A similar qRT-PCR analysis was previously performed on tissue collected from a SAR experiment where the *dir1-1* mutant was SAR-defective rather than competent, and similar results were obtained (Champigny et al., 2013). Thus changes to *DIR1* and *DIR1-like* expression profiles cannot explain the occasional SAR competent phenotype of the *dir1-1* mutant.

Light plays a major role in both plant resistance and pathogen virulence (Reviewed in Griebel and Zeier, 2008; Roden and Ingle, 2009). Recently, the circadian clock has been shown to be important for innate immunity (Zheng et al., 2013). Environmental factors such as light may be responsible for the occasional SAR competent phenotype of the *dir1-1* mutant. In support of this, the robustness of SAR induction seems to depend on the hours of light received after *Pst* infection. Daytime inoculations stimulate stronger SAR responses (Griebel and Zeier, 2008). The need for plants to detect light during SAR is supported by the fact that phytochrome mutants have been shown to be SAR-defective (Griebel and Zeier, 2008). To determine if DIR1 or MeSA participation during SAR

depended the hours of light received after inoculation, Liu et al. (2011b) conducted SAR experiments were they varied the hours of light received after inoculation. They discovered that inoculations of *dir1-1* and MeSA-deficient *bsmt1* plants in the morning resulted in plants capable of mounting a SAR response, while *dir1-1* and *bsmt1* plants inoculated in the afternoon were SAR-defective (Liu et al., 2011a). They propose that the number of hours of light after inoculation is critical for both MeSA and DIR1 participation in SAR (Liu et al., 2011a). Thus, light may be an environmental factor responsible for the variability in the *dir1-1* SAR phenotype. Attempts to replicate these findings in our own lab have been unsuccessful as *dir1-1* is SAR competent or SAR defective regardless of morning or afternoon inoculations, suggesting that there may be more than one environmental factor affecting *dir1-1* SAR phenotype. Thus further experimentation is required to address this question.

It may be possible that DIR1-like is occasionally participating in SAR and this explains the occasional *dir1-1* SAR-competent phenotype. This hypothesis can be tested after the creation of a *dir1-1 dir1-like* double mutant. If DIR1-like is the cause of variability then we would expect the *dir1-1 dir1-like* double mutant to be consistently SAR defective. If DIR1-like is not responsible for occasional SAR-competence observed in *dir1-1*, then other environmental factors may be the cause and should be tested.

In the Agro-SAR assay, a DIR1-like-sized band was detected in distant petiole exudates of SAR-induced *dir1-1* plants provides preliminary evidence that DIR1-like may also move to distant tissues during SAR (Chapter 3, Figure 3.3). It is likely that the DIR1 antibody is detecting DIR1-like since our DIR1 antibody was shown to bind recombinant DIR1 and DIR1-like but not a highly similar LTP2sw protein (Champigny et al., 2013). It

would be informative to perform the same experiment in the *dir1-1dir1-like* double mutant to ensure that DIR1-like is the true cause of the DIR1-like sized band. If DIR1-like is responsible for the DIR1-like sized band, then this band should disappear in the *dir1-1dir1-like* double mutant. Another way to improve this experiment would be to tag DIR1-like with a small epitope tag and collect SAR-induced petiole exudates either from transgenic plants stabily expressing DIR1-like-tag or using transient DIR1-like-tag expression in the Agro-SAR assay. Then protein gel blots using an epitope-specific antibody could be used to detect DIR1-like in petiole exudates. Both the *dir1-1dir1-like* double knockout (screening T1s) and DIR1-like epitope tagged constructs (screening T2s) are being created as tools to monitor DIR1 and DIR1-like movement during SAR (Chapter 3, sections 3.2.4 and 3.2.5).

Transgenic T1 plants in Col-0, Ws and *dir1-1* backgrounds expressing a DIR1-like RNAi construct under the control of a 35S or estrogen inducible (XVE) promoter are currently being screened (Chapter 3, section 3.2.5). These plants should produce single *dir1-like* and double *dir1dir1-like* mutants for further dissection of the involvement of these proteins during SAR. These plant lines will allow us to determine if DIR1-like is occasionally participating in SAR and causing the occasional SAR-competent phenotype of the *dir1-1* mutant. In addition, the estrogen inducible (XVE) RNAi lines will allow us to test the hypothesis that our antisense lines did not yield a double knockout because loss of DIR1-like is lethal to the plant. If this is the case then conditional expression of DIR1-like RNAi will allow us to dissect DIR1-like's involvement during SAR.

If this RNAi strategy fails to produce a *dir1-1dir1-like* double mutant due to silencing of our RNAi transgene, our collaborator Jean Greenburg is

creating a *dir1-1dir1-like* double mutant by using a genome engineering tool, transcription activator-like effector nucleases (TALEN). Similar to zinc-finger nucleases (ZFN), TALENs are chimeric proteins composed of a DNA binding domain bound to a nuclease. The DNA binding domain can be modified to be specific for almost any DNA sequence. Since the nuclease works as a dimer, two TALENS are designed to bind the gene of interest in two locations. An advantage of TALENS over ZFN is their ability to bind a larger number of gene target sites. The DNA is cleaved between the TALENS and then the non-homologous end joining (NHEJ) DNA repair system rejoins the split chromosome but with high probability of introducing mutations (Reviewed in Mussolino and Cathomen, 2012; Zhang et al., 2013). This technology has been adapted to plants opening up new possibilities in genome engineering and targeted mutagenesis (Zhang et al., 2013).

There are disadvantages to ZFN/TALEN technology which include designing a TALEN DNA binding domain with the correct specificity for a target sequence, off target cleavage, recalcitrance of certain DNA segments to the technology, and overall difficulty in delivering these enzymes into crop plants as some crop plants are recalcitrant to *Agrobacterium* transformation. In addition, ZFN/TALEN technology requires extensive screening for mutants as the NHEJ repair system sometimes rejoins the DNA segments without making a mistake. Another technology for site-directed mutagenesis in plants is the use of the clustered regularly interspaced, short palindromic repeats (CRISPR) system (Shan et al., 2013). The CRISPR system is used by bacteria to defend themselves against genome integrated bacteriophage DNA. The CRISPR-associated protein (CAS) is directed to foreign DNA by a CRISPR single

guide sgRNA where the CAS endonuclease cleaves out the foreign bacteriophage double stranded DNA (Reviewed in Shan et al., 2013). This system has a higher mutation rate than ZFN/TALEN technology because a large chunk of DNA is removed and has been adapted to plants by modifying the specificity of the sgRNA to guide the CAS protein to a plant gene of interest for cleavage. This technology represents an alternative if the *DIR1-like* sequence proves resistant to ZFN/TALEN technology.

6.2 DIR1 orthologs

Although DIR1 orthologs were shown to exist in tobacco (Liu et al., 2011b), and a putative ortholog was identified in tomato (Mitton et al., 2009), Chapter 4 identified new putative DIR1 orthologs in *A.lyrata, B.rapa*, *E. salsugineum*, cucumber, and soybean (Chapter 4 figure 4.1). All orthologs share 44-93% sequence identity which is highly suggestive of a common ancestry. However, it is unclear how high sequence identity values must be to say that it is unlikely that the sequences are conserved by chance alone. To determine the range of sequence identity values that might be obtained by chance alone, a global alignment of DIR1 and random sequences was performed. A random sequence generator (http://www.bioinformatics.org) was used to produce DIR1-sized amino acid sequences (76 bp) and a global alignment of ten random sequences produced an average of 5% sequence identity (See appendix Table 7.2). Further evidence of the relationship between sequence identity and orthology is provided by Rost et al. (1999) who found that below 25% sequence identity, 90% of orthologs identified are false positives. At 30% sequence identity only 10% of orthologs identified were false positives (Rost, 1999). Thus most scientists assume that a high

sequence identity is anything above 40%. All of the sequences identified as putative DIR1 orthologs have between 44-93% sequence identity, which supports the idea that they are DIR1 orthologs.

The phylogeny of DIR1 orthologs produced two distinct clades: the *Brassicaceae* clade and the crop plant clade (Chapter 4, Figure 4.1). Looking at this larger phylogeny, an alternative hypothesis for the timing of the tandem duplication of DIR1 and DIR1-like is observed. It is possible that *Thellungiella* and *Rapa* may have lost a paralog instead of the duplication event occurring post *Rapa* and *Thellungiella* speciation. Further analysis with additional DIR1 orthologs in the *Brassicaceae* family may provide additional information to determine which hypothesis is most parsimonious. Parsimony simply indicates that the simplest explanation is usually correct. The most parsimonious hypothesis is the one which requires the fewest evolutionary changes to occur.

Soybean, tomato, and cucumber are diploid plants whereas tobacco is a tetraploid. Despite being a tetraploid, tobacco does not have twice as many DIR1 orthologs than the other diploid crop plants. However, it is possible that tobacco lost paralogous genes or that all DIR1 orthologs have not been annotated in the preliminary tobacco genome. *AtDIR1* and *AtDIR1-like* are tightly linked tandem copies separated by approximately 1000bp. The duplications in soybean, tomato and cucumber DIR1 orthologs are not tandemly located on their respective chromosomes (see Appendix Table 7.3 for scaffold/genomic locations). Tobacco orthologs are not on the same contigs, however the short contig lengths (~2000bp) means that these genes could be within 2000 bp of each other, but the current state of the *Nicotiana tabacum* genome makes it impossible to tell. The absence of tandem duplications in these

crop plants suggests that the duplication events leading to these paralogs were caused by larger chromosomal rearrangements than tandem duplications such as unequal crossover during meiosis, retrotransposition, or whole genome duplications (polyploidy).

By comparing DIR1 and DIR1-like protein structure using homology modeling, several residues were hypothesized to be important for AtDIR1 function (Chapter 5, Figure 5.1). These included a hydrophobic cavity, the presence of polar residues as docking sites at the cavity entrance and a possible protein-protein interaction motif (PxxPxxP) (Lascombe et al., 2008). Since sequence information reveals little about where residues are located in the protein tertiary structure, homology modeling was used to compare AtDIR1 and the cucumber DIR1 orthologs proteins structure (Chapter 4, Figure 4.2). It was of interest to determine if the cucumber orthologs possessed the features of hypothesized importance for DIR1 as this would provide addition evidence of their importance. The homology model of CucDIR1 and CucDIR2 revealed that both of the putative cucumber orthologs of DIR1 possess all three regions of putative importance. This suggests that sequence similarity translates into a conserved protein structure, that CucDIR1/CucDIR1 may possess the motifs necessary for participation in SAR and is further evidence of orthology between AtDIR1 and CucDIR1/CucDIR2.

The PxxP motif (where P is proline and x is any residue) is present on all three proteins. The hypothesis that the PxxP in AtDIR1, CucDIR1 and CucDIR2 is a protein-protein interaction motif is strengthened by the fact that it is exposed to the solvent and it is located towards the bottom of the protein away from the cavity entrance where a protein interaction would not interfere with ligand binding. Many protein-protein interaction

domains are quite small averaging less than 10 residues (Kay et al., 2000). The Src homology (SH3) interaction domain acts as protein docking site for PxxP- containing proteins, mediating transient protein-protein interactions. These SH3 domains interact with proline rich motifs with a minimum motif of PxxP. The SH3 domain is composed of 3 pockets. The proline residues extends into two SH3 pockets while a third pocket binds a positively charged specificity- determining residue (Figure 6.). There are two types of PxxP motifs, class I and class II which are determined by the position of a positive residue relative to the proline motif. Class I motifs have a positive residue at the beginning of the motif while class II have a positive residue at the end. The position of the positive residue determines the orientation of binding (Reviewed in Zarrinpar et al., 2003).

AtDIR1 contains a PxxPxxP while CucDIR1 contains a PxPxxxPP and CucDIR2 contains a PPxPxPP motif. If we look at the positions of the positive residues (Lysine K, Histidine H or Asparagine N) relative to the PxxP motifs we see that all three proteins have class I motifs. AtDIR1 with NPxxPxxP, CucDIR1 with KPxPxxxPP and CucDIR2 with PPNPXPP. Notice that in CucDIR2 the only positive residue is in the middle of the motif. This suggests that the functional motif of CucDIR2 is shorter than hypothesized motif and becomes NPxPP. Repeated PxxP motifs like in AtDIR1 are hypothesized to strengthen the protein-protein interactions (Williamson, 1994). The variation in PxxP motifs suggests that perhaps these motifs are modified for slightly different binding partners. However, SH3 domains often display flexibility in their binding partners (Kay et al., 2000).

SH3 interactions tend to be transient and there are several examples where transient binding mediates the coming together of two different proteins into a higher affinity interaction. For example, the SH3

domain may act as a scaffold for a protein and its receptor. Therefore it is reasonable to predict that an SH3 domain may be responsible for bringing AtDIR1/CucDIR1/CucDIR2 into proximity of proteins involved in a SAR long distance signaling complex or into proximity of a distant leaf receptor protein to initiate SAR. However, only a handful of SH3 domain proteins have been confirmed in *Arabidopsis* and they seem to be involved in the vesicle trafficking (Lam et al., 2001; Isono et al., 2010). A blast search of the *Arabidopsis* genome for SH3 domains only produces six hits. In comparison eukaryotic organisms have substantially higher number of proteins with SH3 domain (C.elegans 55, Drosophila 63) (Mayer, 2001). This may suggest that perhaps an SH3-like domain exists in *Arabidopsis* that has yet to be characterized and may participate in transient interactions with these PxxP motifs or these conserved PxxP motifs perform some other function.

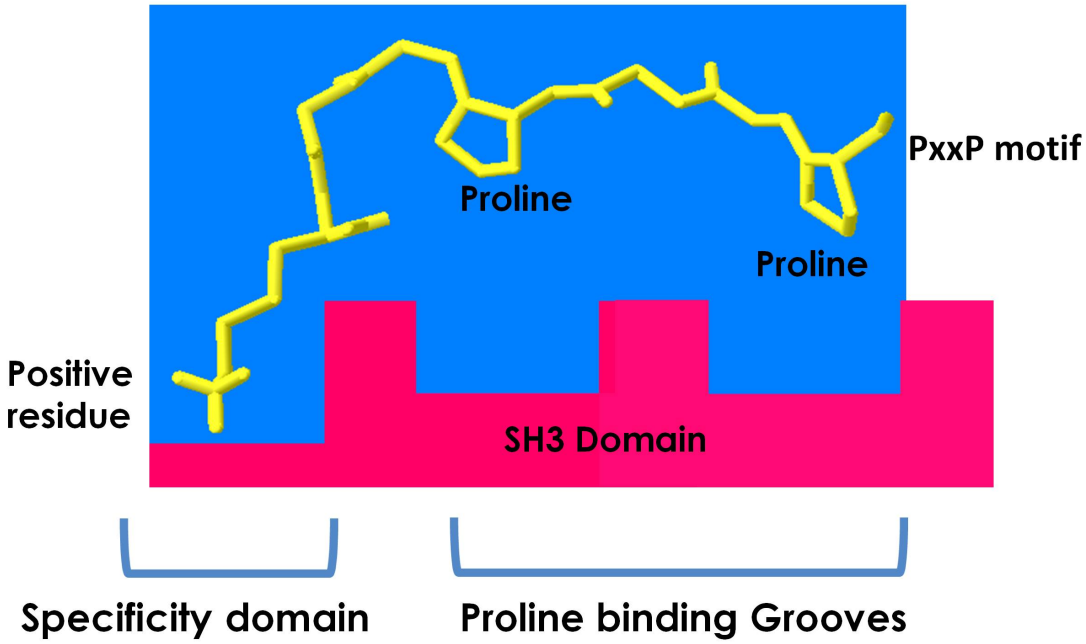

Figure 6.1: Illustration of SH3 domain binding a PxxP motif. The proline residues extend into two SH3 pockets while a third pocket binds a positive specificity-determining residue. The positive residue can be on either side of the PxxP motif and therefore determines the orientation of the PxxP containing protein relative to the SH3 domain. This figure is based on a figure from (Zarrinpar et al., 2003).

Agrobacterium expression of CucDIR1 in one leaf of the *Arabidopsis dir1-1* mutant rescued the SAR defect (Chapter 4, Figure 4.3). This suggests that CucDIR1 is functionally equivalent to AtDIR1 and is a DIR1 ortholog. If

CucDIR1 is an ortholog of AtDIR1, then CucDIR1 should move to distant tissues during SAR. To test this theory petiole exudates collected from cucumber plants were probed with the AtDIR1 antibody. A 7kDa AtDIR1-sized band was detected in mock- and SAR-induced petiole exudates of cucumber plants but it is unclear if this band corresponds to CucDIR1, CucDIR2 or both proteins (Cameron lab, unpublished). A protein gel blot using the AtDIR1 antibody to probe recombinant CucDIR1 and CucDIR2 showed that AtDIR1 antibody detects both proteins but not a highly similar AtLTP2sw protein suggesting that the antibody is specific for proteins similar to DIR1. CucDIR1 and CucDIR2 are present in the phloem before SAR induction, therefore an alternative method is required to monitor movement. Future experiments will include *Agrobacterium* expression of epitope-tagged CucDIR1-HA and CucDIR2-HA in cucumber or *Arabidopsis* followed by mock or SAR-induction. Petiole exudates will be collected from induced and distant tissues and probed with an HA-specific antibody to determine if these proteins have migrated to distant tissues upon SAR induction. In addition, testing the ability of CucDIR2 to complement the *Arabidopsis dir1-1* mutant along with the other crop orthologs (tomato, and soybean) is required to provide evidence that CucDIR2 and additional putative orthologs are in fact orthologous to AtDIR1.

Liu et al. 2011 found that tobacco TobDIR2 and TobDIR3 could complement the *dir1-1* mutation in *Arabidopsis*, while TobDIR1, which shares 62% sequence similarity with *Arabidopsis* DIR1, could not. There are no obvious differences between TobDIR1, 2, and 3 that explain the differences in *dir1-1* complementation (Figure 6.2). All three have a PxxP-like motif (PxPxPP, PxPxxP, PPxPxxP), polar head groups around their cavity

entrance and none of them have obvious hydrophilic residues in their hydrophobic pockets that might disrupt ligand binding.

```
TobDIR2 GSGDSPCGLSIGDLMSCKPAVSGPKPLPPSEKCCAALGKADLPCLCTFKNSPMISAFKIN
TobDIR1    LSLCNMGDDGLTACKPSVTKPNPVEPSASCCEALSGADLQCLCSYRNSLLLPSLGID
TobDIR3  ---QGICNISGEGLMSCKPSVTPPNPSAPTAKCCSALAHADWGCLCSYMNSHWLPSLGVD
            . *.:.  .* :***:*: *:*  *: .** **. **  ***:: **  :.:: ::

TobDIR2         ATLAMDLPSKCNLNSP-NCAA
TobDIR1         PELALALPPKCNLTSPANC--
TobDIR3         PTLAMQLPQKCKLPNPPHC--
                . **: ** **:* .* :*
```

Figure 6.2: Tobacco DIR1 ortholog mature protein sequence alignment using ClustalW. PxxP motif is highlighted in blue.

It may be more informative to compare the TobDIR1 sequence to a more similar protein like TomDIR1 to discover a mutation responsible for TobDIR1's inability to participate in SAR. Given that the phylogeny predicts with relatively high certainty (Bootstrap 73%) that TobDIR1 and TomDIR1 (95% sequence similarity, 86% sequence identity to each other at the amino acid level) are orthologs, it may be reasonable to predict that TomDIR1 may not complement the *Arabidopsis dir1-1* mutation either. Testing the ability of TomDIR1 to complement *dir1-1* will address this question. If TomDIR1 complements the *dir1-1* mutant then the high sequence similarity between TomDIR1 and TobDIR1 may allow the identification of the TobDIR1 residue responsible for SAR-defective phenotype in *dir1-1* complementation assays. There are only 10 differences in amino acids between the two proteins. Three of these amino acid substitutions result in a change in the R group characteristics (polar/aromatic/non-polar). For example, there is a glycine (small non-charged) to aspartic acid (negatively charged) substitution at residue 8. Thus, if the complementation data shows that TomDIR1 but not TobDIR1 can complement the *dir1-1* mutant than we can look more closely at these three substitutions through mutagenesis studies as this suggests that they are responsible for the lack of TobDIR1 complementation.

```
TobDIR1            1 -LSLCNMGDDGLTACKPSVTKPNPVEPSASCCEALSGADLQCLCSYRNSL     49
                       :::|||.|||||:|||||||:|||||||||||||||||||||||||||.
TomDIR1            1 XMNICNMDDDGLTSCKPSVTQPNPVEPSASCCEALSGADLQCLCSYRNSF     50

TobDIR1           50 LLPSLGIDPELALALPPKCNLTSPANC     76
                     :|||||||||||||||.|||||||:||
Tom1              51 VLPSLGIDPELALALPTKCNLTSPSNC     77
```

Figure 6.3: TobDIR1 and TomDIR1 mature protein sequence alignment using ClustalW.

6.3 TNS Inhibition/Displacement Binding Assays: Searching for the DIR1 Ligand

Only one biologically important *in vivo* ligand for an LTP has been identified. Buhot et al. (2004) showed that tobacco LTP1 binds the plant hormone jasmonic acid (JA) and application of this complex to plants increased pathogen resistance but application of LTP1 or JA alone did not. TNS inhibition/displacement binding assays were conducted in the hopes of identifying an *in vitro* DIR1 ligand. Little *in vitro* binding to any of the putative SAR ligands was observed using recombinant DIR1, DIR1 variants, DIR1-like, CucDIR1 and CucDIR2 (Chapter 4,5). TNS fluoresces in the hydrophobic cavity of the LTP2s. If a ligand binds to the LTP2 then it will displace TNS and cause a decrease in TNS fluorescence. Therefore ligands with high affinity for the LTP2 pocket will display TNS fluorescence inhibition. A similar TNS inhibition/displacement study by Buhot et al. (2004) examined ligand binding to an LTP1 protein. In previous LTP TNS inhibition/displacement binding studies TNS fluorescence inhibition above 75% was considered high, inhibition 50%-75% was moderate and inhibition between 30-50% was considered low (Buhot et al., 2004; Krasikov et al., 2011). Our highest TNS fluorescence inhibition was 35% (CucDIR2-AA) suggesting that all ligands bound with low affinity. Although pipecolic

acid (PA), azelaic acid (AA) or glycerol-3-phosphate (G3P) do not appear to bind DIR1 *in vitro* it is still possible that one of these molecules could be the *in vivo* ligand. Although DIR1 variants showed little *in vitro* binding to the putative ligands they did have a reduced capacity to bind TNS in the folding-assay. This suggests that these DIR1 variants have modifications that have affected the structure of their internal binding cavity to some capacity and support the idea that they maybe important to DIR1 function.

Ligand binding experiments using purified CucDIR1 and CucDIR2 revealed 30-35% TNS fluorescence inhibition suggesting a low levels of binding with azelaic acid (AA) (Chapter 4, Figure 4.5). Since AA is a dicarboxylic acid with polar oxygen molecules at both ends it is unclear how the CucDIR1 or CucDIR2 hydrophobic cavity could bind this molecule. It is difficult to imagine that either of the polar ends would be accommodated in the hydrophobic lipid binding pocket. However, nuclear magnetic resonance of a wheat LTP1 protein revealed that it bound prostaglandin which, like AA, contains a carboxyl group at the end of one of its chains (Tassin-Moindrot et al., 2000). AtDIR1 does not bind AA in the in vitro TNS assay suggesting that there are enough differences in structure between the cucumber DIR1 orthologs and DIR1 to cause differential affinities for the ligands tested. This was not predicted by the homology modeling as the 3-dimensional models of the cucumber orthologs and AtDIR1 are very similar. None of the putative ligands tested bound with high affinity. This suggests that these molecules are not ligands of AtDIR1 and cucumber DIR1 or that differential conditions exist *in vivo* which promote ligand binding. This could include the creation of a

protein complex or perhaps modifications to protein structure which allow binding of these putative ligands.

Sequence logo and DIR1/DIR1-like homology modeling revealed several residues that were highly conserved and may be important for protein function during SAR. Mutation in these residues produced several DIR1 variants and similar to DIR1, DIR1-like and the cucumber orthologs, these variants did not bind any of the putative ligands with high affinity. In one of the variants a mutation was made to disrupt the hydrophobic cavity as a negative control for our binding experiments. The location of Leu43 between two cysteine residues is hypothesized as critical for cysteine bond pairing (Samuel et al., 2002) and mutations in this residue in a rice LTP2 protein resulted in pocket disruption (Cheng et al., 2008). The hydrophobic Leu43 was converted to a hydrophilic aspartic acid (L43D) which was expected to completely disrupt cysteine pairing and pocket formation. However, in our protein folding experiment L43D seemed to have folded sufficiently to bind TNS. Cheng et al. (2008) measured pocket disruption using circular dichroism, therefore it is possible that a misfolded L43D protein provides a hydrophobic environment that binds TNS and allows it to fluoresce, either in a hydrophobic pocket or perhaps the protein is aggregating into some kind of micellar shape providing a hydrophobic environment at its center. It will be informative to use this L43D mutant in the Agro-SAR assay to test if the structure has changed sufficiently to inhibit *dir1-1* complementation.

A complementary *in vivo* strategy is also required to identify the DIR1 SAR ligand. The Cameron lab is pursuing this and plans to immunoprecipitate AtDIR1 from SAR-induced petiole exudates in hopes of pulling out any proteins or small molecules in complex with DIR1. We will

collaborate with Dr Corina Vlot to identify proteins that interact with DIR1 using LC-MS/MS or molecules in complex with DIR1 using GC/MS. This technique could reveal the DIR1 ligand and other proteins in the DIR1 signal complex.

There are several studies that support the idea of a DIR1 SAR complex. When expressed in Tobacco, DIR1(LTP2) and AZI1 (LTP1) were determined to form homo and heterodimers using bimolecular fluorescence complementation and co-immunoprecipitation, (Yu et al., 2013). The DIR1-AZI1 complex needs to be confirmed in its native *Arabidopsis* system but there is an example of a Barley LTP1-LTP2 complex in the literature (Stanislava, 2007). DIR1 homodimer formation is supported in our protein gel blots of petiole exudates from SAR-induced plants where we see DIR1 monomer (7kDa) and dimer-sized (14kDa) bands (Champigny et al., 2013). Although it is possible that a heterodimer is responsible for the 14kDa band, Champigny et al. (2013) showed that protein gel blots of SAR-induced petiole exudates from transgenic plants expressing DIR1-GFP contained both a ~40 and a ~66 kDa bands using both GFP and DIR1 antibodies. This suggests the presence of a DIR1-GFP monomer (~40kDa) and DIR1-GFP dimer (~60kDa). Protein gel blots of recombinant DIR1 protein show only a DIR1 monomer suggesting that dimerization may be a SAR-induced or activating event.

Studies of the putative SAR signal molecule, Dehydroabietinal (DA) have shown that DA is always present in the phloem, while in naïve plants DA exists in a low molecular weight complex and in SAR-induced plants DA becomes part of a high molecular weight complex (Chaturvedi et al., 2012). Chaturvedi et al. (2012) hypothesized that DIR1 may be part of the high MW complex. Shah et al. revealed in a recent review that DIR1 is

present in the high molecular weight complex (Shah and Chaturvedi, 2013) providing evidence for a DIR1 SAR complex during SAR.

To investigate DIR1 complex formation it would be informative to conduct protein gel blots under native conditions (BlueNative Page) with our DIR1 antibody to see if DIR1 from SAR -activated petiole exudates is part of a complex. Another interesting experiment would be to conduct native protein gel blot analysis on cucumber exudates from mock- or SAR-induced plants. Since CucDIR1 and/or CucDIR2 are present in the phloem at all times, a change in band size after SAR induction might suggest that a cucumber DIR1 complex forms. Further research is required to understand the role of DIR1 complexes during SAR.

6.4 DIR1/DIR1-like model for SAR

I hypothesize that DIR1 and DIR1-like are in the process of sub-functionalization, however residual function to participate in SAR and seed development is possible. I base this hypothesis on the fact that *dir1-1* mutants germinate poorly on soil and DIR1 and DIR1-like are highly expressed during seed development (Toronto BAR (Winter et al., 2007)). Perhaps DIR1 has become the prime participant in SAR while DIR1-like is required for seed development. Further investigation is required to address this hypothesis.

Our studies to date suggest that DIR1 and its orthoglogs are activated by a SAR-inducing pathogen. This is supported by the fact that in *Arabidopsis,* DIR1 is only detected in the phloem after SAR induction. In addition, DIR1 overexpression lines do not display constitutive SAR (Maldonado et al., 2002). This suggests that DIR1 must be activated either through a protein complex or a cellular change that allows DIR1 to be

loaded into the phloem upon SAR induction in *Arabidopsis*. In cucumber, CucDIR1 and CucDIR2 appear to be present in the phloem before SAR induction (Cameron lab unpublished) suggesting that some change occurs to activate these proteins. Thus both AtDIR1 and the DIR1 cucumber orthologs require SAR induction for activation.

DIR1 binds two monoacylated phospholipids in its hydrophobic cavity *in vitro* (Lascombe et al., 2006; Lascombe et al., 2008), however DIR1 *in vivo* ligand(s) are still unknown. Several candidates for the SAR mobile signal have been proposed including MeSA, G3P, AA and DA but some are more likely than others be a DIR1 ligand. MeSA levels in distant tissues of SAR-induced plants are higher in the *dir1-1* mutant than in wild-type plants (Liu et al., 2011b). This suggests that if MeSA does travel to distant tissues during SAR, MeSA can travel there without DIR1. It is important to note that exogenous MeSA application does not induce SAR in the *dir1-1* mutant (Liu et al., 2011b). Thus MeSA may require DIR1 in distant tissues but due to its distant leaf accumulation in the absence of DIR1, MeSA is unlikely to be a DIR1 ligand. The ability of AA to travel systemically during *Pst* (*avrRpt2*)-induced SAR was confirmed by isotopically labeling AA (Jung et al., 2009). Azelaic acid accumulates in exudates in response to avirulent *Pst* (Jung et al., 2009) but not in response to virulent *Pst* (Navarova et al., 2012). Navarova et al. (2012) have suggested that AA may amplify and strengthen SAR manifestation in distant leaves but its movement is not essential for the SAR response. In addition, Yu et al. (2013) found that transport of AA to distant tissues during SAR was unaffected in the *dir1-1* mutant (Yu et al., 2013) although AA requires functional DIR1 to enhance SAR priming (Jung et al., 2009).

Therefore I predict that AA is also unlikely to be part of the DIR1 signal complex.

In order to be a candidate for a DIR1-ligand SAR long distance signal complex, molecules must be shown to travel from induced to distant tissue and there should be evidence of complex formation with DIR1. Pipecolic acid (PA), dehydroabietinal (DA) and a lipid derivative of glycerol-3-phosphate (G3Pd) are all strong candidates for the DIR1-ligand SAR complex. PA is a small molecule that could easily fit into the DIR1 hydrophobic cavity. Although the requirement for DIR1 in pipecolic acid (PA)- induced resistance has not been tested, PA is able to travel systemically when administered through the roots, a key characteristic of a long distance signal. Evidence for PA movement was provided when PA deficient *ald1* plants, were watered with PA and PA was detected in distant tissues (Navarova et al., 2012).

DA is another small molecule that could bind to the hydrophobic pocket of DIR1. Radiolabeled exogenously applied DA was shown to move to distant tissues (Chaturvedi et al., 2012). It seems likely that DIR1 and DA are part of a high molecular weight complex identified by Chaturvedi et al. (2012) (Shah and Chaturvedi, 2013). Whether or not DIR1 binds DA directly or is in a complex with a putative DA carrier-protein remains to be determined. Thus DA possesses both key characteristics of a candidate for the DIR1-ligand SAR long distance signal, systemic movement and evidence of DIR1 complexation.

G3P is also a good DIR1 ligand candidate. Evidence of G3P movement and requirement of DIR1 was shown when exogenously applied radiolabeled G3P was coinfiltrated with recombinant DIR1 protein and a G3P derivative was detected in distant tissues (Chanda et al.,

2011). Chanda et al. failed to test if DIR1 protein folded and the level of DIR1 protein applied may have induced cell death which itself has been shown to induce SAR and maybe responsible for G3P movement. In addition G3P was tested for its ability to cause DIR1 movement in tobacco by co-infiltration *Agrobacterium* expressing DIR1-RFP and TMV movement protein tagged with GFP. Although not clearly stated, it is assumed that TMV movement protein-GFP is used as a plasmodesmata marker to show that DIR1 is traveling through the plasmodesmata in the phloem. However, TMV movement protein is known to affect plasmodesmata size exclusion limits (Wolf et al., 1989) by modifying the cytoskeleton (Liu and Nelson, 2013) and therefore is a poor choice of marker for DIR1 movement through the plasmodesmata as it could enhance movement. In addition, this group failed to include a random similarly sized protein as a control to ensure that the addition of TMV movement protein did not cause all proteins to move through the plasmodesmata. Therefore additional evidence is required to determine if G3P moves to distant tissue and if this movement is dependent on DIR1. G3P establishment of resistance in distant tissues does require DIR1 and AZI1 as G3P plus naïve exudate could induce SAR in wild-type but not *dir1-1* or *azi1* plants (Chanda et al., 2011; Yu et al., 2013). Thus G3P remains a possible DIR1 ligand.

I predict that a DIR1/AZI1 protein complex binds DA and possibly PA, and or a G3P derivative and transports the signal(s) to distant tissues for SAR activation. It is interesting to note that the high molecular weight DA complex is approximately 100kDa. DIR1 and AZI1 are only 7 and 9 kDa respectively. This suggest that several other proteins participate in this SAR complex. It is unclear how DIR1 or DIR1-ligands or DIR1-ligand-protein complex enters the phloem but both secreted and cytosolic DIR1 proteins

participate in SAR (Champigny et al., 2011). Perhaps the DIR1 complex moves cell-to-cell first and then is loaded into the phloem enabling DIR1 to travel to distant leaves. In distant leaves I predict that DIR1 interacts with a receptor protein. It is possible that an SH3 domain-containing protein acts as a scaffold to mediate DIR1 docking to a receptor in distant tissue. Another possibility is that the receptor contains a SH3 domain and through a PxxP and SH3 domain interaction, a conformational change occurs in DIR1 that releases the SAR mobile signal(s) that DIR1 chaperoned through the phloem. AA, MeSA, DA, PA, and a G3P derivative then act synergistically to increase SA accumulation leading to the activation of NPR1 and SAR establishment in distant leaves.

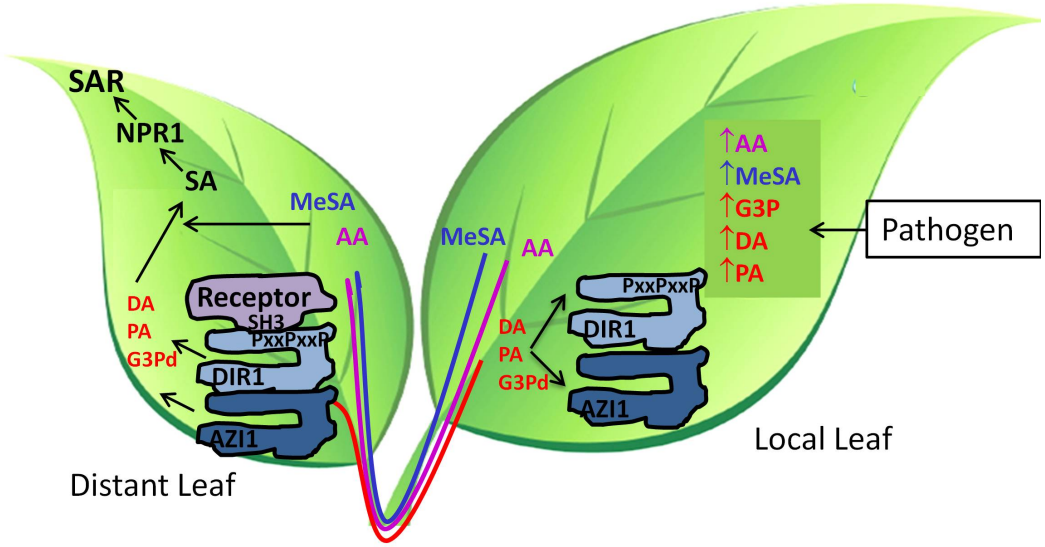

Figure 6.4: Simplified model of DIR1 and putative SAR signal movement from a local SAR-induced leaf to distant leaf. Pathogen exposure leads to increased accumulation of AA, MeSA, G3P, DA and PA. MeSA does not require DIR1 for movement to distant tissues although SAR establishment requires MeSA and DIR1. AA seems to participate and amplify SAR in response to avirulent but not virulent pathogen infection and therefore is not likely part of the DIR1 SAR complex but travels to distant tissues on its own or as part of some other complex. DA, PA and G3Pd are good candidates for DIR1 or AZI1 ligand binding and are likely transported to distant tissues by these LTPs during SAR. In distant tissues DIR1 ligand release may be triggered by interaction with a SH3 domain containing receptor protein. The different signaling molecules act synergistically to increase SA which induces transcription changes through key SAR regulator NPR1 thus priming the plant against future attack.

Conclusion:

By examining DIR1 and DIR1-like in *Arabidopsis* and Cucumber, this thesis has increased our understanding of DIR1-like involvement during Systemic Acquired Resistance and DIR1 protein structure. A phylogenetic

analysis provided evidence that DIR1 and DIR1-like arose from a recent tandem duplication event. Furthermore, our data suggests that similar to DIR1, DIR1-like travels from induced to distant tissues during SAR. This supports our hypothesis that DIR1-like may be able to replace DIR1 function resulting in the occasional SAR competent phenotype of the *dir1-1* mutant. This work provides useful tools for future dissection of the roles of DIR1 and DIR1-like during SAR through the creation of a *dir1-1dir1-like* double knockdown lines as well as SS-HA-DIR1-iLOV and SS-FLAG-DIR1-like-phiLOV transgenic plants. Understanding the role of DIR1-like during the SAR response may help explain why there is variation in data between SAR labs. Through homology modeling and sequence Logo analysis, new protein motifs in DIR1 were identified that may be critically important for SAR function. The importance of these residues is supported by the reduced TNS binding in these DIR1 variants. In addition, new putative DIR1 orthologs were identified and complementation studies support the idea that AtDIR1 and CucDIR1 are functionally orthologous, providing additional evidence that SAR mechanisms are conserved among plant species.

Appendix

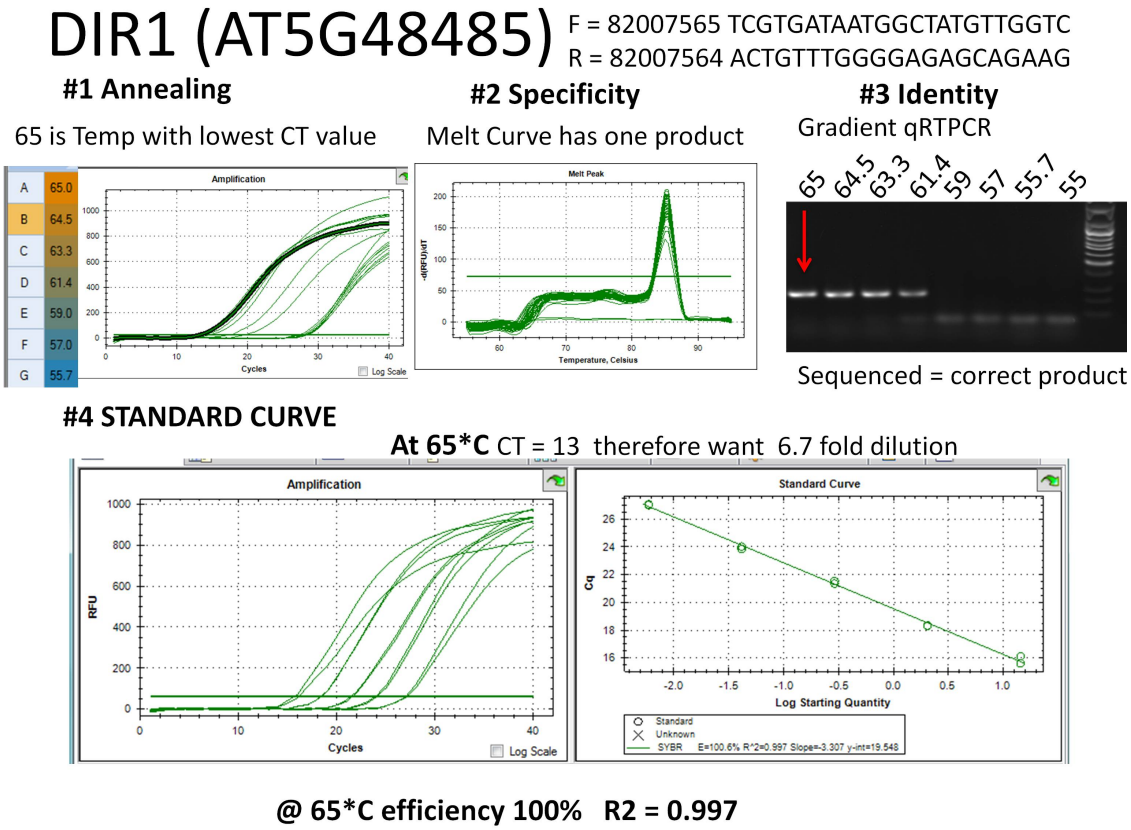

Figure 7.1: Summary of DIR1 primer validation. First a gradient PCR was performed to check for optimal primer annealing temperature which was shown to be 65°C. The Melt Curve was assessed at the annealing temperature selected to ensure that a single product was being produced (one peak). The 65°C annealing temperature products were then run on a gel to check that the product was of the anticipated size. These bands were excised from the gel, purified and sent for sequencing to ensure that the correct product was being produced. Based on the CT value obtained in the gradient qRT-PCR, a dilution was designed to cover the entire qRT-PCR working range (10-35CTs). An 8 point standard curve was created by diluting the cDNA and this was used to calculate primer efficiency. Points could be removed from the beginning or the end of the standard curve with a minimum of 5 points remaining.

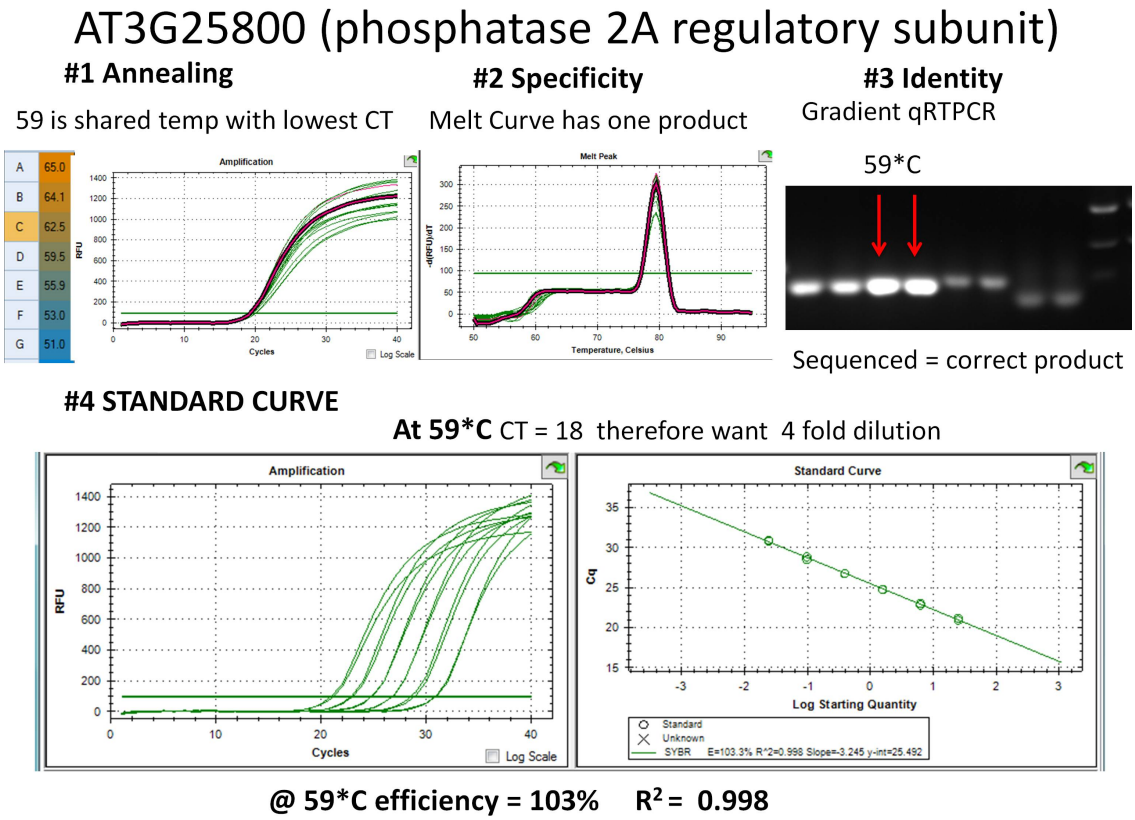

Figure 7.2: Summary of reference gene AT3G25800 primer validation. First a gradient PCR was performed to check for optimal primer annealing temperature which was shown to be 59°C. The Melt Curve was assessed at the annealing temperature selected to ensure that a single product was being produced (one peak). The 59°C annealing temperature products were then run on a gel to check that the product was of the anticipated size. These bands were excised from the gel, purified and sent for sequencing to ensure that the correct product was being produced. Based on the CT value obtained in the gradient qRT-PCR, a dilution was designed to cover the entire qRT-PCR working range (10-35CTs). An 8 point standard curve was created by diluting the cDNA and this was used to calculate primer efficiency. Points could be removed from the beginning or the end of the standard curve with a minimum of 5 points remaining.

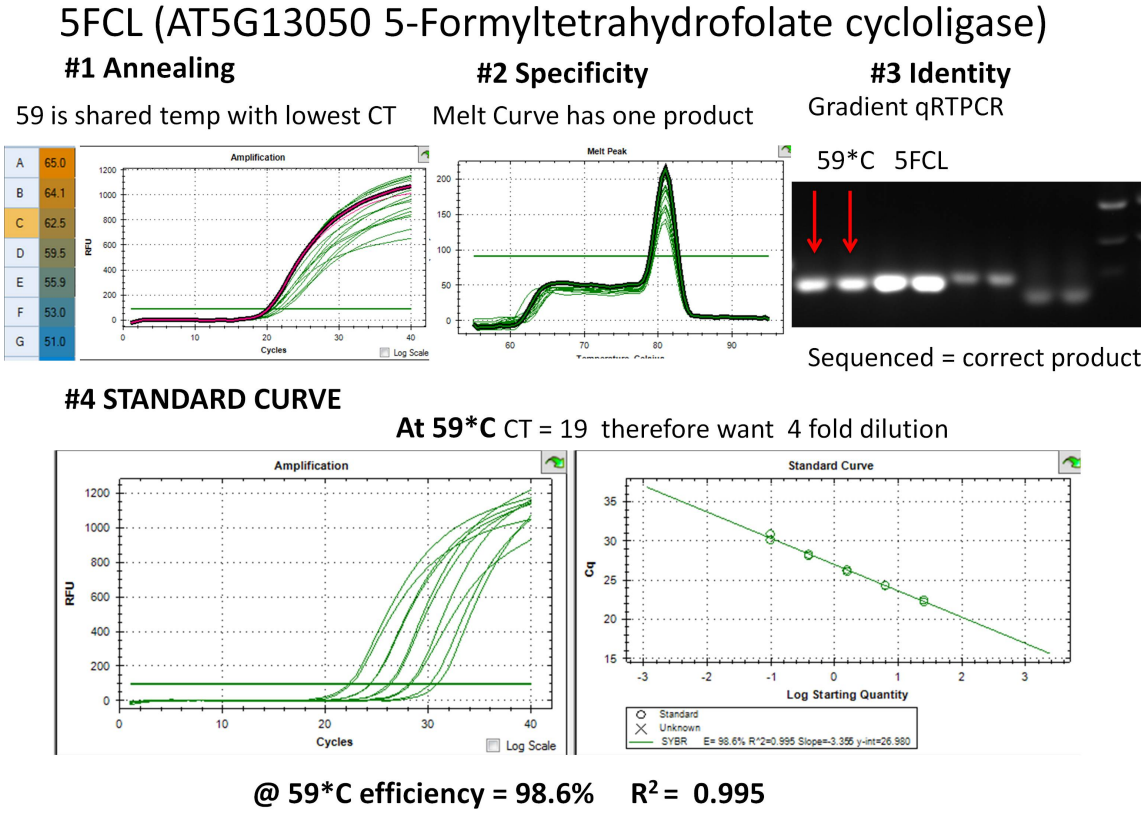

Figure 7.3: Summary of reference gene 5FCL primer validation. First a gradient PCR was performed to check for optimal primer annealing temperature which was shown to be 59°C. The Melt Curve was assessed at the annealing temperature selected to ensure that a single product was being produced (one peak). The 59°C annealing temperature products were then run on a gel to check that the product was of the anticipated size. These bands were excised from the gel, purified and sent for sequencing to ensure that the correct product was being produced. Based on the CT value obtained in the gradient qRT-PCR, a dilution was designed to cover the entire qRT-PCR working range (10-35CTs). An 8 point standard curve was created by diluting the cDNA and this was used to calculate primer efficiency. Points could be removed from the beginning or the end of the standard curve with a minimum of 5 points remaining.

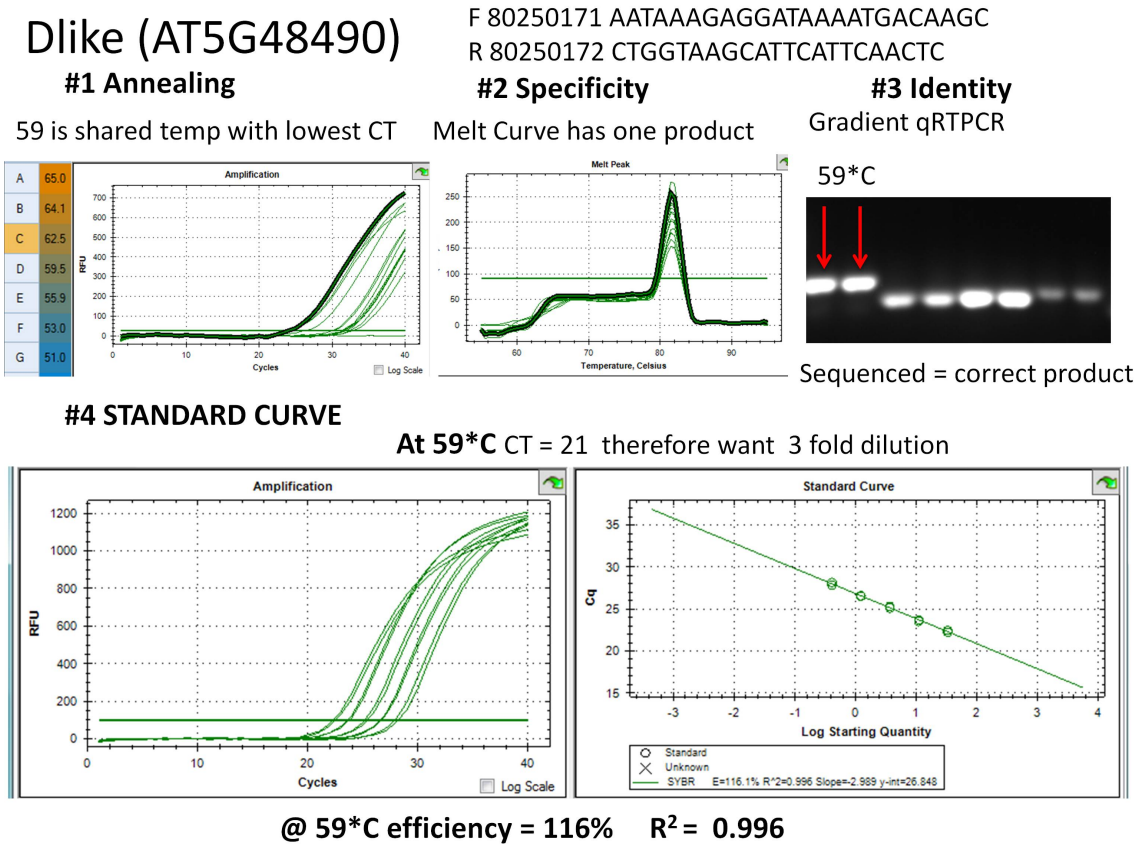

Figure 7.4: Summary of DIR1-like primer validation. First a gradient PCR was performed to check for optimal primer annealing temperature which was shown to be 59°C. The Melt Curve was assessed at the annealing temperature selected to ensure that a single product was being produced (one peak). The 59°C annealing temperature products were then run on a gel to check that the product was of the anticipated size. These bands were excised from the gel, purified and sent for sequencing to ensure that the correct product was being produced. Based on the CT value obtained in the gradient qRT-PCR, a dilution was designed to cover the entire qRT-PCR working range (10-35CTs). An 8 point standard curve was created by diluting the cDNA and this was used to calculate primer efficiency. Points could be removed from the beginning or the end of the standard curve with a minimum of 5 points remaining.

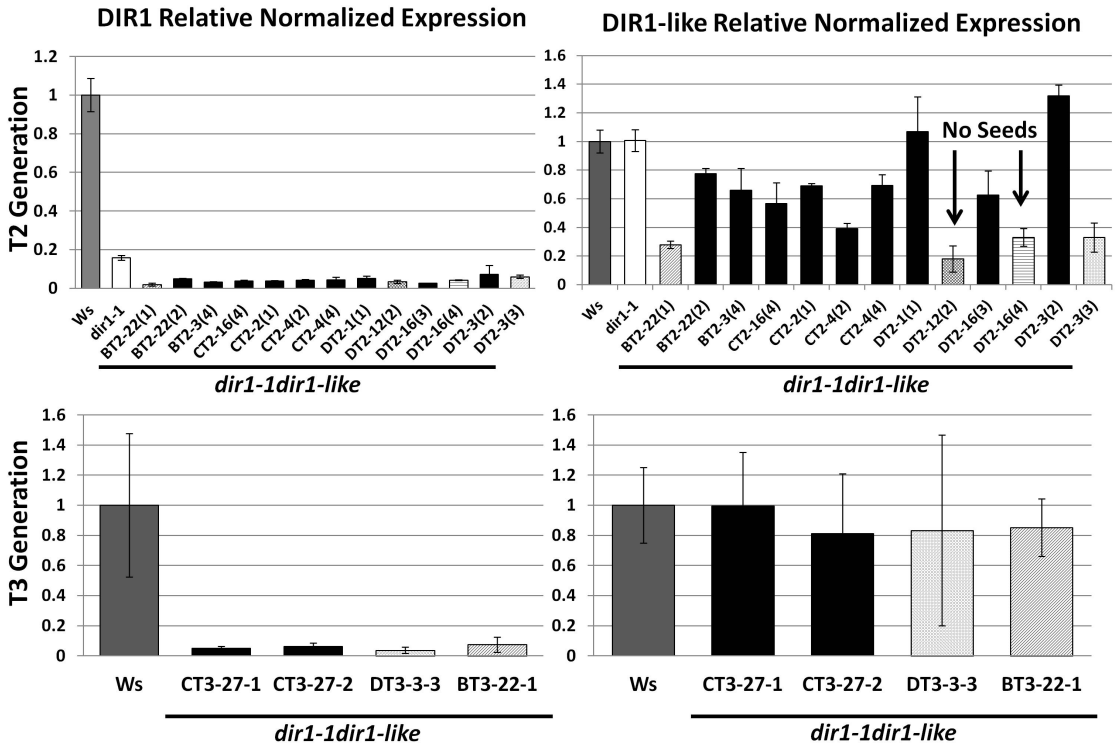

Figure 7.5: Additional Screen of quantitative Real Time PCR (qRT-PCR) analysis of *DIR1* and *DIR1-like* transcript abundance relative to wild-type Ws plants in untreated T2 and T3 plants collected at 3wpg. Values were normalized to 5CFL and AT5G25800 reference genes. Fold-expression was calculated relative to the wild-type Ws control. T2 tissue was collected from a single plant and analyzed in three technical replicates. T2 error bars represent the standard deviation of the technical variation. Homozygous T3 tissue was collected in biological triplicate and analyzed in technical triplicates. T3 error bars represent the standard deviation of the biological variation. A Students T-test was used to identify significant differences ($p<0.05$) compared to Ws plants and is denoted by (*). B,C,D abbreviations indicate the type of antisense construct used (See table 3.1). Expected mutation is identified bellow the construct identifier.

Table 7.1: Control wells containing TNS and ligand or MES show similar levels to TNS alone.

Contents of Control Wells	Average Fluorescence
TNS alone	918
TNS + AA	868
TNS + PA	940
TNS + G3P	856
TNS + MES	865

Table 7.2: Sequence Similarity and Identity due to chance alone.

Random Sequence	Sequence Similarity	Sequence Identity
1	0	0%
2	5%	2%
3	1%	1%
4	13%	9%
5	4%	3%
6	12%	10%
7	5%	3%
8	16%	9%
9	14%	7%
10	16%	9%

Table 7.3: Genome or scaffold locations of the DIR1 orthologs.

AtDIR1 Ortholog	Location in the Genome/Scaffold
CucDIR1	scaffold03967: 503773 – 504645
CucDIR2	scaffold00919: 595227 – 595904
SoyDIR1	Gm18: 30001494 – 30003858
SoyDIR2	Gm10: 50833656 – 50833967
SoyDIR3	Gm08: 45094410 - 45095370
TomDIR1	SL1.00sc05992:831,746..832,316
TomDIR2	Unknown genomic location EST only
TomDIR3	SL1.00sc05477:392,537..393,262

TobDIR1	C59324: 2309-2623
TobDIR2	C43434: 646-966
TobDIR3	C32287: 78-530

References

Afzal A.J., Cunha L., and Machey D. (2011). Separable fragments and membrane tethering of *Arabidopsis* RIN4 regulate its suppression of PAMP-triggered immunity. The Plant Cell **23,** 3798-3811.

Arnold K., Bordoli L., Kopp J., and Schwede T. (2006). The SWISS-MODEL workspace: a web-based environment for protein structure homology modelling. Bioinformatics **22,** 195-201.

Attaran E., Zeier T.E., Griebel T., and Zeier J. (2009). Methyl salicylate production and jasmonate signaling are not essential for Systemic Acquired Resistance in *Arabidopsis*. The Plant Cell **21,** 954-971.

Bakan B., Hamberg M., Perrocheau L., Maume D., Rogniaux H., Tranquet O., Rondeau C., Blein J., Ponchet M., and Marion D. (2006). Specific adduction of plant lipid transfer protein by an allene oxide generated by 9-lipoxygenase and allene oxide synthase. The Journal of Biological Chemistry **281,** 38981-38988.

Beckers G.J., Jaskiewicz M., Liu Y., Underwood W.R., He S.Y., Zhang S., and Conrath U. (2009). Mitogen-Activated Protein Kinases 3 and 6 are required for full priming of stress responses in *Arabidopsis thaliana*. The Plant Cell **21,** 944-953.

Beilstein M.A., Nagalingum N.S., Clements M.D., Manchester S.R., and Mathews S. (2010). Dated molecular phylogenies indicate a Miocene origin for *Arabidopsis thaliana*. PNAS **107,** 18724-18728.

Blanc G. and Wolfe K.H. (2004). Functional divergence of duplicated genes formed by polyploidy during *Arabidopsis* evolution. The Plant Cell **16,** 1679-1691.

Boller T. and Gomez-Gomez L. (1999). A single locus determines sensitivity to bacterial flagellin in *Arabidopsis thaliana*. The Plant Journal **18,** 277-284.

Booler T. and He S.Y. (2009). Innate Immunity in Plants: An arms race between pattern recognition receoptors in plants and effectors in microbial pathogens. Science **324,** 742-744.

Buhot N., Gomes E., Milat M., Ponchet M., Marion D., Lequeu J., Delrot S., Coutos-Thevenot P., and Blein J. (2004). Modulation of the biological activity of a tobacco LTP1 by lipid complexation. Molecular Biology of the Cell **15,** 5047-5052.

Cameron R.K., Dixon R.A., and Lamb C.J. (1994). Biologically induced systemic acquired resistance in *Arabidopsis thaliana*. The Plant Journal **5,** 715-725.

Cameron R.K., Paiva N.L., Lamb C.J., and Dixon R.A. (1999). Accumulation of salicylic acid and PR-1 gene transcripts in relation to the systemic aquired resistance (SAR) response induced by *Pseudomonas syringae* pv. *tomato* in *Arabidopsis*. Physiological and Molecular Plant Pathology **55,** 121-130.

Caruso F.L. and Kuc J. (1979). Induced resistance of cucumber to anthracnose and angular leaf spot to *Pseudomonas lachrymans* and *Colletotrichum lagenarium*. Physiology Plant Pathology **14,** 191-201.

Carvalho A.d.O. and Gomes V.M. (2007). Role of plant lipid transfer proteins in plant cell physiology - A concise review. Peptides **28,** 1144-1153.

Champigny M., Shearer H., Faubert J., Mohammad A., Haines K., Neumann M., Thilmoney R., He S.Y., Fobert P., Dengler N., and Cameron R.K. (2011). Localization of DIR1 at the tissue, cellular and subcellular levels during Systemic Acquired Resistance in *Arabidopsis* using DIR1:GUS and DIR1:EGFP reporters. BMC Plant Biology **11,** 1-16.

Champigny M.J., Isaacs M., Carella P., Faubert J., Fobert P.R., and Cameron R.K. (2013). Long distance movement of DIR1 and investigation of the role of DIR1-like during systemic acquired resistance in *Arabidopsis*. Frontiers in Plant Science **4,** 1-20.

Champigny M.J. and Cameron R.K. (2009). Chapter 4 Action at a Distance: Long-Distance Signals in Induced Resistance in Advances in Botanical Research. Volume 51, L.C. Van Loon, ed (Academic Press) pp. 123-171, doi/DOI: 10.1016/S0065-2296(09)51004-X.

Chanda B., Xia Y., Mandal M.K., Yu K., Sekine K., Gao Q., Selote D., Hu Y., Stromberg A., Navarre D., Kachroo A., and Kachroo P. (2011). Glycerol-3-phosphate is a critical mobile inducer of systemic immunity in plants. Nature Genetics **43,** 421-427.

Chapman S., Faulkner C., Kaiserli E., Garcia-Mata C., Savenkov E.I., Roberts A.G., Oparka K.J., and Christie J.M. (2008). The photoreversible

fluorescent protein iLOV outperforms GFP as a reporter of plant virus infection. Proceedings of the National Academy of Sciences **105**.

Chaturvedi R., Venables B., Retros R.A., Nalam V., Li M., Wang X., Takemoto L.J., and Shah J. (2012). An abietane diterpenoid is a potent activator of systemic acquired resistance. Plant Journal **71,** 161-172.

Chaturvedi R., Krothapalli K., Makandar R., Nandi A., Sparks A.A., Roth M.R., Welti R., and Shah J. (2008). Plastid *w*3-fatty acid desaturase-dependent accumulation of a systemic aquired resistance inducing activity in periole exudates of *Arabidopsis thaliana* is independent of jasmonic acid. The Plant Journal **54,** 106-117.

Chen Z., Agnew J.L., Cohen J.D., He P., Shen L., Sheen J., and Kunkel B.N. (2007). *Pseudomonas syringae* type III effector AvrRpt2 alters *Arabidopsis thaliana* auxin physiology. PNAS **104,** 20131-20136.

Cheng C.S., Chen M.N., Lai Y.T., Chen T., Lin K.F., Liu Y.J., and Lyu P.C. (2008). Mutagenesis study of rice non-specific lipid transfer protein 2 reveals residues that contribute to structure and ligand binding. Proteins **70,** 695-706.

Christie J.M., Hitomi K., Arvai A.S., Hartfield K.A., Mettlen M., Pratt A.J., Tainer J.A., and Getzoff E.D. (2012). Structural Tuning of the Fluorescent Protein iLOV for Improved Photostability. The Journal of Biological Chemistry **287,** 22295-23304.

Clough S.J. and Bent A.F. (1998). Floral dip: a simplified method for *Agrobacterium*-mediated transformation of *Arabidopsis thaliana*. The Plant Journal **16,** 735-743.

Crooks G.E., Hon G., Chandonia J., and Brenner S.E. (2004). WebLogo: A Sequence Logo Generator. Genome Research **14,** .

Cui F., Wu S., Sun W., Coaker G., Kunkel B., He P., and Shan L. (2013). The *Pseudomonas syringae* Type III Effector AvrRpt2 Promotes Pathogen Virulence via Stimulating *Arabidopsis* Auxin/Indole Acetic Acid Protein Turnover. Plant Physiology **162,** 1018-1029.

Cunnac S., Lindeberg M., and Collmer A. (2009). *Pseudomonas syringae* type III secretion system effectors: repertoires in search of functions. Current Opinion in Microbiology **12,** 53-60.

Curtis M.D. and Grossniklaus U. (2003). A Gateway Cloning Vector Set for High-Throughput Functional Analysis of Genes *in Planta*. Plant Physiology **133,** 462-469.

Dean R.A. and Kuc J. (1986). Induced systemic protection in cucumbers: the source of the "signal". Physiological and Molecular Plant Pathology **28,** 227-233.

DeBono A., Yeats T.H., Rose J.K.C., Bird D., Jetter R., Kunst L., and Samuels L. (2009). *Arabidopsis* LTPG is a Glycosylphosphatidylinositol-Anchored Lipid Transfer Protein Required for Export of Lipids to the Plant Surface. The Plant Cell **21,** 1230-1238.

Delaney T.P., Friedrich L., and Ryals J.A. (1995). *Arabidopsis* signal transduction mutant defective in chemically and biologically induced disease resistance. PNAS **92,** 6602-6606.

Delaney T.P., Uknes S., Vernooji B., Friedrich L., Weymann K., Negrotto D., Gaffney T., Gut-Rella M., Kessmann H., Ebon M., and Ryals J. (1994). A central role in salicylic acid in plant disease resistance. Science **266,** 1247.

Dempsey D.A. and Klessig D.F. (2012). SOS - too many signals for systemic acquired resistance? Trends in Plant Science **17,** .

Dodds P.N. and Rathjen J.P. (2010). Plant immunity: towards an integrated view of plant-pathogen interactions. Nature Reviews **11,** 539-548.

Dong X., Mindrinos M., Davis K.R., and Ausubel F.M. (1991). Induction of *Arabidopsis* defense genes by virulent and avirulent *Pseudomonas syringae* strains and by a cloned avirulence gene. The Plant Cell **3,** 61-72.

Dong X. and Durrant W.E. (2004). Systemic Acquired Resistance. Annual Review of Pytopathology **42,** 185-209.

Dong X. and Spoel S.H. (2013). How do plants achieve immunity? Defence without specialized immune cells. Nature Reviews **12,** 89-100.

Douliez J.P., Pato C., Rabesona H., Molle D., and Marion D. (2001). Disulfide bond assignment, lipid transfer activity and secondary structure of a 7-kDa plant lipid transfer protein, LTP2. FEBS **268,** 1400-1403.

Dowen R.H., Pelizzola M., Schmitz R.J., Lister R., Dowen J.M., Nery J.R., Dixon J.E., and Ecker J.R. (2012). Widespread dynamic DNA methylation in response to biotic stress. PNAS **109,** 12858-12859.

Drummond A.J., Suchard M.A., Dong X., and Rambaut A. (2012). Bayesian phylogenetics with BEAUti and the BEAST 1.7. Molecular Biology and Evolution **29,** 1969-1973.

Felsenstein J. (1985). Confidence limits on phylogenies: An approach using the bootstrap. Evolution **39,** 783-791.

Fire A., Xu S., Montgomery M.K., Kostas S.A., Driver S.E., and Mello C.C. (1998). Potent and Specific genetic interference by double-stranded RNA in *Caenorhabditis elegans*. Nature **391,** 806-811.

Fu Z.Q., Yan S., Saleh A., Wang W., Ruble J., Oka N., Mohan R., Spoel S.H., Tada Y., Zheng N., and Dong X. (2012). NPR3 and NPR4 are receptors for the immune signal salicylic acid in plants. Nature **487,** 228-233.

Fu Z.Q. and Dong X. (2013). Systemic Acquired Resistance: Turning local infection into global defense. Annual Reviews in Plant Biology **64,** 839-863.

Gaffney T.F., Leslie, Vernooij B., Negrotto D., Nye G., Uknes S., Ward E., Kessmann H., and Ryals J. (1993). Requirement of salicylic acid for the induction of Systemic Acquired Resistance. Science **261,** 754-756.

Girault T., Fancais J., Rogniaux H., Pascal S., Delrot S., Coutos-Thevenot P., and Gomes E. (2008). Exogenous application of a lipid transfer protein-jasmonic acid complex induces protection of grapevine towards infection by *Botrytis cinerea*. Plant Physiology and Biochemistry **46,** 140-149.

Goodstein D.M., Shu S., Howson R., Neupane R., Hayes R.D., Fazo J., Mitros T., Dirks W., Hellsten U., Putnam N., and Rokhsar D.S. (2012). Phytozome: a comparative platform for green plant genomics. Nucleic Acids Research **40,** 1178-1186.

Griebel T. and Zeier J. (2008). Light regulation and daytime dependency of inducible plant defenses in *Arabidopsis*: Phytochrome signaling controls Systemic Acquired Resistance rather than local defense. Plant Physiology **147,** 790-801.

Guedes M.E.M., Richmond S., and Kuc J. (1980). Induced systemic resistance to anthracnose in cucumber as influenced by the location of the inducer inoculation with *Colletotrichum lagenarium* and the onset of flowering and fruiting. Physiological Plant Pathology **17,** 229-233.

Guex N. and Peitsch M.C. (1997). SWISS-MODEL and the Swiss-Pdb Viewer: an environment for comparative protein modeling. Electrophoresis **18,** 2714-2723.

Han M.V. and Zmasek C.M. (2009). phyloXML: XML for evolutionary biology and comparative genomics. BMC Bioinformatics **10,** 356-363.

Huang S., Li R., Zhang Z., Li L., Gu X., Fan W., Lucas W.J., Wang X., Xie B., Ni P., Ren Y., Zhu H., Li J., Lin K., Jin W., Fei Z., Li G., Staub J., Kilian A., Vossen E.A.G., Wu Y., Guo J., He J., Jia Z., Ren Y., Tian G., Lu Y., Ruan J., Qian W., Wang M., Huang Q., Li B., Xuan Z., Cao J., Asan, Wu Z., Zhang J., Cai Q., Bai Y., Zhao B., Han Y., Li Y., Li X., Wang S., Shi Q., Liu S., Cho W.K., Kim J., Xu Y.,

Hller-Uszynska K., Miao H., Cheng Z., Zhang S., Wu J., Yang Y., Kang G., Li M., Liang H., Ren X., Shi Z., Wen M., Jian M., Yang H., Zhang G., Yang Z., Chen R., Liu S., Li J., Ma L., Liu D., Zhou Y., Zhao J., Fang X., Li G., Fang L., Li Y., Liu D., Zheng H., Zhang Y., Qin N., Li Z., Yang G., Yang S., Bolund L., Kristiansen K., Zheng H., Li S., Zhang X., Yang H., Wang J., Sun R., Zhang B., Jiang S., Wang J., Du Y., and Li S. (2009). The genome of the cucumber, *Cucumis sativus L.*. Nature Genetics **advanced online publication,** 1-9.

Isono E., Katsiarimpa A., Muller I.K., Anzenberger F., Stierhof Y., Geldner N., Chory J., and Schwechheimer C. (2010). The Deubiquitinating Enzyme AMSH3 Is Required for Intracellular Trafficking and Vacuole Biogenesis in *Arabidopsis thaliana*. The Plant Cell **22,** 1826-1837.

Hoh F., Pns J., Fautier M., Lamotte F.d., and Dumas C. (2005). Structure of a liganded type 2 non-specific lipid-transfer protein from wheat and the molecular basis of lipid binding. Biological Christallography **61,** 397-406.

Holsters M., Silva B., Van Vliet F., Genetello C., De Block M., Dhaese P., Depicker A., Inze D., Engler G., Villarroel R., van Montagu M., and Schell J. (1980). The functional organization of the nopaline *A.tumefaciens* plasmid pTiC58. Plasmid **3,** 212-230.

Jambunathan N., Siani J.M., and McNellis T.W. (2001). A humidity-sensitive *Arabidopsis* copine mutant exhibits percocious cell death and increased disease resistance. The Plant Cell **10,** 2225-2240.

Jaskiewicz M., Conrath U., and Peterhansel C. (2011). Chromatin modification acts as a memory for systemic acquired resistance in the plant stress response. EMBO **12,** 50-55.

Jenns A.E. and Kuc J. (1979). Graft Transmission of Systemic Resistance of Cucumber to Anthracnose Induced by *Colletotrichum lagenarium* and Tobacco Necrosis Virus. The Americal Phytopathological Society **7,** 753-756.

Jones J.D.G. and Dangl J.L. (2001). Plant pathogens and integrated defence responses to infection. Nature **411,** 826-833.

Jones J.D.G. and Dangl J.L. (2006). The plant immune system. Nature **444,** 323-329.

Jung H.W., Tschaplinski T.J., Wang L., Glazebrook J., and Greenberg J.T. (2009). Priming in Systemic Plant Immunity. Nature **324,** 89-91.

Katagiri F., Thilmony R., and He S.Y. (2002). The *Arabidopsis Thaliana-Pseudomonas Syringae* Interaction. The American Society of Plant Biologist, pp. 1-61.

Kay B.K., Williamson M.P., and Sudol M. (2000). The importance of being proline: the interaction of proline-rich motifs in signaling proteins with their cognate domains. FASEB **14,** 231-241.

Kiefer F., Arnold K., Kunzli M., Bordoli L., and Schwede T. (2009). The SWISS-MODEL Repository and associated resources. Nucleic Acids Research **37,** 387-392.

Kiefer I.W. and Slusarenko A.J. (2003). The pattern of Systemic Aquired Resistance induction within the *Arabidopsis* rosette in relation to the pattern of translocation. Philos Trans R Soc Lond B Biol Sci.an **132,** 840-847.

Kim M.G., Cunha L., McFall A.J., Belkhadir Y., DebRoy S., Dangl J.L., and Mackey D. (2005). Two *Pseudomonas syringae* Type III effectors inhibit RIN4-regulated basal defense in *Arabidopsis*. Cell **121,** 749-759.

Kimura M. (1980). A Simple method for estimating evolutionary rate of base substitutions through comparative studies of nucleotide sequences. Journal of Molecular Evolution **16,** 111-120.

King R.W. and Zeevaart J.A.D. (1974). Enhancement of phloem exudation from cut petioles by chelating agents. Plant Physiology **53,** 96-103.

Koonin E.V. (2005). Orthologs, paralogs, and evolutionary genomics. Annual Reviews in Genetics **39,** 309-338.

Krasikov V., Dekker H., Rep M., and Takken F.L.W. (2011). The tomato xylem sap protein XSP10 is required for full susceptibility to Fusarium wilt disease. Journal of Experimental Botany **62,** 963-973.

Kuc J. (1982). Induced immunity to plant disease. BioScience **32,** 854-860.

Kumar D. and Klessig D. (2003). High-affinity salicylic acid-binding protein 2 is required for plant innate immunity and has salicylic acid-stimulated lipase activity. PNAS **100,** 16101-16106.

Kunkel B.N., Bent A.F., Dahlbeck D., Innes R.W., and Staskawicz B.J. (1993). *RPS2,* an *Arabidopsis* Disease Resistance Locus Specifying Recognition of *Pseudomonas syringae* Strains Expressing the Avirulence Gene *avrRpt2*. The Plant Cell **5,** 865-875.

Lam B.C.H., Sage T.L., Bianchi F., and Blumwald E. (2001). Role of SH3 Domain-Containing Proteins in Clatherin-Mediated Vesicle Trafficking in *Arabidopsis*. The Plant Cell **13,** 2499-2512.

Lascombe M., Buhot N., Bakan B., Marion D., Blein J.P., Lamb C.J., and Prange T. (2006). Crystallization of DIR1, a LTP2-like resistance signalling protein from *Arabidopsis thaliana*. Acta Cryst. **F62,** 702-704.

Lascombe M., Bakan B., Buhot N., Marion D., Blein J., Larue V., Lamb C., and Prange T. (2008). The structure of "defective in induced resistance" protein of *Arabidopsis thaliana,* DIR1, reveals a new type of lipid transfer protein. Protein Science **17,** 1522-1530.

Lawton K., Weymann K., Friedrich L., Vernooij B., Uknes S., and Ryals J. (1995). Systemic Acquired Resistance in *Arabidopsis* requires salicylic acid but not ethylene. MPMI **8,** 863-870.

Leister D. (2004). Tandem and segmental gene duplication and recombination in the evolution of plant disease resistance genes. Trends in Genetics **20,** 116-122.

Lindorff-Larsen K., Lerche M.H., Poulsen F.M., Roepstorff P., and Winther J.R. (2001). Barley Lipid Transfer Protein, LTP1, contains a new type of lipid-like post-translational modification. Journal of Biological Chemistry **276,** 33547-33553.

Liu C. and Nelson R.S. (2013). The cell biology of Tobacco mosaic virus replication and movement. Frontiers in Plant Science **4,** 1-10.

Liu P., Dahl C.C., and Klessig D.F. (2011a). The extent to which methyl salicylate is required for signaling Systemic Acquired Resistance is dependent on exposure to light after Infection. Plant Physiology **157,** 2216-2226.

Liu P., Dahl C.C.v., Park S., and Klessig D.F. (2011b). Interconnection between methyl salicylate and lipid-based long-distance signaling during the development of Systemic Acquired Resistance in *Arabidopsis* and tobacco. Plant Physiology **155,** 1762-1768.

Lorenc-Kukula K., Chaturvedi R., Roth M., Welti R., and Shah J. (2012). Biochemical and molecular-genetic characterization of SFD's involvement in lipid metabolism and defense signaling. Frontiers in Plant Science **3,** 1-11.

Luna E., Bruce T.J.A., Roberts M.R., Flors V., and Ton J. (2012). Next-Generation Systemic Acquired Resistance. Plant Physiology **158,** 844-853.

Luna E. and Ton J. (2012). The epigenetic machinery controlling transgenerational systemic acquired resistance. Plant Signaling & Behaviour **7,** 615-618.

Mackey D., Belkhadir Y., Alonso J.M., Ecker J.R., and Dangl J.L. (2003). *Arabidopsis* RIN4 is a target of the Type III virulence effector AvrRpt2 and modulates RPS2-mediated resistance. Cell **112,** 379-389.

Malamy J., Carr J.P., Klessig D.F., and Raskin I. (1990). Salicylic acid: a likely endogenous signal in the resistance response of tobacco to viral infection. Science **250,** 1002-1004.

Maldonado A.M., Doerner P., Dixon R.A., Lamb C.J., and Cameron R.K. (2002). A putative lipid transfer protein involved in systemic resistance signalling in *Arabidopsis*. Nature **419,** 399-403.

Mayer B.J. (2001). SH3 domains: complexity in moderation. Journal of Cell Science **114,** 1253-1263.

McClure W.O. and Edelman G.M. (1966). Fluorescent probes for conformational states of proteins, I. mechanism of fluorescence of 2-p-Toluidinylnaphthalene-6-sulfonate, a hydrophobic probe. Biochemistry **5,** 1908-1919.

Metraux J.P., Signer H., Ryals J., Ward E., Wyss-Benz M., Gaudin J., Raschdorf K., Schmid E., Blum W., and Inverardi B. (1990). Increase in salicylic acid at the onset of Systemic Acquired Resistance in cucumber. Science **250,** 1004-1006.

Mishina T.E. and Zeier J. (2007). Pathogen-associated molecular pattern recognition rather than development of tissue necrosis contributes to bacterial induction of systemic aquired resistance in *Arabidopsis*. The Plant Journal **50,** 500-513.

Mishna T.E. and Zeier J. (2006). The *Arabidopsis* Flavin-Dependent Monooxygenase FMO1 is an essential component of biologically induced Systemic Acquired Resistance. Plant Physiology **141,** 1666-1675.

Mitton F.M., Pinedo M.L., and Canal L. (2009). Phloem sap of tomato plants contains a DIR1 putative ortholog. Journal of Plant Physiology **166,** 543-547.

Moffett P. (2011). Fragment complementation and co-immunoprecipitation assays for understanding R Protein structure and function in plant immunity: Methods and Protocols, J. M. McDowell, ed (: Springer Science) pp. 9-20.

Mou Z., Fan W., and Dong X. (2003). Inducer of plant Systemic Acquired Resistance regulate NPR1 Function through redox changes. Cell **113,** 935-944.

Mudgett M.B. and Staskawicz B.J. (1999). Characterization of the *Pseudomonas syringae pv. tomato* AvrRpt2 protein: demonstration of secretion and processing during bacterial pathogenesis. Molecular Microbiology **32,** 927-941.

Mur L.A.J., Kenton P., Lloyd A.J., Ougham H., and Prats E. (2008). The hypersensitive response; the centenary is upon us but how much do we know? Journal of Experimental Botany **59,** 501-520.

Mussolino C. and Cathomen T. (2012). TALE nucleases: tailored genome engineering made easy. Current Opinion in Biotechnology **23,** 644-650.

Nandi A., Welti R., and Shah J. (2004). The *Arabidopsis thaliana* Dihydroxyacetone Phosphate Reductase Gene *SUPPRESSOR OF FATTY ACID DESATURASE DEFICIENCY1* is required for glycerolipid metabolism and for the activation of Systemic Acquired Resistance. The Plant Cell **16,** 465-477.

Navarova H., Bernsdorff F., Doring A., and Zeier J. (2012). Pipecolic acid, an endogenous mediator of defense amplification and priming, is a critical regulator of inducible plant immunity. The Plant Cell 1-20.

Nürnberger T., Brunner F., Kemmerling B., and Piater L. (2004). Innate immunity in plants and animals: striking similarities and obvious differences. Immunological reviews **198,** 249-266.

Oerke E.C. and Dehne H.W. (2004). Safeguarding production - losses in major crops and the role of crop protection. Crop Protection **23,** 275-285.

Pajerowska-Mukhtar K.M., Wang W., Tada Y., Oka N., Tucker C.L., Fonseca J.P., and Dong X. (2012). The HSF-like transcription factor TBF1 is a major molecular switch for plant growth-to-defense transition. Current Biology **22,** 103-312.

Park S., Liu P., Forouhar F., Vlot A.C., Tong L., Tietjen K., and Klessig D.F. (2009). Use of a synthetic salicylic acid analog to investigate the roles of methyl salicylate and its esterases in plant disease resistance. Journal of Biological Chemistry **284,** 7307-7317.

Park S., Kaimoyo E., Kumar D., Mosher S., and Klessig D. (2007). Methy salicylate is a critical mobile signal for plant Systemic Aquired Resistance. Science **318,** 113-116.

Peitsch M.C. (1995). Protein modeling by E-mail. Biotechnology **13,** 658-660.

Perterson T.N., Brunak S., von Heijne G., and Nielsen H. (2011). SignalP 4.0: discriminating signal peptides from transmembrane regions. Nature Methods **8,** 785-786.

Prince V.E. and Pickett F.B. (2002). Splitting Pairs: The diverging fates of duplicated genes. Nature Reviews **3,** 827-837.

Pyee J., Yu H., and Kolattukudy P.E. (1994). Identification of a lipid transfer protein as the major protein in the surface wax of broccoli (*Brassica oleracea*) leaves. Archives of Biochemistry and Biophysics **331,** 460-468.

Rasmussen J.B., Hammerschmidt R., and Zook M.N. (1991). Systemic induction of salicylic acid accumulation in cucumber after inoculation with *Pseudomonas syringae* pv *syringae*. Plant Physiology **97,** 1342-1347.

Roden L.C. and Ingle R.A. (2009). Lights, Rhythms, Infection: The role of light and the circadian clock in determining the outcome of plant-pathogen interactions. The Plant Cell **21,** 2546-2552.

Ross A.F. (1961a). Systemic Acquired Resistance induced by localized virus infections in plants. Virology **14,** 340-358.

Ross A.F. (1961b). Localized acquired resistance to plant virus infection in hypersensitive hosts. Virology **14,** 329-339.

Rost B. (1999). Twilight zone of protein sequence alignment. Protein Engineering **12,** 85-94.

Samuel D., Liu Y., Cheng C., and Lyu P. (2002). Solution structure of plant non-specific lipid transfer protein-2 from rice (*oryza sativa*). Journal of Biological Chemistry **277,** 35267-35273.

Schlaich N.L. (2007). Flavin-containing monooxygenases in plants: looking beyond detox. Trends in Plant Science **12,** 412-418.

Schneider T.D. and Stephens R.M. (1990). Sequence Logos: A new way to display consensus sequences. Nucleic Acids Research **18,** 6097-6100.

Schranz M.E., Song B., Windsor A.J., and Mitchell-Olds T. (2007). Comparative genomics in the *Brassicaceae*: a family-wide perspective. Current Opinion in Plant Biology **10,** 168-175.

Schwede T., Kopp J., Guex N., and Peitsch M. (2003). SWISS-MODEL: an automated protein homology-modeling server. Nucleic Acids Research **31,** 3381-3385.

Schwessinger B. and Zipfel C. (2008). News from the frontline: recent insights into PAMP-triggered immunity in plants. Current Opinion in Plant Biology **11,** 389-395.

Shah J. and Chaturvedi R. (2013). Long-Distance Signaling in Systemic Acquired Resistance in Long-distance systemic signaling and communication in plants, F. Baluska, ed (Germany: Springer-Verlag) pp. 1-21.

Shah J. and Zeier J. (2013). Long-distance communication and signal amplificaton in systemic acquired resistance. Frontiers in Platn Science **4,** 1-40.

Shan Q., Wang Y., Li J., Zhang Y., Chen K., Liang Z., Zhang K., Liu J., Xi J.J., Qui J., and Gao C. (2013). Targeted genome modification of crop plants using a CRISPR-Cas system. Nature Biotechnology **31,** 686-688.

Slaughter A., Daniel X., Flors V., Luna E., Hohn B., and Mauch-Mani B. (2012). Descendants of Primed *Arabidopsis* Plants Exhibit Resistance to Biotic Stress. Plant Physiology **158,** 835-843.

Smith J.A., Hammerschmidt R., and Fulbright D.W. (1991a). Rapid induction of systemic resistance in cucumber by *Pseudomonas syringae* pv. *syringae*. Physiological and Molecular Plant Pathology **38,** 223-235.

Smith J.A., Hammerschmidt R., and Fulbright D.W. (1991b). Rapid induction of systemic resistance in cucumber by *Pseudomonas syringae* pv. *syringae*. Physiological and molecular plant pathology **38,** 223-235, doi/DOI: 10.1016/S0885-5765(05)80126-2.

Song J.T., Lu H., McDowell J.M., and Greenberg J.T. (2004). A key role for ALD1 in activation of local and systemic defenses in *Arabidopsis*. The Plant Journal **40,** 200-212.

Stam M., Mol J.N.M., and Kooter J.M. (1997). The silence of genes in transgenic plants. Annals of Botany **79,** 3-12.

Stanislava G. (2007). Barley grain non-specific lipid-transfer proteins (ns-LTPs) in beer production and quality. Journal of the Institute of Brewing **113,** 310-324.

Tamura K., Peterson D., Peterson N., Stecher G., Nai M., and Kumar S. (2011). MEGA5: Molecular Evolutionary Genetics Analysis using maximum likelihood, evolutionary distance, and maximum parsimony methods. Molecular Biology and Evolution **In Press,** .

Tassin-Moindrot S., Caille A., Douliez J.P., Marion D., and Vovelle F. (2000). The wide binding properties of a wheat nonspecific lipid transfer protein. Solution structure of a complex with prostaglandin B2. European Journal of Biochemistry **267,** 1117-1124.

Theologis A., Ecker J.R., Palm C.J., Federspiel N.A., Kaul S., White O., Alonso J., Altafi H., Araujo R., Bowman C.L., Brooks S.Y., Buehler E., Chan A., Chao Q., Chen H., Cheuk R.F., Chin C.W., Chung M.K., Conn L., Conway A.B., Conway A.R., Creasy T.H., Dewar K., Dunn P., Etgu P., Feldblyum T.V., Feng J., Fong B., Fujii C.Y., Gill J.E., Goldsmith A.D., Haas B., Hansen N.F.,

Hughes B., Huizar L., Hunter J.L., Jenkins J., Johnson-Hopson C., Khan S., Khaykin E., Kim C.J., Koo H.L., Kremenetskaia S., Kurtz D.B., Kwan A., Lam B., Langin-Hooper S., Lee A., Lee J.M., Lenz C.A., Li J.H., Li Y., Lin X., Liu S.X., Liu Z.A., Luros J.S., Maiti R., Marziali A., Militscher J., Miranda M., Nguyen M., Nierman W.C., Osborne B.I., Pai G., Peterson J., Pham P.K., Rizzo M., Rooney T., Rowley D., Sakano H., Salzberg S.L., Schwartz J.R., Shinn P., Southwick A.M., Sun H., Tallon L.J., Tambunga G., Toriumi M.J., Town C.D., Utterback T., Aken S.V., Vaysberg M., Vysotskaia, V,S, Walker M., Wu D., Yu G., Fraser C.M., Venter J.C., and Davis R.W. (2000). Sequence and analysis of chromosome 1 of the plant *Arabidopsis thaliana*. Nature **408,** 816-820.

Thomas S., Kaneko Y., and Somerville C. (1993). A non-specific lipid transfer protein from *Arabidopsis* is a cell wall protein. The Plant Journal **3,** 427-436.

Truman W., Bennett M.H., Kubigsteltig I., Turnbull C., and Grant M. (2007). *Arabidopsis* systemic immunity uses conserved defense signaling pathways and is mediated by jasmonates. Proceedings of the National Academy of Sciences **104,** 1075-1080.

Tuzun S. and Kuc J. (1985). Movement of a factor in tobacco infected with *Peronospora tabacina* which systemically protects against blue mold. Physiological Plant Pathology **26,** 321-330.

van Hulten M., Pelser M., van Loon L.C., Pieterse C.M.J., and Ton J. (2006). Costs and benefits of priming for defense in *Arabidopsis*. PNAS **103,** 5602-5607.

van Loon L.C. and Dijkstra J. (1976). Virus-specific expression of systemic acquired resistance in tobacco mosaic virus- and tobacco necrosis virus-infected 'Samsun NN' and 'Samsun' tobacco. Netherlands Journal of Plant Pathology **82,** 231-236.

Vernooij B., Friedrich L., Morse A., Reist R., Kolditz-Jawhar R., Ward E., Uknes S., Kessmann H., and Ryals J. (1994). Salicylic acid is not the translocated signal responsible for inducing Systemic Acquired Resistance but is required in signal transduction. The Plant Cell **6,** 959-965.

Vlot A.C., Dempsey D.A., and Klessig D.F. (2009). Salicylic acid, a multifaceted hormone to combat disease. Annual Review of Pytopathology **47,** 177-206.

Vlot A.C., Liu P., Cameron R.K., Park S., Yang Y., Kumar D., Zhou F., Padukkavidana T., Gustafsson C., Pichersky E., and Klessig D.F. (2008). Identification of likely orthologs of tobacco salicylic acid-binding protein 2

and their role in systemic acquired resistance in *Arabidopsis thaliana*. The Plant Journal **56,** 445-456.

Vogel-Adghough D., Stahl E., Navarova H., and Zeier J. (2013). Pipecolic acid enhances resistance to bacterial infection and primers salicylic acid and nicotine accumulation in tobacco. Plant Signaling and Behaviour **8,** .

Wang D., Weaver N.D., Kesarwani M., and Dong X. (2005). Induction of protein secretory pathway is required for Systemic Acquired Resistance. Science **308,** 1036-1040.

Wang D., Pajerowska-Mukhtar K., Culler A.H., and Dong X. (2007). Salicylic acid inhibits pathogen growth in plants through repression of the auxin signaling pathway. Current Biology **17,** 1784-1790.

Weigel R.R., Bauscher C., Pfitzner A.J., and Pfitzner U.M. (2001). NIMIN-1, NIMIN-2 and NIMIN-3, members of a novel family of proteins from *Arabidopsis* that interact with NPR1/NIM1, a key regulator of systemic acquired resistance in plants. Plant Molecular Biology **46,** 143-160.

Wesley S.V., Helliwell C.A., Smith N.A., Wang M., Rouse D.T., Liu Q., Gooding P.S., Singh S.P., Abbott D., Stoutjesdijk P.A., Robinson S.P., Gleave A.P., Green A.G., and Waterhouse P.M. (2001). Construct design for efficient, effective and high-throughput gene silencing in plants. The Plant Journal **27,** 581-590.

Whalen M.C., Innes R.W., Bent. A.F., and Staskawicz B.J. (1991). Identification of *Pseudomonas syringae* pathogens of *Arabidopsis* and a bacterial locus determining avirulence on both *Arabidopsis* and soybean. The Plant Cell **3,** 49-59.

Williamson M.P. (1994). The structure and function of proline-rich regions in proteins. Biochem Journal **297,** 249-260.

Winter D., Vinegar B., Nahal H., Ammar R., Wilson G.V., and Provart N.J. (2007). An "Electronic Fluorescent Pictograph" browser for exploring and analyzing large-scale biological data sets. PLoS ONE **2,** 1-12.

Wolf S., Deom C.M., Beachy R.N., and Lucas W.J. (1989). Movement protein of tobacco mosaic virus modifies plasmodesmatal size exclusion limit. Science **246,** 377-379.

Wroblewski T., Tomczak A., and Michelmore R. (2005). Optimization of *Agrobacterium*-mediated transient assays of gene expression in lettuce, tomato and *Arabidopsis*. Plant Biotechnology Journal **3,** 259-273.

Wu Y., Chu J.Y., Boyle P., Wang Y., Brindle I.D., Luca V.D., and Despres C. (2012). The *Arabidopsis* NPR1 protein is a receptor for the plant defense hormone salicylic acid. Cell Reports **1,** 639-647.

Xiao S., Brown S., Patrick E., Brearley C., and Turner J.G. (2003). Enhanced transcription of the *Arabidopsis* disease resistance genes *RPW8.1* and *RPW8,2* via salicylic acid-dependent amplification circuit is required for hypersensitive cell death. Plant Cell **15,** 33-45.

Xin X. and He S.Y. (2013). *Pseudomonas syringae pv. tomato* DC3000: A model pathogen for probing disease susceptibility and hormone signaling in plants. Annual Review of Pytopathology **51,** .

Yu K., Soares J.M., Mandal M.K., Wang C., Chanda B., Gifford A.N., Fowler J.S., Navarre D., Kachroo A., and Kachroo P. (2013). A feedback regulatory look between G3P and lipid transfer proteins DIR1 and AZI1 mediates azelaic-acid-induced systemic immunity. Cell Reports **3,** 1266-1278.

Zarrinpar A., Bhattacharyya R.P., and Lim W.A. (2003). The structure and function of proline recognition domains. Science Signaling **179,** 1-10.

Zeidler D., Zahinger U., Gerber I., Bubery I., Hartung T., Bors W., Hutzler P., and Durner J. (2004). Innate immunity in *Arabidopsis thaliana*: Lipopolysaccharides activate nitric oxide synthase (NOS) and induce defense genes. PNAS **101,** 15811-15816.

Zhang X., Henriques R., Lin S., Niu Q., and Chua N. (2006). *Agrobacterium*-mediated transformation of *Arabidopsis thaliana* using the floral dip method. Nature Protocols **1,** 1-6.

Zhang Y., Zhang F., Li X., Baller J.A., Qi Y., Starker C.G., Bogdanove A.J., and Voytas D.F. (2013). Transcription activator-like effector nucleases enable efficient plant genome engineering. Plant Physiology **161,** 20-27.

Zheng C., Xie Q., Anderson R.G., Ng G., Seitz N.C., Peterson T., McClung C.R., McDowell J.M., Kong D., Kwak J.M., and Lu H. (2013). Crosstalk between the circadian clock and innate immunity in *Arabidopsis*. PLOS Pathogens **9,** 1-14.

Zhou J., Trifa Y., Silva H., Pontier D., Lam E., Shah J., and Klessig D.F. (2000). NPR1 differentially interacts with members of the TGA/OBF family of transcription factors that bind an element of the *PR-1* gene required for induction by salicylic acid. Molecular Plant-Microbe Interactions **13,** 191-202.

Zoeller M., Stingl N., Krischke M., Fekete A., Waller F., Berger S., and Mueller M.J. (2012). Lipid profiling of the *Arabidopsis* hypersensitive response

reveals sepcific lipid peroxidation and fragmentation processes: biogenesis of pimelic and azelaic acid. Plant Physiology **160,** 365-378.

Zuo J., Niu Q., and Chua N. (2000). An estrogen receptor-based transactivator XVE mediates highly inducible gene expression in transgenic plants. The Plant Journal **24,** 265-273.